UNITED STATES
PARTMENT OF
)MMERCE
IBLICATION

ESSA Technical Memorandum WBTM HYDRO 11

U.S. DEPARTMENT OF COMMERCE
Environmental Science Services Administration
Weather Bureau

Joint Probability Method of Tide Frequency Analysis Applied to Atlantic City and Long Beach Island, N.J.

VANCE A. MYERS

'ER SPRING
MARYLAND

PRIL 1970

ESSA TECHNICAL MEMORANDA

Office of Hydrology Series

The Office of Hydrology develops procedures for making river and water supply forecasts, analyzes hydrometeorological data for planning and design criteria for other agencies, and conducts pertinent research and development.

ESSA Technical Memoranda in the Office of Hydrology series facilitate prompt distribution of scientific and technical material by staff members, cooperators, and contrctors. Results presented in this series may be preliminary in nature and may be published formally elsewhere at a later date.

Memoranda listed below are available from the Clearinghouse for Federal Scientific and Technical Information, U.S. Department of Commerce, Sills Bldg., 5285 Port Royal Road, Springfield, Va. 22151. Price: $3.00 hard copy; $0.65 microfiche. Order by accession number shown in parentheses at end of each entry.

TN 44 HYDRO 1   Infrared Radiation from Air to Underlying Surface. Vance A. Myers, May 1966. In former Weather Bureau Technical Notes series. (PB-170 664)

WBTM HYDRO 2   Annotated Bibliography of ESSA Publications of Hydro-meteorological Interest. J. L. H. Paulhus, February 1967. (Superseded by WBTM HYDRO 8)

WBTM HYDRO 3   The Role of Persistence, Instability, and Moisture in the Intense Rainstorms in Eastern Colorado, June 14-17, 1965. F. K. Schwarz, February 1967. (PB-174 609)

WBTM HYDRO 4   Elements of River Forecasting. Marshall M. Richards and Joseph A. Strahl, October 1967. (Superseded by WBTM HYDRO 9)

WBTM HYDRO 5   Meteorological Estimation of Extreme Precipitation for Spillway Design Floods. Vance A. Myers, October 1967. (PB-177 687)

WBTM HYDRO 6   Annotated Bibliography of ESSA Publications of Hydro-meteorological Interest. J. L. H. Paulhus, November 1967. (Superseded by WBTM HYDRO 8)

WBTM HYDRO 7   Meteorology of Major Storms in Western Colorado and Eastern Utah. Robert L. Weaver, January 1968. (PB-177 491)

WBTM HYDRO 8   Annotated Bibliography of ESSA Publications of Hydro-meteorological Interest. J. L. H. Paulhus, August 1968. (PB-179 855)

WBTM HYDRO 9   Elements of River Forecasting (Revised). Marshall M. Richards and Joseph A. Strahl, March 1969. (PB-185 969)

WBTM HYDRO 10   Flood Warning Benefit Evaluation - Susquehanna River Basin (Urban Residences). Harold J. Day, March 1970. (PB-190 984)

U.S. DEPARTMENT OF COMMERCE
Environmental Science Services Administration
Weather Bureau

ESSA Technical Memorandum WBTM HYDRO 11

JOINT PROBABILITY METHOD OF TIDE FREQUENCY ANALYSIS
APPLIED TO ATLANTIC CITY AND LONG BEACH ISLAND, N.J.

Vance A. Myers

Part of a study by ESSA for the Federal Insurance Administration,
Department of Housing and Urban Development, under the National
Flood Insurance Act of 1968.

Office of Hydrology

Silver Spring, Md.
April 1970

UDC 551.466.713:551.465.755:551.515.23(74)(76)

551.46		Oceanography
	.465	Dynamics of sea
	.755	Storm surges
	.466	Waves and high tides
	.713	High tide frequency analysis
551.5		Meteorology
	.515	Weather - storms, etc.
	.23	Hurricane tracks and frequencies
(74)		Northeastern U.S.
(76)		Gulf States

CONTENTS

iii

JOINT PROBABILITY METHOD OF TIDE FREQUENCY ANALYSIS

Applied to Atlantic City and Long Beach Island, N. J.

Vance A. Myers
Office of Hydrology
ESSA-Weather Bureau

Chapter I

INTRODUCTION

The "National Flood Insurance Act of 1968" (Public Law 448, 90th Congress, title XIII), provides for the first time a national program for insuring residences and small businesses against the hazard of damage or destruction by floods. The law is administered by the Secretary of Housing and Urban Development through the Federal Insurance Administration. Other federal agencies are assisting HUD in implementing this law by making appropriate technical studies. Thus, HUD requested the Environmental Science Services Administration (ESSA) to make a technical study of Long Beach Island, N.J. for this purpose, calling on the combined experience of the Coast and Geodetic Survey and the Weather Bureau, both components of ESSA.

Essential to implementing the flood insurance program in any community, whether coastal or river valley, is a flood frequency analysis. Flood heights at certain frequencies are the guide for dividing the community into zones of different flood risks, are the actuarial basis for calculating flood insurance rates, and also are criteria in local zoning and flood plain occupancy ordinances. Such ordinances are required by the Act of 1968 as a condition of community eligibility for federal sponsorship of flood insurance.

This paper describes the frequency analysis of combined storm surges and periodic tides prepared by ESSA as part of the Long Beach Island study. These frequencies apply to the ocean beach. Studies of wave action and possible variations in water levels inshore from the ocean side of the Island are not covered here, nor are other parts of the ESSA study such as mapping of the community and elevation determination of structures.

The Long Beach Island study is a pilot study in a new area. It is intended to serve as a guide to other studies of other coastal communities as well as to provide needed criteria at this one location. Thus, a few

comments are included in the report on similarities and differences between Long Beach Island and other locations. Technical procedures are set forth in some detail in this report, to facilitate not only their emulation but also their criticism and modification in future studies for other coastal communities.

Previous tide frequency analysis

The most recent tide frequency analysis for southern New Jersey prior to the present study was prepared by the Philadelphia District of the Corps of Engineers (1) in 1963 under Public Law 71, 84th Congress. That law provided for a survey of hurricane damage potential and for possible remedial measures along the coast. In the Corps of Engineers study the tide frequency curve for Atlantic City was extended from past recorded storm tides at the Atlantic City gage to a tide calculated to result from a hypothetical storm delineated by the Weather Bureau, the "Standard Project Hurricane" (8). For purposes of that particular analysis, the Standard Project Hurricane was assigned a probability of occurrence in any one year of 0.2 percent. The surge (rise of water level) resulting from this storm was assumed to occur simultaneously with mean high astronomical tide.

This same tide frequency analysis, together with records from past storms, was used by the Corps of Engineers in preparing Flood Plain Information Studies for several southern New Jersey communities under the Flood Control Act of 1960, and as amended in 1966.

Present tide frequency analysis

Since insurance rates are intimately related to the frequencies of the events insured against, it was considered essential in the present study to evolve the most reliable tide frequency estimates that existing data and present technology would permit. The present study, like the 1963 frequency analysis cited above, extends the frequency curve beyond observed storm data by including hypothetical tides calculated from hypothetical storms chosen so as to represent future possibilities. Recent advances in the technique of computing surges from hurricane wind fields (2, 3) by solving simplified forms of the applicable dynamic equations make it possible to determine surges in a statistical manner for several hundred hypothetical hurricanes, representing different combinations of climatological hurricane characteristics. Another advance in the present study is that in calculating hypothetical tides, storm surges are combined with the astronomical tide in a random manner rather than being made coincident with astronomical high tide only. This joint probability approach is described in the next chapter.

List of symbols

The following symbols are employed in this report. Some of them are also defined in the text where first used. The units used in this report are indicated in parenthesis.

A – astronomic or periodic tide (feet above a specified reference datum, usually mean sea level in this report).

S – storm surge. Deviation of observed water level from "A" (feet).

T – water level, or total tide. Sum of S and A (feet above a specified reference datum, usually above mean sea level in this report).

A_x – maximum A. Commonly called "high tide" (feet above reference datum).

S_{1x} – local maximum S. Highest surge during a storm at a specified distance from storm track. Defined only for landfalling hurricanes (feet).

S_x – landfalling hurricanes: Maximum S_{1x} along coast in a storm (feet). Other storms: Maximum S during a storm (feet).

T_x – maximum T from a particular combination of time profiles of S and A (feet above reference datum).

t – time

$t_{2/3}$ – scaling parameter for surge-time profiles. $S = (2/3)S_x$ at $t = \pm (1/2)t_{2/3}$

d – landfalling hurricanes: Distance along coast from point of occurrence of S_x.

        alongshore hurricanes: Distance of storm track from coast.

$d_{2/3}$ – scaling parameter for surge-distance profiles in landfalling hurricanes. $S_{1x} = (2/3) S_x$ at $d = \pm (1/2)d_{2/3}$

D – pressure depression at center of hurricane below peripheral pressure (mb).

f – forward speed of hurricane (kt or mph).

R – radial distance from center of hurricane to location of maximum windspeeds (statute miles).

D_s – D for a hurricane of "standard" intensity in (3). Varies with R (mb).

F_h – frequency of hurricane track penetrations of a coastal region (storms per nautical mile per year).

F_H — frequency that tracks of hurricanes moving approximately parallel to shore cross a line perpendicular to the coast (storms per nautical or statute mile per year).

F_d — frequency of hurricane tracks through a specified distance interval. Product of F_H and length of interval (per year).

F_R — frequency of a representative climatological alongshore hurricane with D, f, R, and d within specified ranges (per year).

F_w — frequency that a "winter" (Nov-Apr) storm surge equals or exceeds a specified height (per year).

F_c — frequency of T_x resulting from a specific combination of storm parameters, astronomical tide amplitude, and phase displacement from A_x to S_x (per year).

P_i, P_f, P_r — fraction of hurricanes having D, f, and R within certain ranges, respectively (dimensionless probability).

P_a — fraction of A_x's falling within specified range (dimensionless probability).

P_z — phasing displacement probability (dimensionless).

P_s — fraction of hurricanes having a specified combination of D, f, and R (dimensionless).

H_o — height of the mean level of the sea for a month, year, or epoch (feet above reference datum).

H_n, f_n, a_n, t, α_n, m — factors in equation (19). See page 50.

W — mean period of astronomical tide = one-half mean lunar day = 12.42 hours.

S_B, S_A — upper and lower boundaries of a standard surge height interval in surge frequency analysis (feet)

S_M — $(1/2)(S_B + S_A)$.

F_{A-B} — frequency with which local maximum surge height, S_{1x}, falls within interval $S_B \overline{>} S_{1x} \overline{>} S_A$ (feet).

d_B, d_A — 2d for $S_{1x} = S_B$, $S_{1x} = S_A$

Chapter II

JOINT PROBABILITY METHOD OF TIDE FREQUENCY DETERMINATION

Method for hurricanes

High tides in storms result from the superposition of storm effects on the normal gravitational or astronomical tide. This may be represented by the equation

$$T = S + A \tag{1}$$

Here T is the total water level, or "tide," in feet at a particular time above some specified datum such as gage zero or local mean sea level, A is the periodic astronomical tide in feet above the same datum, and S is the storm surge in feet. At tide gage locations element A is calculated in advance by the Coast and Geodetic Survey and published in tide tables (4), T is the total tide observed on a tide recorder, and S is the difference, due principally to wind. Atmospheric pressure has a lesser effect on the surge. In a given hurricane not only is the maximum surge height, S_x, generally almost independent of the magnitude A but also its time variation. If maximum storm surge, S_x, is coincident with maximum astronomical tide, A_x, then the maximum total tide, T_x, is the sum

$$T_x = S_x + A_x \tag{2}$$

But such phasing is neither more likely nor less likely than other phasings. In general it is necessary to maximize the sum

$$T_x = (S + A)_x \tag{3}$$

Thus the height of the maximum total tide in a given hurricane is highly dependent on whether the surge peak, S_x, is in near coincidence with the astronomical tide peak, A_x, or occurs at some earlier or later time.

This near independence of S and A is recognized in the present study by combining each of a series of calculated hurricane surge profiles with a full range of astronomical tide amplitudes at a full range of displacements in timing (chapter VI) as if S and A were fully statistically and physically independent. Circumstances under which this assumption may not be justified are discussed in a subsequent paragraph.

Hurricane frequency

All climatologically expected hurricanes are represented by a finite number (several hundred) of specific storms with specific characteristics.

Each such representative hurricane has a specific estimated frequency of occurrence, depending on its characteristics. The sum of the assigned frequencies of all the representative hurricanes is equal to the frequency of passages of hurricanes through the area. The climatological assessment of hurricanes and their characteristics on a frequency basis required for this purpose is covered in chapter III.

Astronomical tide probability

The range of the astronomical semi-diurnal tide oscillation depends on the season, relative positions of the earth, sun, and moon, and other factors. All oscillations of the astronomical tide, from lowest neap tide to highest spring tide, are represented by a finite number of specific tidal oscillations, each of which is assigned a probability. The sum of these probabilities is 1.0. The requisite analysis of a 19-year cycle of the astronomical tide is described in chapter V.

Time displacement probability

The time phasing of surge and astronomical tide is handled in a similar probabilistic manner. A finite number of phasing displacements are used, ranging from coincidence of peak storm surge with peak astronomical tide to coincidence of peak storm surge with the low astronomical tide. Each specific time phasing displacement has a probability; the sum of the probabilities is 1.0.

Joint probability

The calculated surge time profile for each of the several hundred representative hurricanes is combined with each of the representative astronomical tide oscillation curves at each of the representative time phasing displacements. Equation (1) is solved for each of these combinations at each of a succession of time steps, and the largest, T_x, of this series discovered by scanning. This is the maximum tide for that particular combination of hypothetical hurricane, astronomical tide oscillation, and phase displacement. The frequency of occurrence of this tide is the product of the frequency of occurrence of the initiating storm, the astronomical tide probability, and the phase displacement probability. The synthetic part of the total tide frequency curve, then, is obtained by arraying the computed T_x's from all these combinations in order of magnitude and accumulating their frequency. This process is described in detail in chapter VI.

Possible non-independence of hurricane surge and astronomical tide

More complex coastal topography might require a more complex treatment of synthetic tide frequency analysis. In an estuary the speed of propagation of the gravitational tidal wave is dependent on water depth and

thereby dependent on S. In shallow water the setup of the water surface due to a given wind depends on the water depth because of the drag between the surface flow in the direction of the wind and the counter current beneath and is therefore also dependent on S.

Non-independence of the occurrence of different component factors offers no fundamental obstacle to a joint probability calculation, provided the interrelationship between these factors can be defined. Where these interrelationships exist, the joint probability or frequency, rather than being the product of the individual probabilities or frequencies, requires more complicated but not insurmountably difficult formulas.

Hurricane surge models

The joint probability approach to synthetic tide frequency determination as described above, can be carried out only if the surges resulting from numerous representative hurricanes can be calculated with acceptable accuracy with an acceptable amount of computation.

Two methods have been published recently for calculating the hurricane surge, S, resulting from a given hurricane moving over coastal waters of stated depth. These are by Jelesnianski (3) and Marinos and Woodward (2). These authors disclaim taking into account fully the very complex natural phenomena in storm tide generation, including non-linear interrelationships. The limitations and assumptions are explained in the cited papers. Particularly, the storm surge dynamics of a hurricane moving parallel or nearly parallel to the coast, appears to be more complex and thus less fully explained than for a storm moving approximately perpendicular into the coast (3). However, it appears that the results of the dynamic models are now sufficiently reliable to warrant the synthetic analysis we have carried out. Further appraisal of the Jelesnianski method is made in chapter X.

The method of Marinos and Woodward is basically a steady state method which determines for a given coastal and water depth configuration the equilibrium water surface and currents that will balance wind stress, gravitational force, bottom frictional stress, and Coriolis forces. This model has been applied by the authors primarily to slow-moving hurricanes in the western Gulf of Mexico. Jelesnianski's model in its present published form works in less detail as to coastal configuration and water depth, in fact it assumes a straight coast and a one-dimensional bottom profile, but is more dynamic in that it takes into account the lag of the mass of water in coming into equilibrium with the imposed forces (inertial effect) and the dynamics of the traveling storm waves. These latter effects are considered of most significance in fast-moving hurricanes. The Jelesnianski model was, therefore, selected for the Long Beach Island study as the majority of hurricanes affecting this region have recurved north or northeastward

Total annual tide frequencies

Total annual tide frequencies at Atlantic City and Long Beach are determined by summing the frequencies from alongshore hurricanes, landfalling hurricanes, and winter storms. This summation is presented in chapter IX.

Chapter III

HURRICANE CLIMATOLOGY

Calculating tide frequencies on the southern New Jersey coast synthet-
ically by the joint probability method described in chapter II requires
specification of certain frequencies and probabilities. For convenience a
distinction is made in the remainder of this paper between "frequency" and
"probability." Frequency is defined as the number of occurrences of some
event per year and has dimensions of time^{-1} while probability is defined as
the fractional part of a total and is dimensionless. The requisite factors
are:

Frequency that hurricanes penetrate the southern New Jersey
coast (storms per mile per year).

Frequency with which storms moving approximately parallel to
the coast of southern New Jersey at sea cross a line normal to
the coast (storms per mile per year).

Probability distribution of forward speeds of these hurricanes.

Probability distribution of radius of maximum winds of these
hurricanes. (Index of the lateral extent of the storm.)

Probability distribution of the central pressure depression of
these storms. (Index of the intensity of the storm.)

Probability distribution of the direction of motion of the land-
falling hurricanes.

Interrelationship among these probabilities if they are not
independent.

We estimate each of these items in turn.

Frequency of hurricane penetration of the southern New Jersey coast, F_h

The basic information on hurricane tracks are the maps published by
Cry (5) of tracks of North Atlantic tropical cyclones for the years 1871
through 1963. Tracks of hurricanes since 1963 are depicted on similar
maps annually in the Monthly Weather Review, for example (6) and (7).
Thus we have in a convenient form relatively homogeneous track information
for the 99 years 1871 through 1969.

During these 99 years only one hurricane has moved inland on the
New Jersey coast. This was on September 16, 1903. The track is shown
in figure 3-1 from Cry (5) and a weather map in figure 3-2.

Tropical storms of less than hurricane intensity penetrated the
Del-Marva Peninsula south of New Jersey on October 23, 1893, and
October 1, 1943. Hurricane coastal penetrations have been rather more
frequent from Norfolk, Va., southward. Examples of storms entering the
coast just south of Norfolk are the hurricane of August 23, 1933, which
produced the highest tides of record at some points in the Chesapeake Bay,
and Hurricane Connie of August 12, 1955.

The New Jersey coast has a length of 105 nautical miles from Sandy
Hook to Cape May. If we consider the September 1903 storm only, there is
one storm penetration per 105 miles of coast for 99 years, or approximately
one storm per 100 nautical miles per 100 years. Delaware Bay plus the
Del-Marva Peninsula adds about 125 nautical miles of "coast." If we count
the three storms mentioned in 99 years over 230 miles of coast, we get
1.3 storms per 100 miles per 100 years. It is, of course, dangerous to
make planning decisions on the basis of such small statistical samples.

On the basis of the information here, it seems reasonably conservative
for calculation of flood insurance rates to assume two penetrations of the
New Jersey coast by hurricanes per hundred years, or .0002 storms per
nautical mile per year. Greater conservatism might be indicated for con-
struction decisions involving safety to persons.

Frequency of alongshore hurricanes at southern New Jersey coast, F_H

To establish this parameter hurricanes and tropical storms passing
at various distances from the New Jersey coast were counted from Cry's
track maps for the years 1871 through 1963 and from maps in the Monthly
Weather Review for subsequent years. For ease in reading from the maps
the track crossings were counted along the 40th parallel instead of along
a line perpendicular to the coast, then adjusted. This count is shown in
table 3-1. The stratification into hurricanes and tropical storms in the
table is discussed later.

The grand totals of table 3-1 show 52 storms crossing 240 nautical
miles of the 40th parallel in 99 years, or .0022 storms per mile per year.
Considering the average storm track direction as parallel to the coast we
project this count on a line normal to the coast at Long Beach Island
(300°-120°) by dividing by cos 30°. The count becomes .0025 storms per
nautical mile normal to the coast per year.

The grand total count from table 3-1, adjusted normal to the coast
and plotted as storm tracks per nautical mile per year, is depicted by the
solid line of figure 3-3. A dashed line shows a smoothed trend. Storm
track frequencies were scaled from the dashed line for certain distance
intervals and are listed in table 3-2 for use in chapter IV.

Probability distribution of hurricane intensity, limited sample

Central pressure is the hurricane intensity index. In their bulletin
on the Standard Project Hurricane, Graham and Nunn have included a compila-
tion of the characteristics of hurricanes affecting the eastern and southern
coast of the United States between 1900 and 1956 (8). This is the best
source of data for establishing the probability distribution of hurricane
intensities because it has the stated goal of including all hurricanes
during the years analyzed that had central pressures below a specified
value (982 mb) at the time the storm crossed or passed near the coast.
Table 3-3 lists the central pressures from Graham and Nunn for seven
storms north of 38°N and the latitudes to which the pressure measurements
or estimates apply. Each central pressure has been adjusted to 39.5°N by
following the trend in the latitudinal variation of the central pressure
index for the Standard Project Hurricane in figure 5a from Graham and
Nunn (8). These adjustments are not intended to provide a precise estimate
of the existing central pressure in each of these hurricanes at 39.5°N but
to provide a statistical body of data applicable to that latitude.

These adjusted central pressures are plotted in figure 3-4 and an
accumulated probability curve fitted by eye.

Probability distribution of hurricane intensity, expanded sample

The list of table 3-3 includes only hurricanes with central pressures
below 982 mb. Tropical storms insufficiently intense to be classed as
hurricanes and a few weaker hurricanes are excluded as specific central
pressures are not available for the weaker storms. Cry's track maps, by
contrast, on which the storm frequency count is based, include tropical
cyclones of all intensities. For validity of the joint probability com-
putations we must enforce consistency at this point, and either expand
the central pressure probability distribution to include the weaker storms,
or else restrict the storm track count to include only storms with central
pressures of 982 mb or less. This is because the frequency of each
representative climatologically specified hurricane of given character-
istics is the product of the frequency of all storms and the probability
of a storm having those particular characteristics.

There is insufficient information to distinguish tropical storms
with central pressures above and below the 982-mb criterion prior to 1900,
as well as in some of the more recent ones traveling offshore; therefore,
we expand the central pressure frequency distribution rather than contract
the storm track count and proceed as follows.

It is noted from table 3-1 that 17 of 27 storms during Cry's period
of most reliable intensity judgments, beginning in 1900, were hurricanes.
This is 63 percent. We compress the probability curve of figure 3-4 to
represent this 63 percent of storms in figure 3-5, and extend the curve
smoothly to 995 mb at 100 percent, thus including the tropical storms.

As a check, we compare the 7 storms of table 3-3 with the total count of hurricane plus tropical storm tracks from Cry's charts for the same period and location. The period is 1900-1956 and the location is the span of the 40th parallel from the coast to 180 nautical miles at sea. Twelve tracks cross this span during this period. If we construe that 7/12 (58%) of the storms have central pressures of less than 976 mb (see figure 3-4) we duplicate the reduction of the figure 3-4 probability curve to figure 3-5 presented in the previous paragraph.

In this manner, the "percent of storms" ordinate of figure 3-5 has been made to refer to the same spectrum of storm intensities as the frequency count of figure 3-1.

Hurricane intensity class intervals

The central pressure probability distribution of figure 3-5 is separated into six class intervals, two representing 10 percent of storms, and four 20 percent each, as depicted by the dashed curve of figure 3-5. For the remainder of the analysis we represent the central pressures of all hurricanes by the six discrete values indicated by figure 3-5 for both alongshore and landfalling hurricanes. These values are listed with their probabilities in table 3-4.

In a similar manner all continuous frequency or probability distributions are replaced by a series of representative discrete values. These values are chosen so as to provide needed resolution of the data and are not necessarily of equal probability.

Probability distribution of forward speeds--alongshore hurricanes

The forward speeds of pertinent hurricanes from (8) are listed in table 3-5. Three hurricanes of later years have been added. Speeds are scaled from Cry's (5) charts for Daisy of 1958 and Alma of 1962, and from an unpublished analysis by the Hydrometeorological Branch of the Weather Bureau for Donna of 1960. A smooth probability distribution of the forward speeds is constructed in figure 3-6. This is replaced by six speeds in six class intervals in the same manner as the intensity probability. These adopted speeds are listed in table 3-6.

All of the hurricanes of table 3-5 were moving approximately parallel to shore, and the resulting climatological speed distribution, table 3-6, applies to this class of storms.

Probability distribution of forward speeds--landfalling hurricanes

Hurricanes typically accelerate after their paths recurve to the north-northeast or northeast. A probability distribution of the forward speed of landfalling hurricanes would be expected to show lower speeds than

alongshore hurricanes at this latitude. The 1903 hurricane entered the
New Jersey coast at a forward speed of approximately 15 knots (5). Lacking
more definite information, for the water level frequency estimate we assume
that in each probability interval the speed of landfalling hurricanes is
20 percent less than for alongshore hurricanes, right-hand column of
table 3-6.

Probability distribution of radius of maximum winds

The principal published information available on the radius of maximum
winds in East Coast hurricanes is in (8), and in the companion publications
(9) and (10), which list some of the same data. Table 3-7 lists the radius
of maximum winds, R, from (8) for hurricanes north of 35°N. These are
plotted as an accumulated probability distribution in figure 3-7.

Computations have not been made with the Jelesnianski model with R's
larger than 45 statute miles (39.1 nautical miles) and it is unconfirmed
that the model works well with very large R's. Study of radar films of
hurricanes occurring since the publication of (8) has failed to provide
visual confirmation of any hurricane having an R as large as 50 nautical
miles. Some of the R's in table 3-7 are directly observed from wind
records, while others are computed from pressure profiles. Both of the
50 nautical mile R's in the table are computed values (reference 9, table
3-1) unconfirmed by direct wind observations. The R=66 nautical miles in
the August 26, 1924 hurricane is at a time of transition to extratropical
characteristics.

Judging these indications together, we ignore the larger R's in esti-
mating tide frequencies on the New Jersey coast by use of the Jelesnianski
model, and adopt 45 statute miles as our largest value of R. We further
assume for the hurricane tide frequency estimate that the hurricane size
variation may be represented by letting R=30, 37.5, and 45 statute miles in
one-third each of storms. This assumed probability distribution was applied
to landfalling hurricanes and is depicted by the dashed line of figure 3-7.

To conserve computation time during program checkout phases, only two
R's were used for alongshore hurricanes, R=30 and R=45 statute miles in
50 percent each of storms. Later tests, introducing R=37.5 storms with
interpolated characteristics, produced only trivial differences in water
level height at a given frequency (0.1 ft) and the computations based on
only two R's were adopted as final.

Direction of forward motion of landfalling hurricanes

The directions of motion of the three hurricanes and the tropical
storms crossing the New Jersey and Del-Marva coasts during the period of
Cry's track charts, are listed in table 3-8. General hurricane behavior

on the East Coast confirms the indication of table 3-8, namely, that a direction of motion from the southeast is the most common for landfalling hurricanes there. We infer from irregularities and loops in hurricane tracks at sea at the latitude of New Jersey, that a hurricane could strike the coast moving from any direction. (Most recent examples of loops and hurricane tracks at this latitude are Hurricane "Esther" of September 1961 and Hurricane "Alma" of September 1962 (5)). A probability distribution of the direction of motion of landfalling hurricanes at the New Jersey coast was derived (not shown) with lowest probabilities of approach from the northeast, and highest probabilities from the south-southeast. This probability distribution was not used for the following reason.

Figure 3-8 is reproduced from Jelesnianski (3) and depicts the maximum surge height for landfalling hurricanes with standard intensity moving over standard water depths ("standard" as defined by Jelesnianski) at various speeds and directions (a water-depth factor would reduce these surge heights for the southern New Jersey coast). We note in the figure that except at slowest speeds storms approaching from a direction of 70° relative to the coast produce the highest surges. Surge heights with this approach are about 15 percent greater than from the more common direction of approach of 120° relative to the coast, for a storm of the same intensity. However, as the track angle decreases from 120° to 70° relative to the coast (150° to 100° true direction) the storm intensity parameter should be diminished as the likelihood of encountering cold water or entraining dry air is increased. Lacking precise information, as an approximation we assume that these effects compensate and that surges computed from hurricanes moving from 120°, with the intensity distribution implied by figure 3-5, also represent surges from hurricanes on more northerly tracks. We assign 120° as the direction of approach for all landfalling hurricanes and base our tide-frequency analysis on this.

The full probability distribution of possible hurricane approach directions would include storms moving directly from the south (150° relative to coast). According to figure 3-8 surge heights are slightly lower from this direction than from 120° for a storm of the same speed and intensity. Substituting the direction of 120° for, say, 150°, may be a slightly conservative step.

Interdependence of hurricane parameter probabilities

Before proceeding further we need to decide whether the hurricane intensity, forward speed, and radius of maximum wind probabilities (figures 3-5, 3-6, and 3-7, respectively) in our study region are essentially independent or whether they are conditional probabilities. On the basis of earlier work by the Hydrometeorological Branch of the Weather Bureau (8), we decide that these three variables are sufficiently independent within the ranges used that they will be treated as such as an

16

approximation in this study. Figures 7 and 17 of (8) show plots of R vs. central pressure for Atlantic Coast and Gulf of Mexico hurricanes, respectively. There is little relationship of one variable to the other within the range of R's and central pressures applicable to Atlantic City and Long Beach Island. The authors of (8) treated R and central pressure as independent; in a table of Standard Project Hurricane characteristics (8-table 1) three categories of R--small, medium, and large--are listed independent of the CPI (central pressure index).

Similarly no dependence of forward speed on central pressure was found and Standard Project Hurricane forward speeds are listed in three categories--slow, moderate, and fast--again independent of CPI (8).

In extending tide frequency studies of this type to other areas the question of conditional probabilities of the basic hurricane climatological parameters should be kept open. The manner of handling such conditional probabilities is illustrated by some initial work at Atlantic City in the present study. Initially the project was designed to treat a frequency distribution of directions of approach of landfalling hurricanes to the coast. Separate frequency distributions of intensity and forward speed were provided for storms moving from the southeast quadrant and the northeast quadrant, with the latter storms less intense and moving more slowly. These conditional probabilities were not required when it was decided to represent all landfalling hurricanes by a single direction of approach for the reasons given on page 14.

Summary

For the purpose of calculating surge and total tide frequencies at Long Beach Island, N. J., future hurricanes are represented by the following specific storms with specific characteristics.

Storms moving parallel to coast. Maximum surge heights and surge time profiles are computed for 432 hurricanes. These are all combinations of 6 nominal distances from coast, 6 forward speeds, 6 intensities, and 2 R's. The frequency of each of these surge profiles is the product of the frequency in the right-hand column of table 3-2 and the probabilities of the other three variables.

$$F_R = F_d P_r P_i P_f \qquad (5)$$

where

F_R = frequency of a particular representative alongshore hurricane (per year)

F_d = frequency of storm tracks through distance interval (storms per year) (table 3-2)

P_r = radius of maximum winds probability

P_i = intensity probability (table 3-4)

P_f = forward speed probability (table 3-6)

Landfalling hurricanes. Maximum surge heights, surge time, and surge distance profiles are calculated for 108 hurricanes. These are all combinations of 6 intensities, 6 forward speeds, and 3 R's. The probability, P_s, of each of these representative hurricanes is given by

$$P_s = P_r P_i P_f \qquad (6)$$

By definition

$$\sum_{n=1}^{n=108} (P_s)_n = \sum_{r=1}^{r=3} P_r = \sum_{i=1}^{i=6} P_i = \sum_{f=1}^{f=6} P_f = 1.0 \qquad (7)$$

The surge frequency distribution at a coastal point from landfalling hurricanes is based on the surges for these 108 hurricanes, with an additional probability factor, namely, how close the storm passes to the point of interest, also taken into account. This is explained in the next chapter.

Table 3-1

FREQUENCY OF DISTANCE FROM COAST OF HURRICANES AND TROPICAL
STORMS CROSSING 40°N, 1871-1969. FROM (5)

Years	Distance from coast along 40th parallel (naut. mi.)				
	0-60	60-120	120-180	180-240	Total
1871-1885	1	5	4	1	11
1886-1899					
Hurricanes	3	3	2	3	11
Tropical storms	2	0	1	0	3
Total	5	3	3	3	14
1900-1969					
Hurricanes	2	4	7	4	17
Tropical storms	3	2	1	4	10
Total	5	6	8	8	27
Grand total	11	14	15	12	52

Table 3-2

FREQUENCIES OF HURRICANE TRACKS AT SEA OPPOSITE SOUTHERN NEW JERSEY

Distance interval, from coast		Nominal distance from coast	Storm track frequency	
Statute miles	Nautical miles	Statute miles	(Tracks per naut. mile per year*)	Tracks within distance interval, per year
0 to 10	0 to 8.7	0	.0021	.0183
10 to 20	8.7 to 17.4	15	.0022	.0191
20 to 30	17.4 to 26.1	25	.0023	.0200
30 to 40	26.1 to 34.7	35	.0023	.0200
40 to 60	34.7 to 52.1	50	.0024	.0418
60 to 120	52.1 to 104.2	90	.0026	.1355

*from figure 3-3.

Table 3-3

HURRICANE CENTRAL PRESSURES AT LATITUDE OF SOUTHERN NEW JERSEY
1900-1956

Storm Date	Central Pressure[#]		Latitude[#]	Adjusted to 39.5°N[ø]		Accum.[*] Probability
	(inches)	(mb)	(°N)	(inches)	(mb)	
Sept. 21, 1938	27.86	943.4	41.8	27.66	936.7	.072
Sept. 11, 1954	27.97	947.2	41.3	27.84	942.8	.215
Sept. 14, 1944	28.31	958.7	41.4	28.20	955.0	.357
Aug. 31, 1954	28.38	961.1	41.8	28.25	956.7	.500
Sept. 16, 1933	28.25	956.6	38.0	28.30	958.4	.643
Sept. 18, 1936	28.53	966.1	38.0	28.56	967.2	.785
Aug. 26, 1924	28.70	971.9	41.3	28.62	969.2	.928

[#]from (8), table A.

[ø] by figure 5a of (8)

[*]$P = \dfrac{M-0.5}{N}$; P = accum. prob., M = serial no. of observations, N = number of observations.

Table 3-4

ADOPTED CENTRAL PRESSURES AND PRESSURE DEPRESSIONS OF CLIMATOLOGICAL
HURRICANES.   SOUTHERN NEW JERSEY

Central Pressure* (mb)	Depression below ambient pressure (mb)	Probability
938.1	75.1	.10
948.3	64.9	.10
960.5	52.7	.20
973.1	40.1	.20
983.1	30.1	.20
991.6	21.6	.20
		1.00

*From figure 3-5.

Table 3-5

FORWARD SPEEDS. HURRICANES PASSING NEW JERSEY COAST AT SEA

Date	Speed (kt)	Latitude	Accum.* Probability	Source
Sept. 12, 1960	18	39.0	.063	(6)
Aug. 29, 1958	27	39.0	.187	(6)
Aug. 28, 1962	28	39.0	.313	(6)
Aug. 26, 1924	29	41.3	.438	(9)
Sept. 14, 1944	30	41.4	.562	(9)
Aug. 31, 1954	33	41.8	.687	(9)
Sept. 11, 1954	40	41.3	.813	(9)
Sept. 21, 1938	47	41.8	.937	(9)

*See table 3-3 for formula.

Table 3-6

ADOPTED FORWARD SPEED OF CLIMATOLOGICAL HURRICANES.
SOUTHERN NEW JERSEY

Along-shore hurricanes		Landfalling hurricanes		Probability
(knots*)	(mph)	(knots#)	(mph)	
16.3	18.7	13.0	15.0	.10
24.5	28.2	19.6	22.6	.20
28.9	33.2	23.1	26.6	.20
32.6	37.5	26.1	30.0	.20
39.4	45.3	31.5	36.2	.20
40.9	57.1	32.7	45.7	.10
				1.00

*From figure 3-6.

#80% of along-shore speed.

Table 3-7

RADIUS OF MAXIMUM WINDS, R, IN EAST COAST HURRICANES
NORTH OF 35°N. FROM (8)

Date	R (naut. mi.)	Latitude (°N)	Accum. Probability*
August 31, 1954	22	41.3	.055
Sept. 18, 1936	34	35.2,38.0	.167
Aug. 23, 1933	36	36.9	.278
Sept. 14, 1944	37	39.5	.390
Interpolated from:			
(Sept. 14, 1944)	(17)	(35.2)	
(Sept. 14, 1944)	(48)	(41.4)	
Sept. 3, 1913	41	35.8	.500
Sept. 16, 1933	42	35.2	.610
Sept. 19, 1955	50	35.0	.722
Sept. 21, 1938	50	41.8	.833
Aug. 26, 1924	56	39.5	.945
Interpolated from:			
(Aug. 25, 1924)	(34)	(35.2)	
(Aug. 26, 1924)	(66)	(41.3)	

*See table 3-3 for formula.

Table 3-8

DIRECTION OF MOTION OF HURRICANES AND TROPICAL STORMS ENTERING
DEL-MARVA AND NEW JERSEY COASTS

Date	Direction (relative to north)	Direction (relative to coast at Long Beach Island, N.J.)
Oct. 23, 1893	150°	120°
Sept. 16, 1903	150°	120°
Oct. 1, 1943	140°	110°
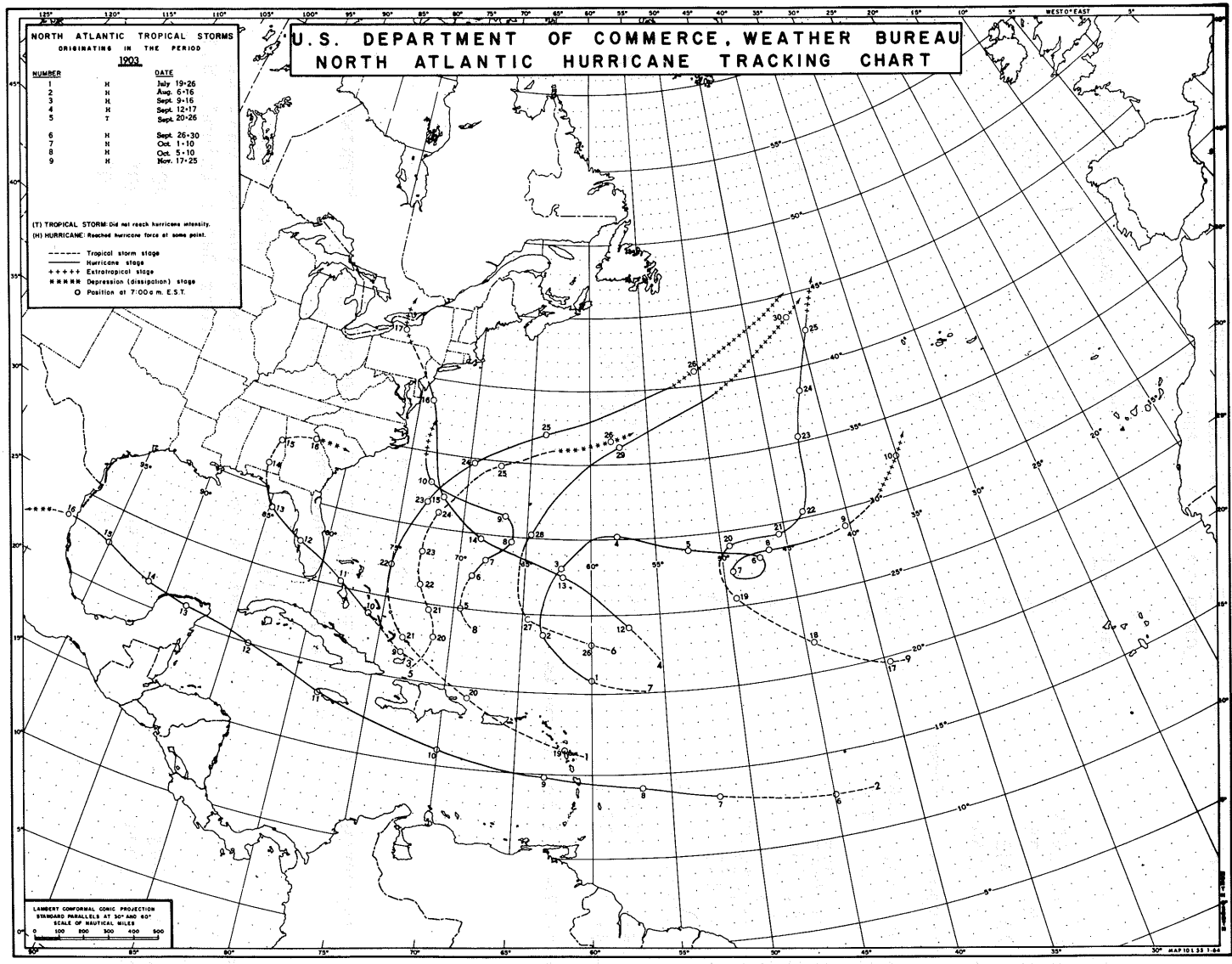
Figure 3-1. Hurricane track chart for 1903 showing hurricane entering New Jersey coast. From (5).
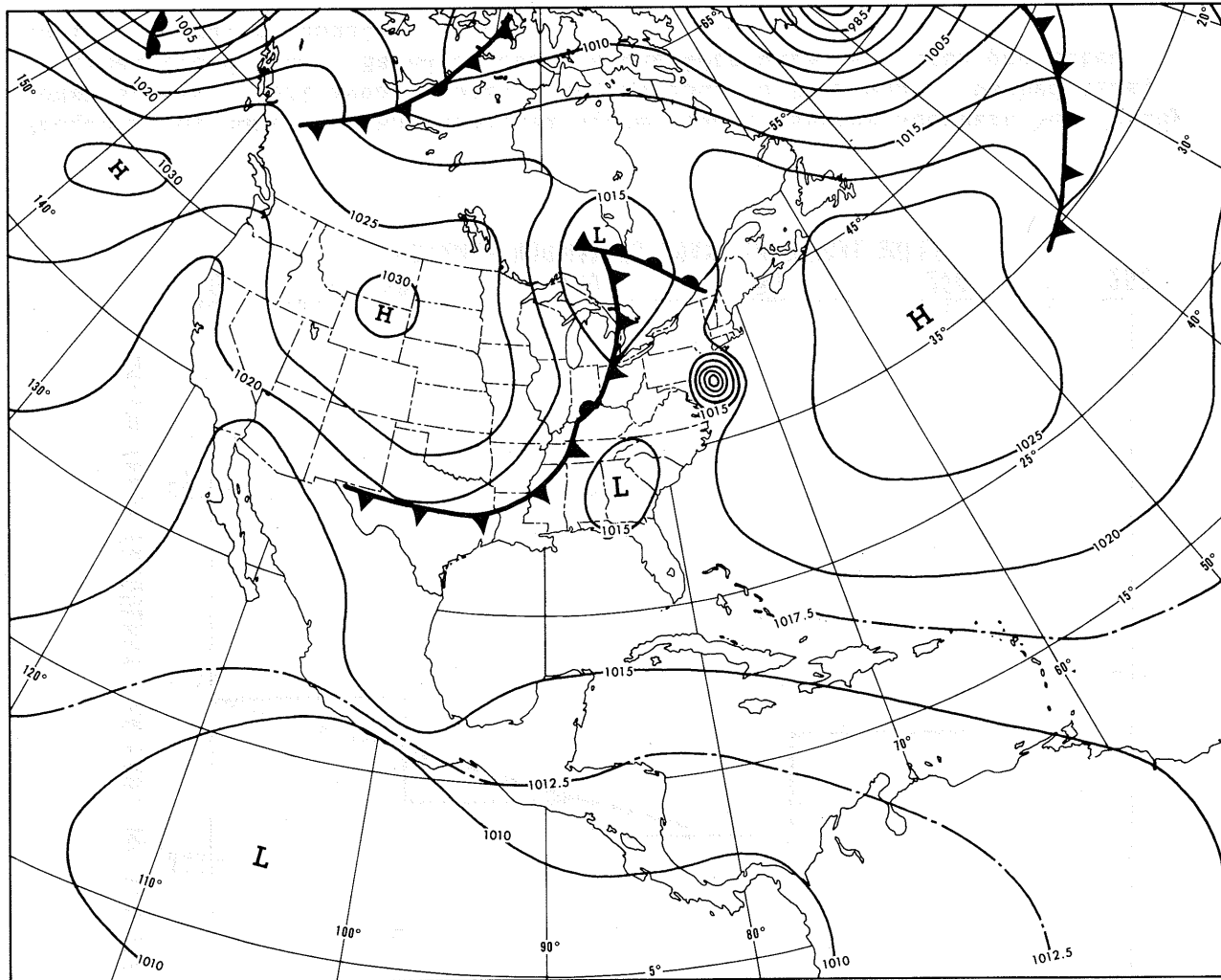
Figure 3-2.   Sea level weather chart depicting hurricane entering New Jersey coast.
1300 GCT Sept. 16, 1903.
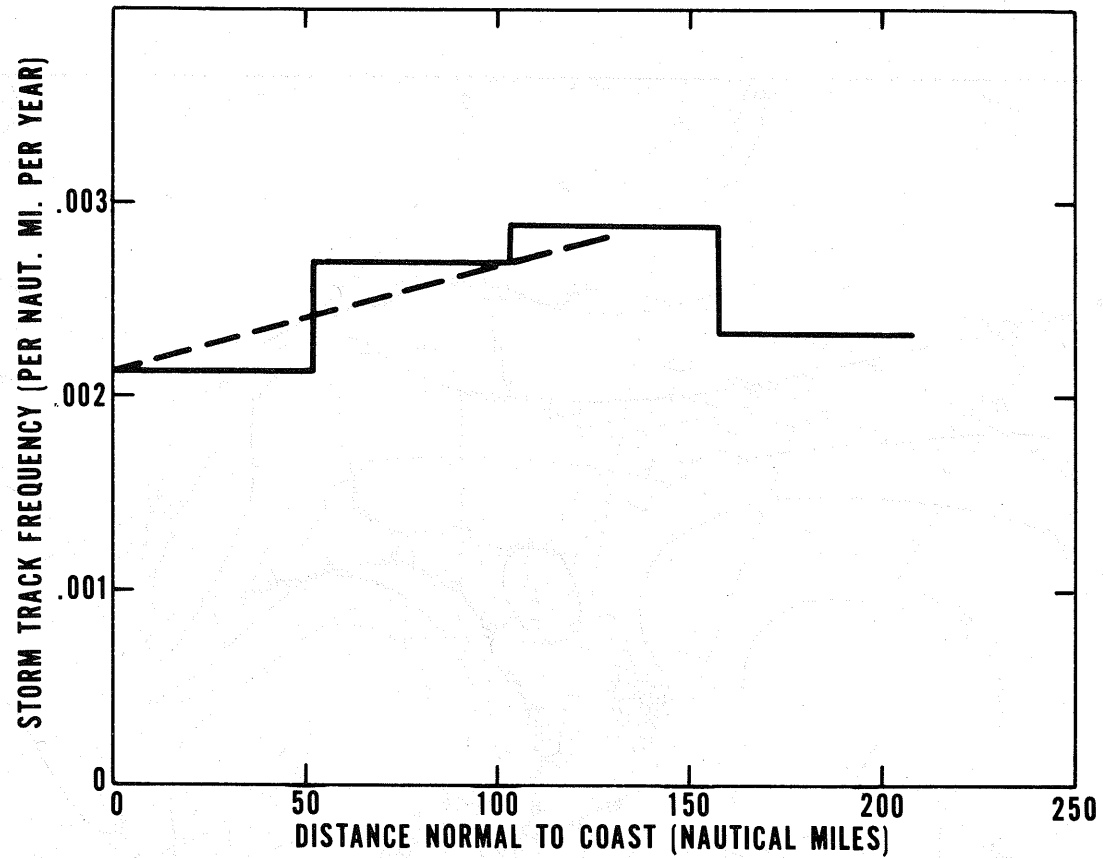
Figure 3-3. Frequency of hurricane and tropical storm tracks passing southern New Jersey coast at sea. 1871-1968. Solid line, as counted from maps. Dashed line, smoothed trend line. Based on count along 40th parallel, then projected on line normal to coast.
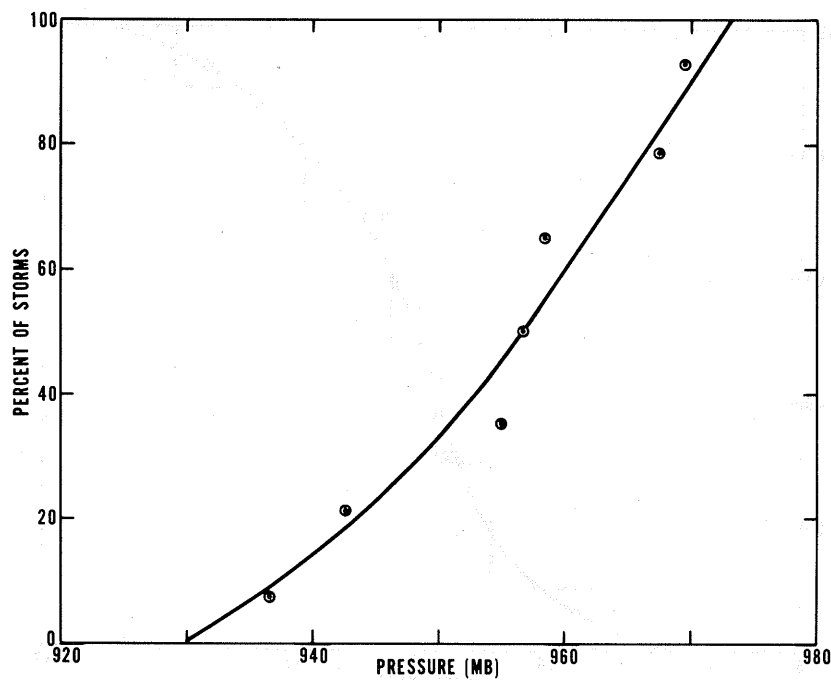
Figure 3-4. Frequency distribution of hurricane central pressures
below 980 mb at 39.5°N. Data from table 3-3.
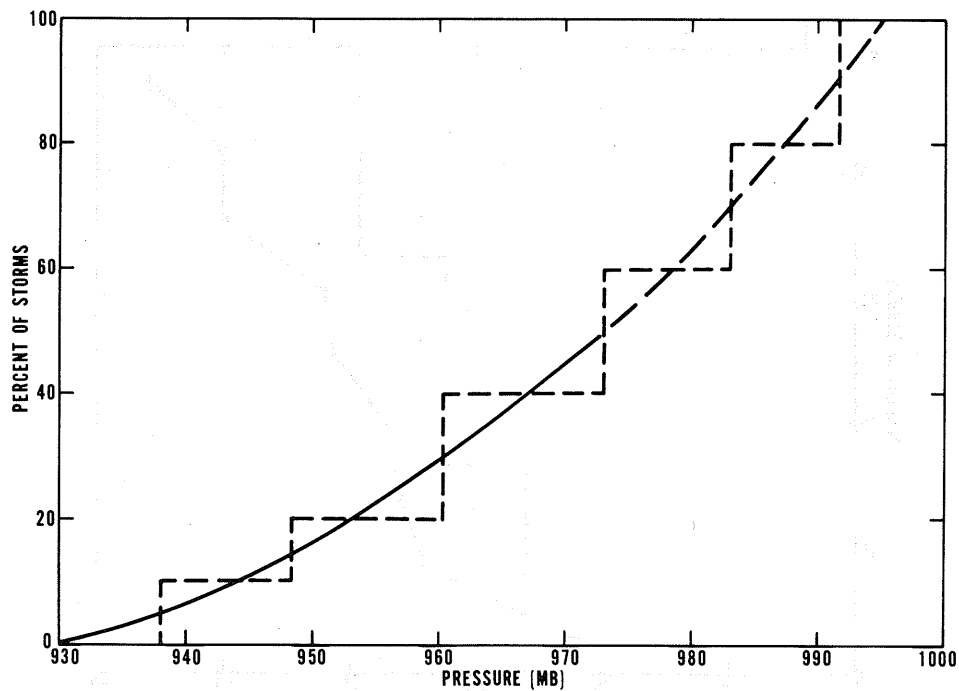
Figure 3-5. Frequency distribution of hurricane and tropical storm
central pressures at 39.5°N. Solid curve reduced from
figure 3-4. Dashed portion, extension for tropical
storms. Dotted curve, division into class intervals
for tide analysis.
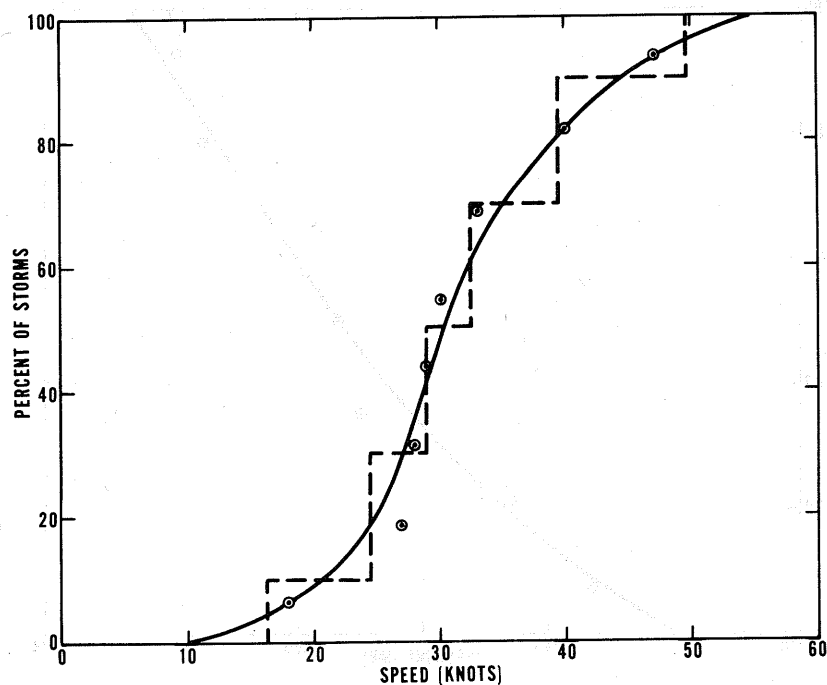
Figure 3-6.   Frequency distribution of forward speed of hurricane passing
New Jersey coast at sea.   Dotted line shows division into
class intervals for tide analysis.
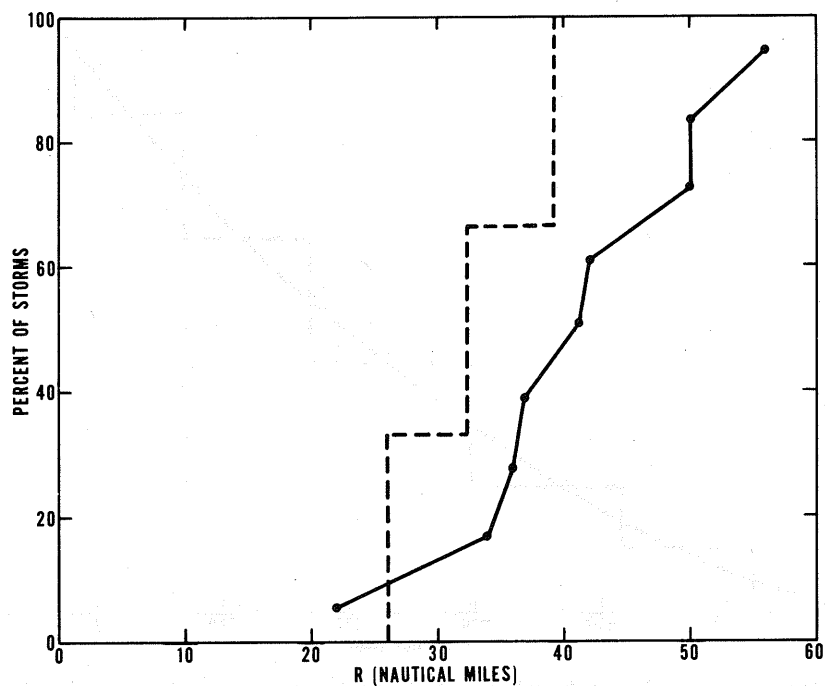
Figure 3-7.   Frequency distribution of radius of maximum winds in hurricanes.
Solid curve, east coast hurricanes from 35° to 42°N, from (9).
Dashed curve, assumed frequency distribution for New Jersey
coast; see text.
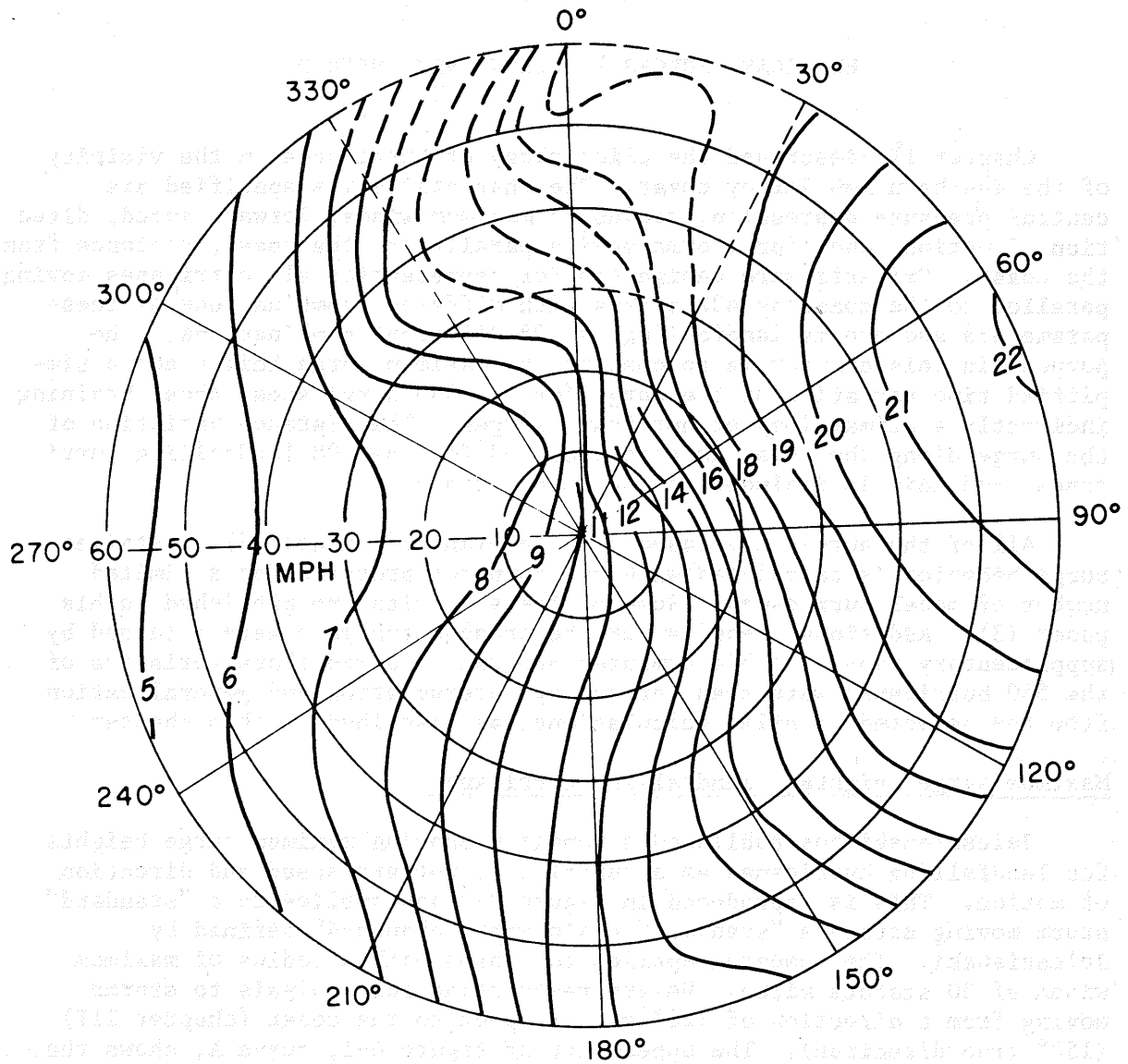
Figure 3-8. Contours of peak coastal surge heights (ft), for "standard" hurricane crossing "standard" basin. Radii storm speed in mph, rays storm direction relative to coast, which runs along 0-180° line with 90° on seaward side. R=30 miles. From (3).

Chapter IV

HURRICANE SURGES - JELESNIANSKI METHOD

Chapter III described the climatology of hurricanes in the vicinity
of the southern New Jersey coast. The characteristics specified are
central pressure depression, radius of maximum winds, forward speed, direc-
tion of motion, and, for storms moving parallel to the coast, distance from
the coast. Criteria were designated for representing all hurricanes moving
parallel to the coast by 432 storms with different combinations of these
parameters and storms landfalling by 108 different combinations. The
purpose in this chapter is to compute the maximum surge height and a sim-
plified time variation of the surge for the 540 hurricanes, thus obtaining
indirectly a climatology of hurricane surges. The distance variation of
the surge along the coast is also required for the 108 landfalling hurri-
canes, and this is included in the computations.

All of the surges are based on Jelesnianski's model (3). Detailed
surge behavior is calculated with his computer programs for a limited
number of model hurricanes. Some of these results are published in his
paper (3). Additional results for the present analysis were obtained by
supplementary runs with his computer programs. Surge characteristics of
the 540 hurricanes were then derived by interpolation and generalization
from the selected detailed calculations, as described in this chapter.

Maximum surge heights - landfalling hurricanes

Jelesnianski has published a nomogram showing maximum surge heights
for landfalling hurricanes as a function of forward speed and direction
of motion. This is reproduced in figure 3-8 and applies to a "standard"
storm moving across a "standard" basin with "standard" defined by
Jelesnianski. The nomogram applies to storms with a radius of maximum
winds of 30 statute miles. We are restricting our analysis to storms
moving from a direction of 120° with respect to the coast (chapter III)
(150° true direction). The upper part of figure 4-1, curve A, shows the
maximum surge height as a function of forward speed along this direction
at this R, scaled from figure 3-8. Curve B is reduced to 81% of curve A.
This is Jelesnianski's adjustment from "standard basin" to the sea bottom
profile at Atlantic City (his figure 17).

The lower part of the figure shows a similar maximum surge vs. storm
speed variation along the 120° direction for model hurricanes with R of
45 statute miles. This is based on a limited number of computations at
this direction and adjacent directions with the basic program for land-
falling storms. The supporting computed S_x's are indicated on the diagram.
The 81% reduction to Atlantic City is also shown.

Adjustment of maximum surge, S_x, for storm intensity

The maximum surge in a hurricane varies approximately in proportion
to the pressure depression at the center, with other storm characteristics
held constant. The chain of physical interrelationships is: maximum storm
surge approximately proportional to stress of wind on water surface, stress
approximately proportional to square of windspeed, square of windspeed
approximately proportional to pressure depression. We follow Jelesnianski
in basing surges on standard storms with prescribed pressure fields and
assume that

$$\frac{S}{S_s} = \frac{D}{D_s} \tag{8}$$

where D is the depression of the central pressure below peripheral pressure
and the subscript s refers to "standard." This conversion applies not only
at the point and time of maximum surge but throughout the storm.

In Jelesnianski's treatment, D_s for R = 30 statute miles is 68 mb (his
figure 2) and for R = 45 miles is 82 mb. We use these values and interpo-
late for R = 37.5 miles. (One may question why D_s is dependent on R. This
is because all "standard" storms have the same windspeed at R. Qualita-
tively it may be noted that a greater total pressure depression is required
at the center to accelerate inflowing air to, say, 100 mph at R = 45 than
to accomplish this at R = 30.)

Probability distribution of maximum surge, S_x, in landfalling hurricanes

Hurricanes landfalling on the southern New Jersey coast have been
represented by 108 storms (6 speeds, 6 intensities, 3 R's). The probabil-
ity distribution of the 108 S_x's is shown in figure 4-2. The S_x's are
scaled from figure 4-1 and adjusted for intensity by equation (8) using the
pressure depressions from table 3-4. Interpreting these probabilities as
frequencies at a coastal point requires taking into account the width along
the coast of the surge profile, discussed later in this chapter.

Time variation of surge - landfalling hurricanes

The time variation of the surge at the coast is required for random
combination at various time phase displacements with the astronomical tide
as described in chapter VI. Figure 4-3, curve A, shows an example of the
computed surge variation with time at the coast from a hurricane moving
along the 120° direction with R = 30 and forward speed of 20 mph. Two
normalizing steps are also illustrated on the figure.

The surge falls more rapidly than it rises in figure 4-3. (The
asymmetry is opposite at the complementary angle of approach of 60°.) For

combining statistically with the astronomical tide the asymmetry of the surge is of no consequence. The effective information required is the time that the surge remains above a given height.

Therefore, the first normalizing step is to replace the asymmetrical surge time profile by a symmetrical profile with equal area under the curve and equal duration at each surge height, curve B, figure 4-3.

The second normalizing step is to approximate the symmetrical surge-time profile by a Gaussian (normal probability) curve,

$$S = S_x \, e^{-kt^2} \tag{9}$$

Here S is the surge at time t and S_x maximum S at t = 0. Curve C of figure 4-3 illustrates this. Curve C is fit to curve B at $S = S_x$, t = 0 and at $S = (2/3)S_x$. For this fit, equation (9) becomes

$$S = S_x \, e^{-.40547(2t/t_{2/3})^2} \tag{10}$$

The scaling parameter, $t_{2/3}$, is the total time, in hours, that S equals or exceeds two thirds of S_x. This is 2.6 hours in figure 4-3.

All surge-time profiles were computed from equation (10). Thus, the designation of the time variation of the surge during a particular model storm is reduced to specifying the two parameters S_x and $t_{2/3}$. It is assumed that the relative time variation of the surge is the same at all coastal points in a particular storm.

S_x has been specified in figure 4-1.

The $t_{2/3}$ factor for hurricanes moving from a single direction is a function of storm speed and R but it is nearly independent of storm intensity and is assumed so. Values of $t_{2/3}$ for R = 30 and R = 45 statute miles for storms moving along the 120° direction and adjacent directions are shown in figure 4-4. These figures are constructed to $t_{2/3}$ factors scaled from plotted surge time profiles at the point on the coast of maximum surge, from runs with Jelesnianski's program.

Distance variation of surge - landfalling hurricanes

The total storm surge experience for any one coastal point derives not only from storms passing immediately over that point but also from storms entering the coast at some distance on either side. This is taken

into account by delineating the along-coast variation of the maximum surge height in each of the 108 landfalling storms. Integrating the effects of storms at varying distances is a statistical procedure explained in chapter VI. The requirement here is to define the along-coast variation of the maximum surge in a concise way.

We make here a distinction from nomograms in Jelesnianski's original paper (3). Certain nomograms define the variation along the coast of the surge height at the time of occurrence of the absolute maximum surge height at the coast. The requirement here is for the profile along the coast of the maximum surge experienced locally in the storm, at each point, not necessarily coincident in time.

The distance variation of the maximum surge is treated in the same manner as the time variation, by imposing symmetry and fitting a Gaussian curve. An example of this fit is shown in figure 4-5. The equation of curve C is

$$S_{1x} = S_x \, e^{-.40547(2d/d_{2/3})^2} \tag{11}$$

Here S_{1x} is the local maximum surge at distance d, S_x the absolute maximum surge at d = 0, and $d_{2/3}$ the total length over which $S_{1x} > (2/3)S_x$.

As before, we develop nomograms depicting $d_{2/3}$ as a function of R and storm speed from individual computer runs with Jelesnianski's program. These are shown in figure 4-6 for the 120° direction. $d_{2/3}$ is treated as independent of storm intensity.

Equation (11) inverts to the form

$$d = \frac{d_{2/3}}{2\sqrt{.40547}} \sqrt{\log(S_x/S_{1x})} = \frac{1.5704 d_{2/3}}{2} \sqrt{\log(S_x/S_{1x})} \tag{12}$$

Calculated frequency distribution of local maximum surge, S_{1x}, landfalling hurricanes

The calculated frequency, F_{A-B}, with which a southern New Jersey coastal point experiences a surge in the range between any two heights S_A and S_B from landfalling hurricanes is given by

$$F_{A-B} = F_h \sum_{n=1}^{n=108} (P_s)_n (d_A - d_B)_n \tag{13}$$

where

F_h = frequency of storms (tracks per mile of coast per year).

d_B, d_A = distance over which $S_{1x} > S_B$ and $S_{1x} > S_A$ in a storm.

P_s = probability of each of 108 representative hurricanes, see chapter III.

From (12),

$$d_B = 1.5704 d_{2/3} \sqrt{\log(S_x/S_B)}$$

$$d_A = 1.5704 d_{2/3} \sqrt{\log(S_x/S_A)} \tag{14}$$

The factor 2 in (12) disappears because d refers to the distance from S_x to one side of the profile while d_B and d_A are total distances across the profile.

Next

$$d_B - d_A = 1.5704 d_{2/3} \left(\sqrt{\log(S_x/S_B)} - \sqrt{\log(S_x/S_A)} \right) \tag{15}$$

Combining (15) and (13)

$$F_{A-B} = 1.5704 F_h \sum_{n=1}^{n=108} (d_{2/3})_n (P_s)_n \left(\sqrt{\log S_x/S_B} - \sqrt{\log(S_x/S_A)} \right),$$

$$S_A < S_B < S_x \tag{16}$$

Solution of (16) for various surge height intervals yields the derived frequency distribution of surges at coastal points from landfalling hurricanes. These frequencies are listed in table 4-3 and graphed in figure 4-7.

Some lack of smoothness in the progression of computed F_{A-B}'s can be noted. We suspect lack of smoothness in first and second differences between input $d_{2/3}$ values contributes to this but we have not tested this.

Observed S_{1x}, landfalling hurricanes

Harris (16) has made an extensive compilation of hurricane surges on the United States coast by subtracting the predicted tide from the observed tide. Further details on his methods are included in the next chapter. Two landfalling hurricanes produced surges of 2.9 feet at Atlantic City, table 4-1. Additional analyses in the present study replicated Harris' method for all likely hurricane candidates since establishment of the Atlantic City tide gage in 1912. No other surges from landfalling hurricanes in excess of 2.5 feet at Atlantic City were found. (This is not surprising in view of the limited landfalling hurricane experience--see chapter III.) Construing table 4-1 as showing a surge of 2.9 feet twice in 58 years two points may be plotted on figure 4-7 for comparison with the calculated surge frequency.

Maximum surge height - alongshore hurricanes

Jelesnianski's paper contains a nomogram depicting maximum surge height for alongshore hurricanes of "standard" intensity as a function of storm speed up to 40 mph and distance from coast (figure 16 of (3)). R = 30 statute miles in this diagram. We have replotted the original data from Jelesnianski's computer outputs on which this nomogram is based in our figure 4-8 and added data for R = 45 and for forward speed of 50 mph. S_x as a function of forward speed, R, and distance from coast is scaled from this figure for hurricanes of "standard" intensity and adjusted to a particular intensity by equation (8).

Calculated frequency distribution of surges from alongshore hurricanes

In concept, an alongshore hurricane sweeps forward at constant velocity parallel to the shore and the surge waves sweep along the coast unmodified except for forward translation. Thus, unlike the landfalling hurricanes, all coastal points within a given reach have the same surge experience in a particular storm. That is:

$$S_{1x} \equiv S_x \qquad (17)$$

The frequency, F_s, with which of a surge height, S, is equaled or exceeded at a coastal point from alongshore hurricanes is simply the sum of the frequencies of representative hurricanes with $S_x \gtrless S$:

$$F_s = \sum_{n=1}^{n=432} F_R, \ (S_x)_R \gtrless S \qquad (18)$$

The 432 F_R's were each calculated from the corresponding climatological probabilities by equation (5).

Seventy-two S_x's were scaled from figure 4-8 for the representative 6 forward speeds, 2 R's and 6 distances from coast, at "standard" intensity. Adjusting to the 6 representative intensities (equation (8)) yielded the requisite 432 representative S_x's.

Applying equation (18) in this manner to selected surge heights, S, yields the computed surge frequency for alongshore hurricanes, table 4-4 and figure 4-9.

Observed S_x, alongshore hurricanes

Harris (16) indicates surges exceeding 2.5 feet in five alongshore hurricanes at Atlantic City, table 4-2. The September 1938 storm destroyed the gage at Atlantic City; the Sandy Hook, N.J., surge has been substituted for Atlantic City in the table. A comparison of surges at Atlantic City and Sandy Hook in fifteen hurricanes observed at both gages showed approximately the same mean surge height.

Search of additional hurricanes since 1912 revealed no additional surges exceeding 2.5 feet (with mean monthly tide as reference sea level-- see chapter V). Thus the five storms in table 4-2 may be construed as representing 58 years, and are plotted as x's on figure 4-9. Part of the difference between the observed and calculated surge frequencies is due to the fact that higher frequencies have been assigned as climatologically representative to intense hurricanes close inshore than have been observed during the 58 years.

Time variation of surge - alongshore hurricanes

For statistical combination of the surge-time profile with astronomical tide profiles at various time displacements the surge, as before, is regarded as a single wave with the shape of the Gaussian curve, defined by the two parameters S_x and $t_{2/3}$. The $t_{2/3}$ parameter is a function of R, forward speed, and distance of storm center from the coast, but is treated as independent of storm intensity. The $t_{2/3}$ parameter abstracted from individual computer runs is plotted in figure 4-10 and the appropriate curves constructed to permit scaling off of this parameter at the requisite speeds, R, and distance from coast.

Jelesnianski's working method is to start with an undisturbed sea and atmosphere at an initial time, then allow a hurricane to grow at a prescribed arbitrary rate. The $t_{2/3}$ factors for zero forward speed in the figure depend on this growth rate and have little real significance. Jelesnianski's discussion of his figure 4 in (3) applies. The other $t_{2/3}$ values are from times after storm has reached maturity and initial oscillations have diminished.

Table 4-1

MAXIMUM SURGES AT ATLANTIC CITY, N. J., FROM HURRICANES ENTERING THE
COAST 1912-1969

Date	Surge* (ft)	Distance, point of landfall to Atlantic City (naut. mi.)
August 23, 1933	2.9	240
October 15, 1954	2.9	150

*from Harris (16)

Table 4-2

MAXIMUM SURGES FROM HURRICANES PASSING ATLANTIC CITY, N. J., AT SEA
1912-1969

Date	Surge* (ft)	Rank	Distance, track to coast (naut. mi.)
September 14, 1944	5.1	1	30
September 12, 1960	4.0	2	45
September 21, 1938	3.2#	3	90
September 18, 1936	3.0	4	45
September 27, 1956	2.6	5	130

*from Harris (16)
#at Sandy Hook, N. J.

Table 4-3

COMPUTED SURGE FREQUENCIES FROM LANDFALLING HURRICANES, ATLANTIC CITY
AND LONG BEACH ISLAND

Range (ft) $S_A - S_B$	Frequency (per year) F_{A-B}	Accum. Frequency (per year) ΣF_{A-B}	Mean Return Period (years) $1/\Sigma F_{A-B}$	Mean Surge Height for Interval (ft) S_M
16.0-16.5	.00001	.00001	132,000	16.25
15.5-16.0	.00003	.00004	25,900	15.75
15.0-15.5	.00003	.00007	14,400	15.25
14.5-15.0	.00006	.00013	7,400	14.75
14.0-14.5	.00008	.00021	4,730	14.25
13.5-14.0	.00010	.00031	3,200	13.75
13.0-13.5	.00016	.00047	2,100	13.25
12.5-13.0	.00017	.00064	1,560	12.75
12.0-12.5	.00019	.00083	1,200	12.25
11.5-12.0	.00021	.00104	957	11.75
11.0-11.5	.00027	.00131	762	11.25
10.5-11.0	.00035	.00167	600	10.75
10.0-10.5	.00042	.00209	479	10.25
9.5-10.0	.00050	.00258	387	9.75
9.0-9.5	.00058	.00316	316	9.25
8.5-9.0	.00060	.00377	265	8.75
8.0-8.5	.00068	.00445	225	8.25
7.0-8.0	.0016	.0061	164	7.5
6.0-7.0	.0021	.0082	122	6.5
5.0-6.0	.0027	.0108	92	5.5
4.0-5.0	.0033	.0141	71	4.5
3.0-4.0	.0045	.0187	54	3.5
2.0-3.0	.0054	.0240	42	2.5

Table 4-4

COMPUTED SURGE FREQUENCIES FOR ALONGSHORE HURRICANES,
ATLANTIC CITY AND LONG BEACH ISLAND

Surge (ft) S_x	Accum. Frequency (per year) F_S	Mean Return Period (years) $1/F_S$
10.7	.000183	5,460
10.5	.000457	2,190
10.4	.000640	1,565
10.3	.00101	994
10.1	.00119	841
9.5	.00240	416
9.0	.00419	239
8.5	.00608	164
8.0	.00870	115
7.5	.0106	95
7.0	.0137	73
6.5	.0196	51
6.0	.0232	43
5.5	.0294	34
5.0	.0374	27
4.5	.0425	24
4.0	.0538	19
3.5	.0636	16
3.0	.0769	13
2.5	.0922	11
2.0	.111	9
1.5	.138	7
1.0	.182	5
0.5	.241	4
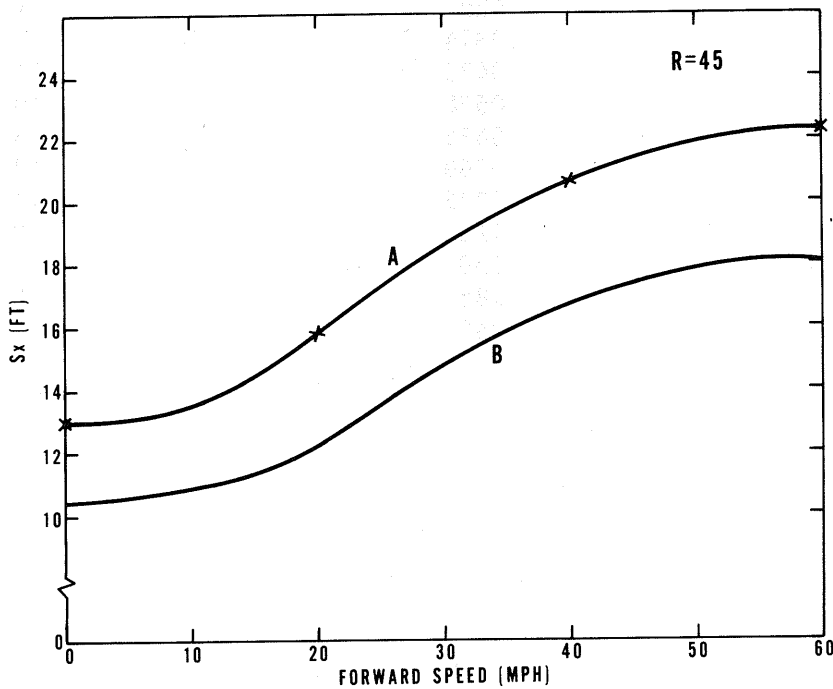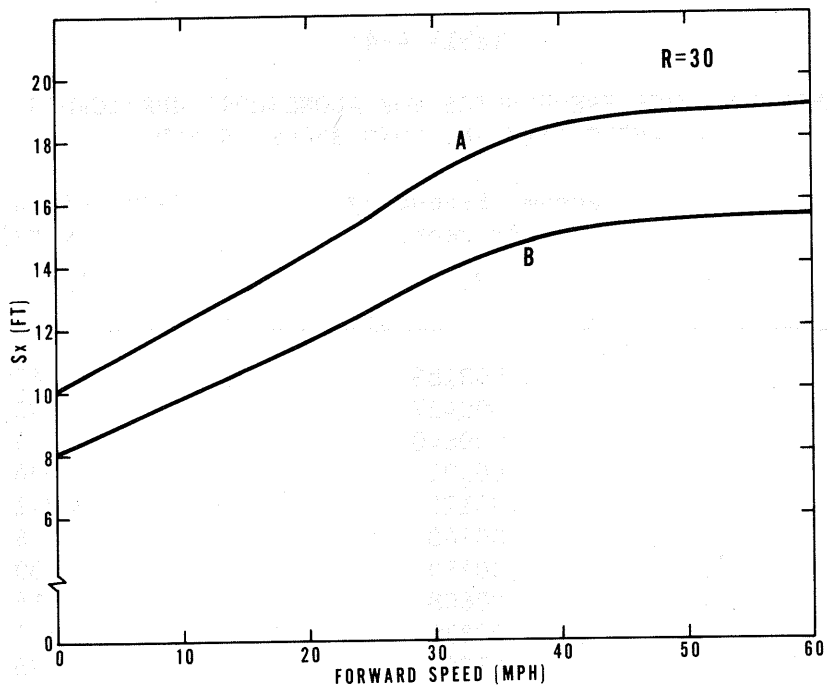
Figure 4-1. Maximum surge at coast (S_x) from landfalling hurricanes after Jelesnianski (3). Direction=120°. A - "Standard" basin. B - Atlantic City (81% of A). Curve A for R=30 scaled from figure 3-8, for R=45 from similar data not shown.
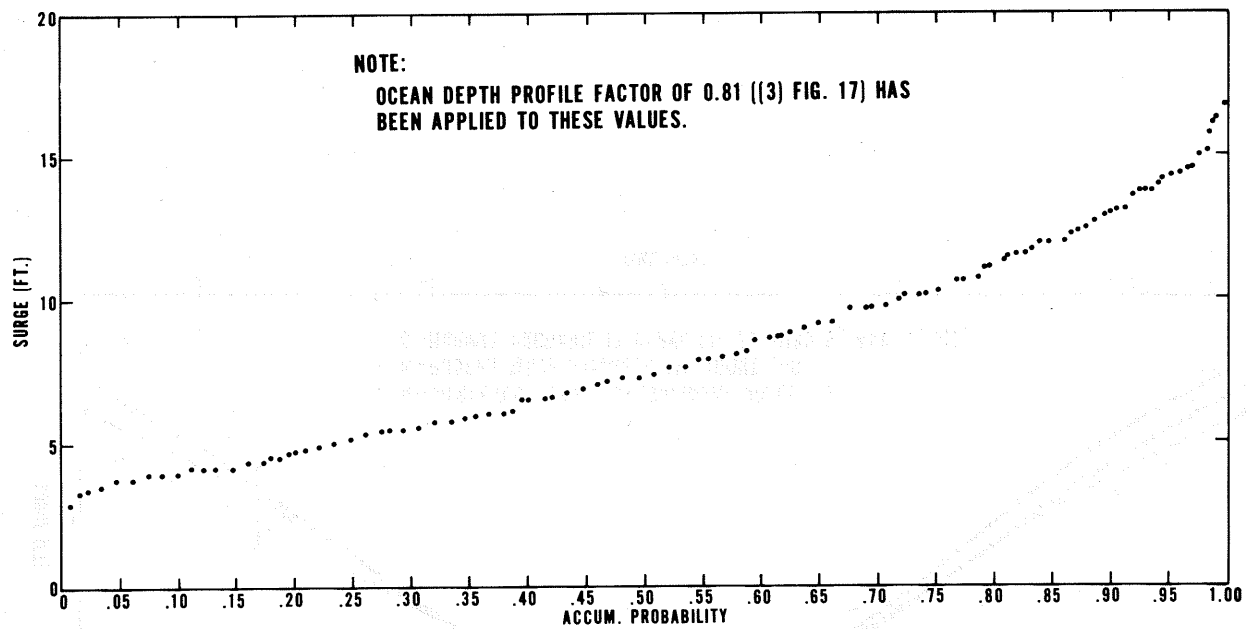
Figure 4-2. Probability distribution of maximum surge height (S_X) in 108 climatological landfalling hurricanes on southern New Jersey coast.
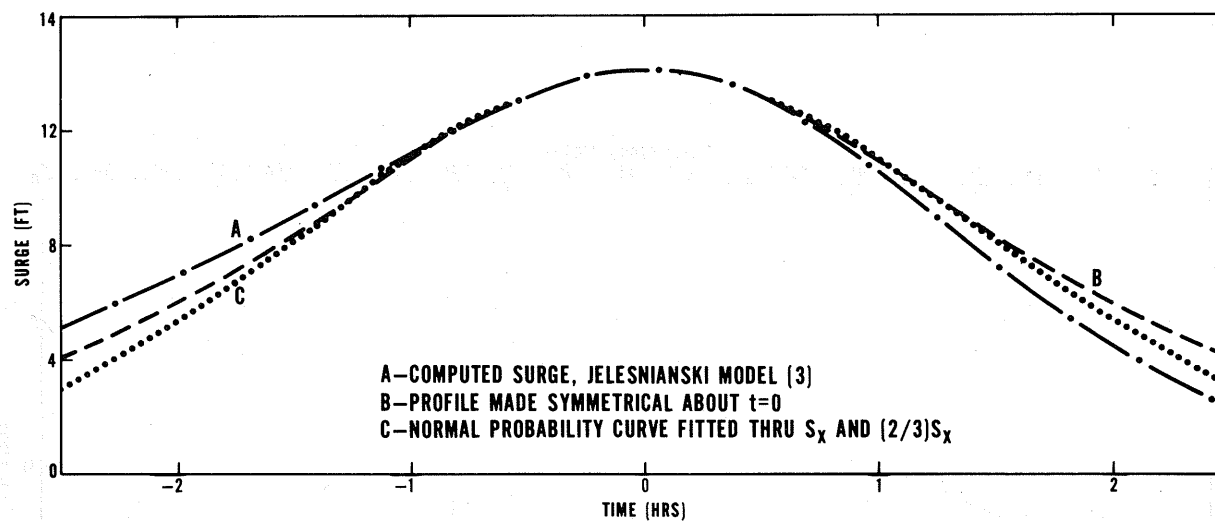
Figure 4-3. Surge-time profiles for landfalling hurricane, standard storm, standard basin. Direction 120° to coast, R=30 mi., speed 20 mph.
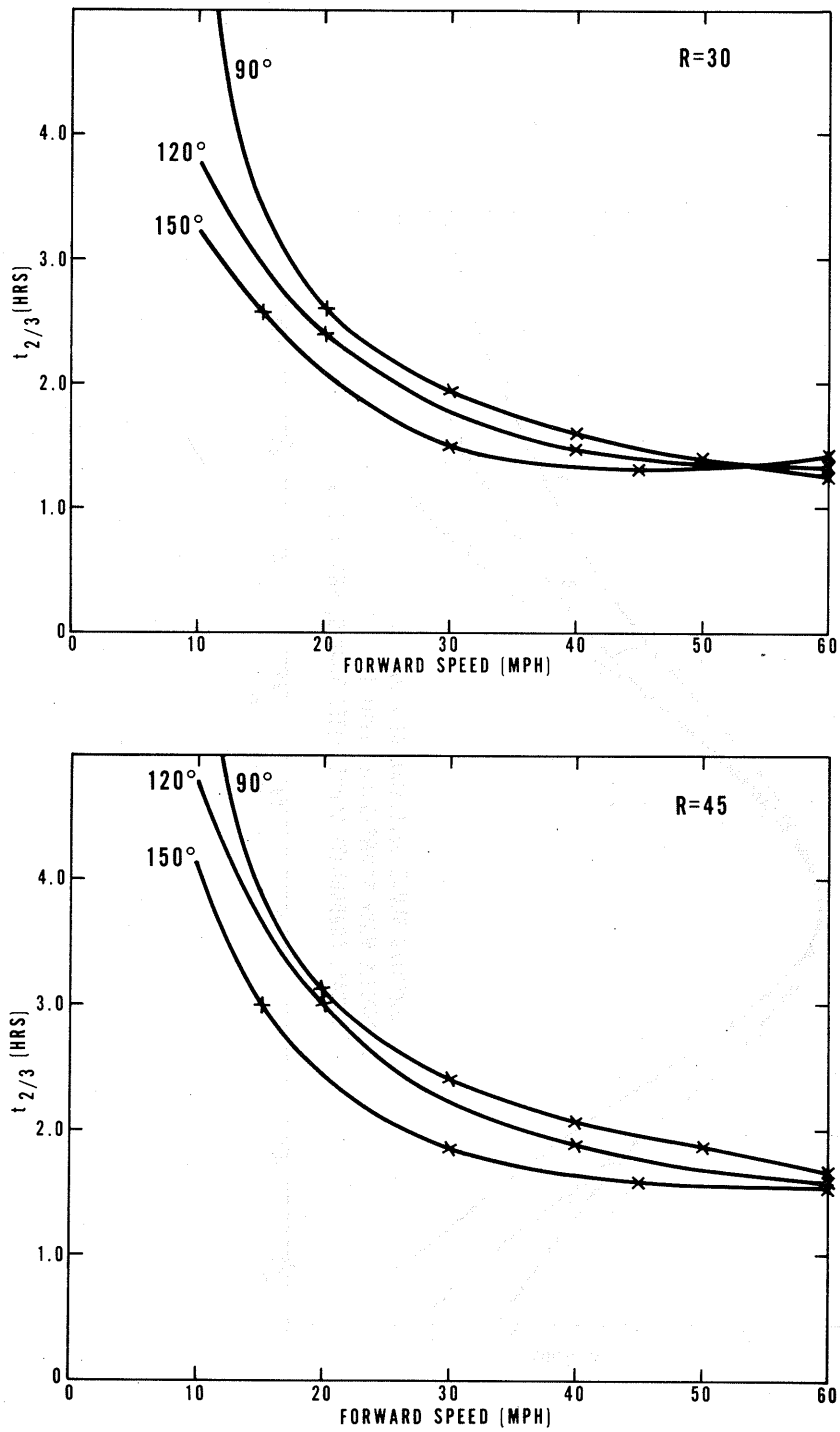
Figure 4-4. Time scale factor ($t_{2/3}$) for surge profiles at coast. Land-falling hurricanes. Directions of storm motion relative to coast as shown.
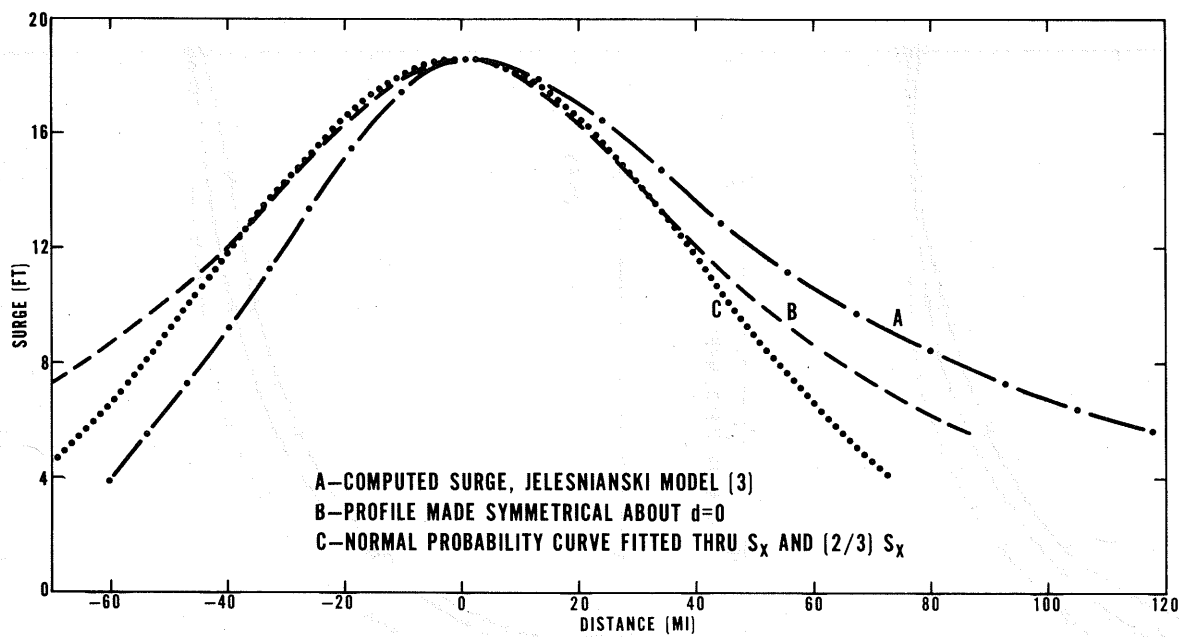
Figure 4-5. Profile of maximum surge height along coast. Standard storm, standard basin. Direction 90° to coast. R=45 mi., speed 20 mph.
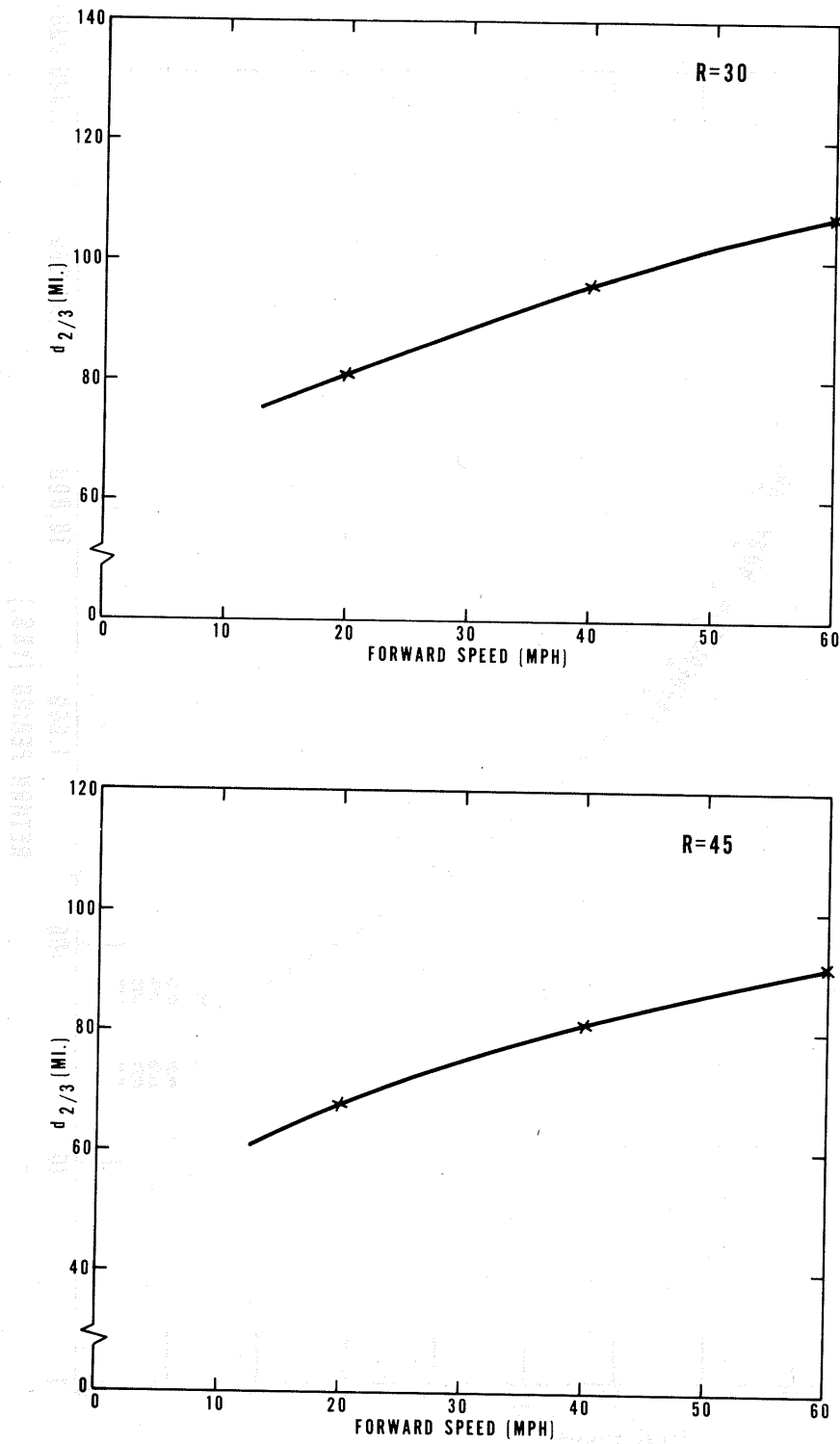
Figure 4-6. Distance scale factor ($d_{2/3}$) for profile at coast of local maximum surge (S_{1x}). Landfalling hurricanes.
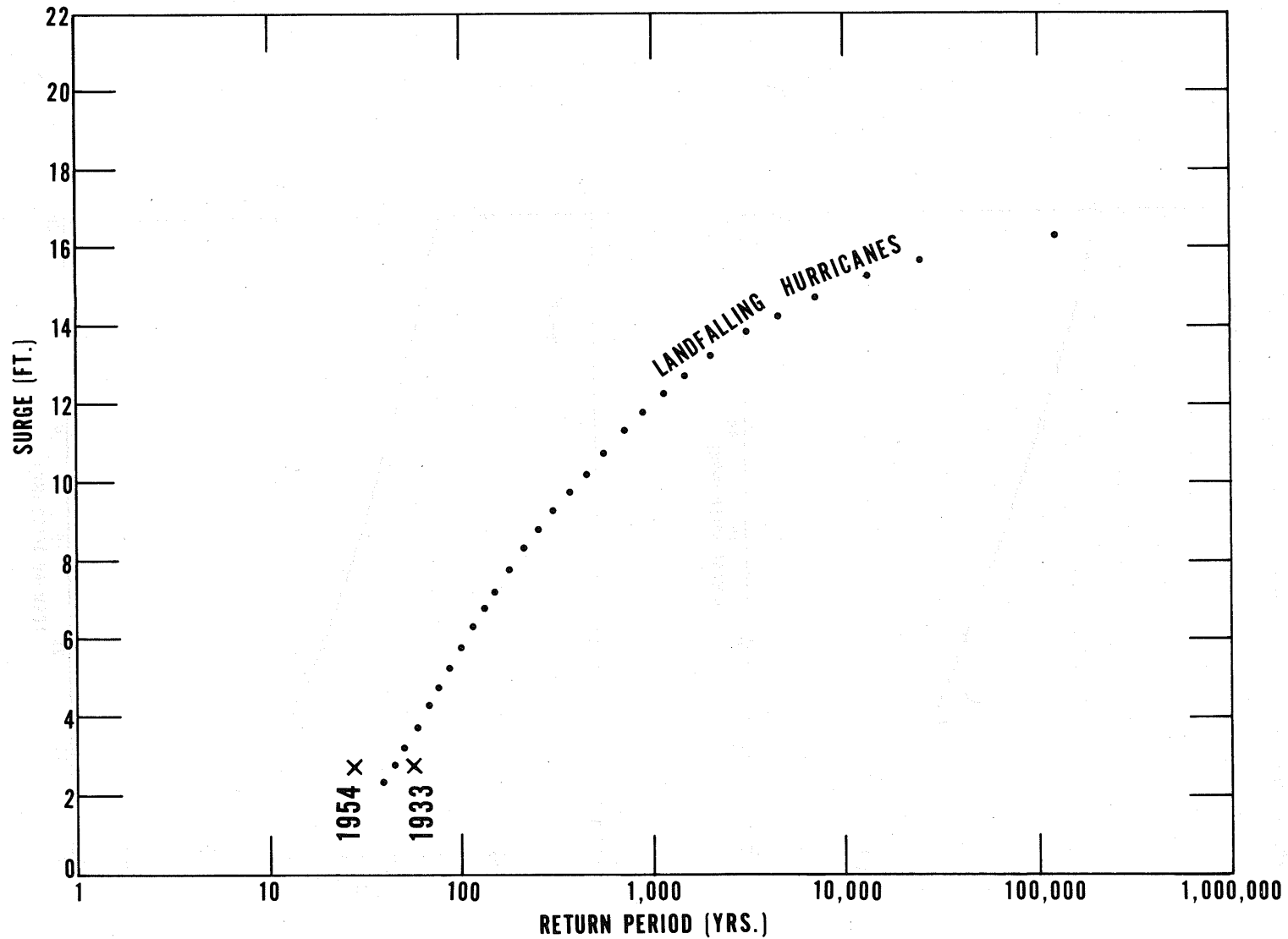
Figure 4-7. Computed frequency distribution of local maximum surge heights, S_{1x}, southern New Jersey coast, from landfalling hurricanes. X – observed surges at Atlantic City (table 4-1).
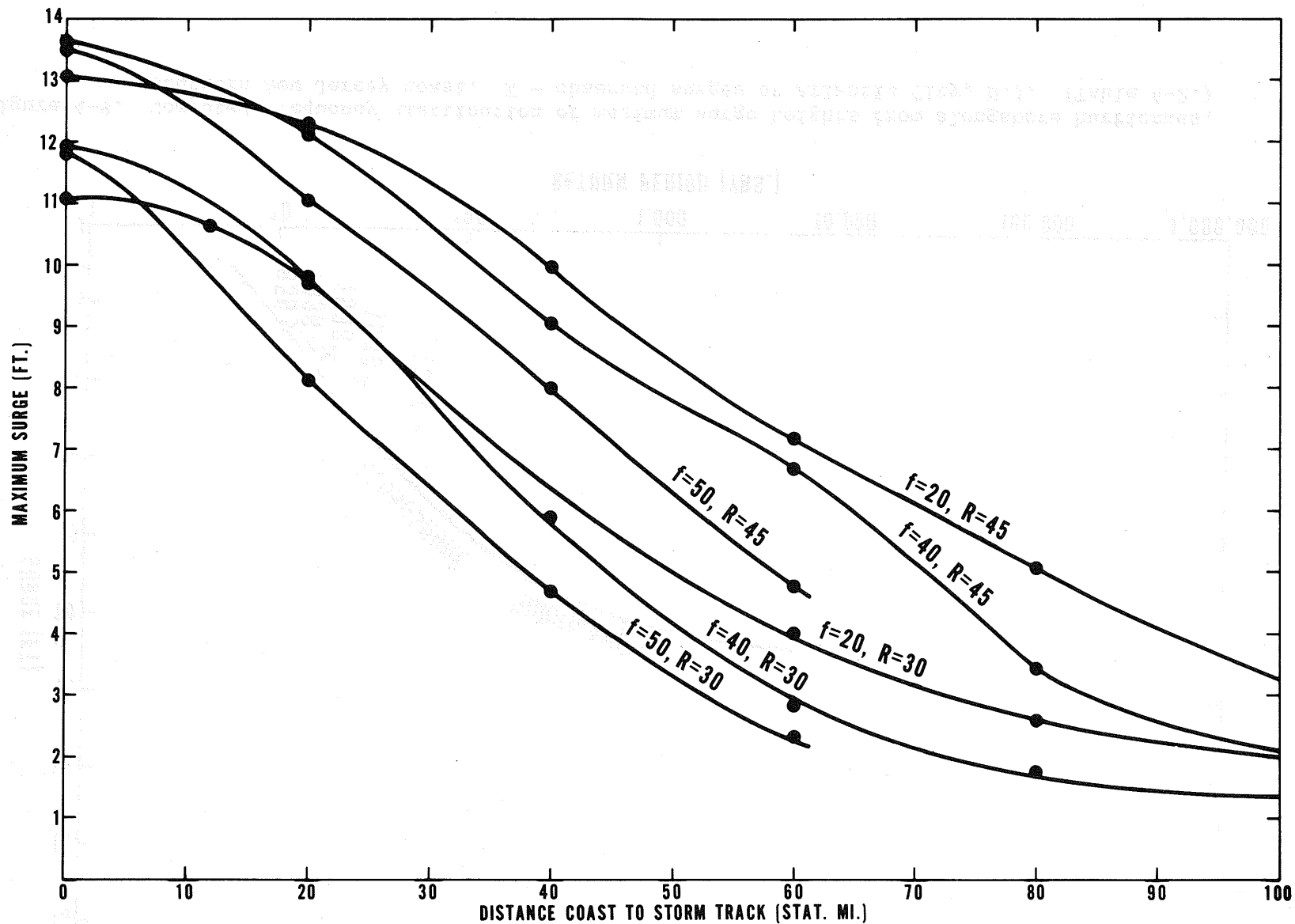
Figure 4-8. Maximum surge on coast from alongshore hurricanes. f = forward speed (mph); R = radius of maximum winds (stat. mi.). R = 30, curves from (3), figure 16.
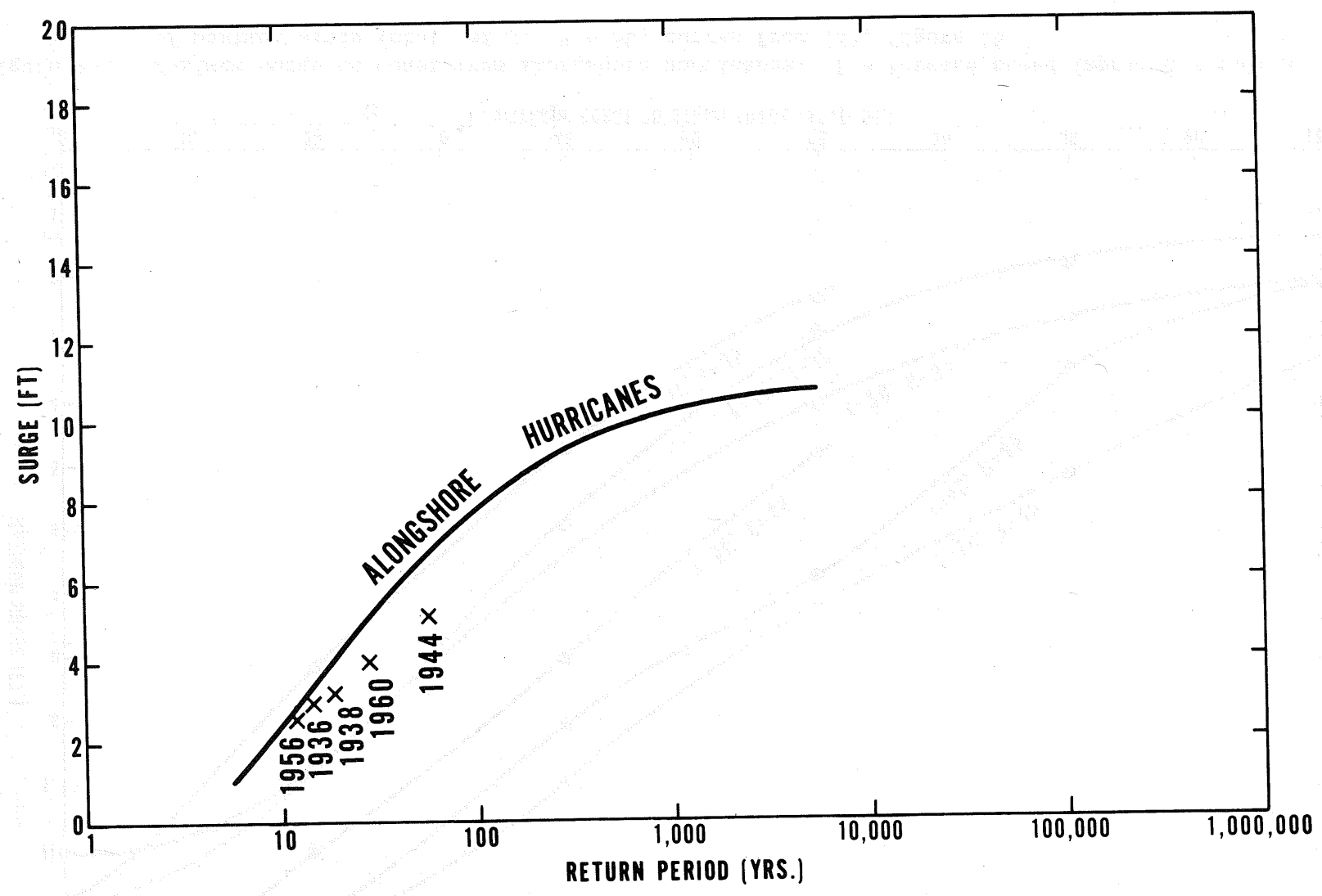
Figure 4-9. Computed frequency distribution of maximum surge heights from alongshore hurricanes, southern New Jersey coast. X - observed surges at Atlantic City, N.J. (Table 4-2.)
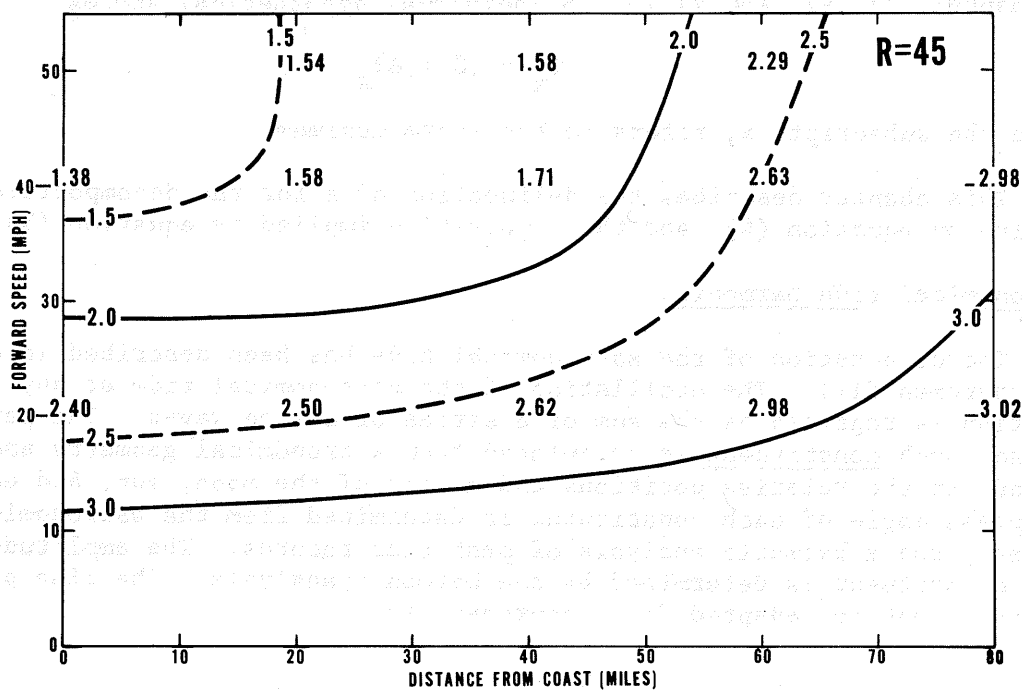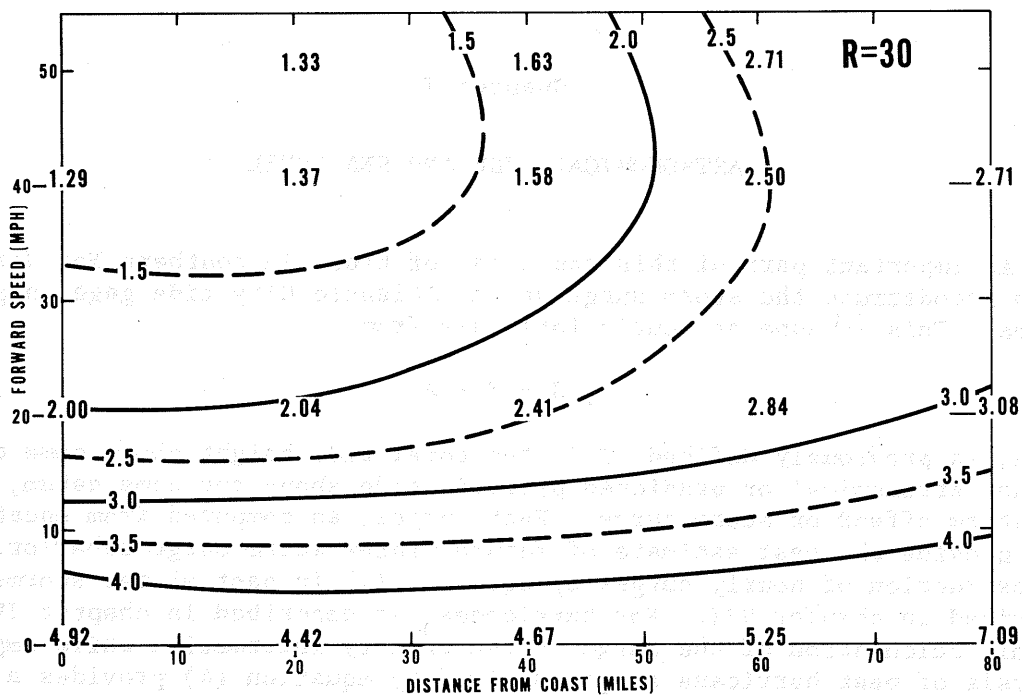
Figure 4-10. Time scale factor, $t_{2/3}$ (hours), of surge profile at coast for hurricanes passing at sea.

Chapter V

ASTRONOMICAL TIDE AND SEA LEVEL

An important part of this appraisal of tides in southern New Jersey is to reconstruct the storm surge at the Atlantic City tide gage in past storms. This is done at hourly intervals from

$$S = T - A \qquad (4)$$

where, as previously defined, T is the total tide height above some datum, A, the astronomical or predicted periodic tide above the same datum, and S the storm effect or storm surge. Past surges, as computed from equation (4), provide the best estimate of future winter storm surge behavior. The reconstruction of hourly surges by equation (1) in past winter storms, is described in chapter VII. For hurricanes, as described in chapter IV, dynamic calculation of the surge is the primary information while empirical analysis of past hurricane surges derived by equation (4) provides a check.

Having obtained estimates of surge behavior in winter storms and hurricanes, this information is combined with the astronomical tide, as described in chapters II, VI, and VIII. In individual hypothetical storms

$$T_x = (S + A)_x \qquad (3)$$

where the subscript, x, refers to the storm maximum.

This chapter describes the delineation of A for the decomposition implied by equation (4), and the composition implied by equation (3).

Astronomical tide harmonics

The computation of the astronomical tide has been described in detail by Schureman (11). The oscillation of the astronomical tide at any one location is regarded as the sum of a series of cosine waves. The period of each such <u>constituent</u> is calculated from astronomical geometry and depends on the relative positions and motion of the moon, sun, and earth. The phase angle of each constituent is determined from the astronomical geometry and a harmonic analysis of past tide records. The amplitude of each constituent is determined by the harmonic analysis. The tide prediction equation, adapted from Schureman, is

$$A = H_o + \sum_{n=1}^{n=m} f_n H_n \cos (a_n t + \alpha_n) \qquad (19)$$

where

A = height of tide at any time t, above selected datum.

H_o = mean height of water level above selected datum.

H_n = mean amplitude of nth tide constituent, determined by harmonic analysis of at least 369 days of tide record.

f_n = factor for reducing mean amplitude H_n to year of prediction. Depends on astronomical factors.

a_n = speed of nth constituent. Depends on astronomical factors.

t = time reckoned from some initial time such as beginning of the first year of predictions.

α_n = initial value of nth constituent at time t = 0 at location for which prediction is made.

m = number of harmonic constituents used for tide prediction. Varies with station.

It will be noted that equation (19) provides for the computation of an oscillation of the tide level about some mean level, H_o, and says nothing about the height of that mean level. Mean sea level at Atlantic City has an annual oscillation with an amplitude of several tenths of a foot, and is therefore different during the winter surge season and the hurricane season. There is also a long-term secular trend which influences the interpretation of past storm surge records.

We next describe the specification of sea level for purposes of this study. We begin with specification of the reference datum plane at the Atlantic City gage.

Atlantic City datum planes

A tide gage recorder was established by the Coast and Geodetic Survey on a pier at Atlantic City in 1912. Tides are published as height in feet above the zero point on the staff gage on this pier (the precise definition of its level is a certain number of feet below a specific permanent inland bench mark; thus, physical destruction or movement of the gage does not change the reference level with respect to the adjacent land).

The shortest period during which all the principal tide generating constituents come close to being given their long-term weights in application of equation (19), is 19 years. A particular 19-year epoch is therefore customarily adopted as a base period for tidal datum plane references (Marmer (13) page 63). All tide work under the jurisdiction of the Coast and Geodetic Survey is currently referred to mean datum levels for the epoch 1941-59.

Reference water levels at the Atlantic City gage, given by Marmer, are, in feet above the gage zero, defined above,

Highest observed (thru 1968)	13.40
Mean high water (1941-59)	8.60
Local mean sea level (1941-59)	6.60
Sea level datum, 1929 adjustment	6.23
Mean low water (1941-59)	4.53
Lowest observed (thru 1968)	0.80
Datum	0.00

Here mean high water and mean low water are the average height of all observed high and low tides, respectively, during the 1941-59 epoch, while local mean sea level is the average of all hourly observed tides during this period. The sea level datum 1929 adjustment refers to a particular geodetic surface determined by adjustment of selected leveling nets in the conterminous United States and used for map making and other purposes.

Secular trend in mean sea level

The mean height of the sea, with respect to the adjacent land, has been rising on the east and west coast of the Continental United States except Alaska and possibly northern New England during the 50 to 60 years of reliable tide observations (14, 15). On the East Coast the rate has been a foot to a foot and a half per century. The apparent change in sea level has been ascribed to a combination of increase of volume of water in the ocean from melting glaciers, and to subsidence of the land. We will not speculate here on the relative importance of these effects.

Mean annual sea level, defined as the average of the observed tide level at a one-hour interval throughout the year, has been tabulated by the Tides and Currents Branch, Oceanography Division, Coast and Geodetic Survey, for a number of stations. These values of local mean sea level at Atlantic City are plotted in figure 5-1. There is a clear upward trend in the mean annual sea level though oscillations appear from year to year. A straight line has been fitted to the data of which the equation is

$$H_o = 5.96 + .01275 \ (Y-1900) \tag{20}$$

where H_o is the mean sea level above gage zero in feet for the given year Y. We adopt the curve of figure 5-1 (and equation (20)) as representing the trend in sea level at Atlantic City for our statistical purposes.

Astronomical tide in winter surge reconstruction

Chapter VII describes the reconstruction of winter surges for the present study by solution of equation (4) at hourly intervals, which in turn depends on the solution of equation (19) at hourly intervals. This

calculation of the hourly astronomical tide for selected storms was carried out by Pore and Cummings, using a computer program prepared by them (12) and which is currently in use by the Coast and Geodetic Survey for routine tide prediction table calculations. Suffice it to say here that these calculations use a fixed H_o for a standard epoch. We therefore adjust all outputs of this program in our selected storms in accordance with

$$A_Y = A_e + ((H_o)_Y - (H_o)_e) \tag{21}$$

$$S_Y = S_e - ((H_o)_Y - (H_o)_e) \tag{22}$$

where the subscript, e, refers to a particular epoch, the subscript, Y, refers to a particular year, A_e is the output of the Pore-Cummings program, H_o is mean annual sea level from equation (20), and $(H_o)_e$ is mean sea level above gage zero for the standard epoch. Values of the secular trend adjustment, $((H_o)_Y - (H_o)_e)$, are listed in table 1, where $(H_o)_e$ is 6.60 feet for the 1941-59 epoch.

Astronomical tide in reconstruction of hurricane surges

Harris has made a comprehensive compilation of reconstructed hurricane surges at a number of coastal points including Atlantic City (16). We use these in our study (chapters IV and X) and have also reconstructed the surges for a few additional hurricanes. Harris adopts the viewpoint that during the quiescent summer season an individual hurricane is of short duration and has little effect on the mean monthly sea level for a calendar month. He defines "surge" as the departure from the astronomical tide based on H_o equal to the observed mean monthly tidal height. This is a convenient assumption because mean monthly observed tides are routinely tabulated by the Coast and Geodetic Survey, Tides and Currents Branch. Two of the tide oscillation constituents, the so-called "SSA" and "SA" constituents, have a semi-annual and an annual period, respectively, and therefore influence mean monthly observed tide levels. To avoid introducing these constituents twice, Harris omits the "SSA" and "SA" constituents in his solution of equation (19) and, in effect, depends on these influences showing up in his values of H_o. The sum of the "SA" and "SSA" constituents at Atlantic City is graphed in figure 5-2, depicting the annual cycle of sea level there.

In the present study, Harris' compilation of hurricane surges was supplemented by computation of additional hurricane surges via Pore and Cummings' program (12), sticking to Harris' definition of surge. As a matter of convenience, the hourly astronomical tide, A, was computed in the standard manner using all constituents and the standard $(H_o)_e$. The output was hand-corrected by subtracting out the sum of "SA" and "SSA" (figure 5-2) and the difference between the observed mean monthly sea level (Coast and Geodetic Survey tabulation) and the standard $(H_o)_e$ (6.60 ft above gage zero).

Astronomical tide in total tide composition

A major feature of the joint probability method of tide frequency estimation is to superimpose storm surges on the full range of astronomical tides, ranging from lowest neap tide to highest spring tide, and a full range of phase displacements between maximum surge and maximum astronomical tide. This requires a simplified semi-analytical description of the astronomical tide. At Atlantic City and Long Beach Island the astronomical tide oscillation can be closely represented by a cosine wave

$$A = A_x \cos (2\pi t/W) \tag{23}$$

where

A_x = astronomical high tide.

t = time in hours before or after high tide.

W = wave period = 12.42 hours = one-half mean lunar day.

At periods of the lunar month when the twice-daily high tides are of different amplitudes, there is necessarily a distortion of the cosine wave but this is of no statistical importance. We impose symmetry on the astronomical tide wave for the same reason that we impose symmetry on the time and space variation of the surge (chapter IV) and regard each tidal cycle from low tide to low tide as a separate symmetrical entity conforming to equation (23).

Probability distribution of astronomical high tide, A_x

We treat the variable astronomical high tide in the same manner as hurricane climatological variables, that is, we construct a smooth probability distribution and then subdivide this into class intervals. All high tides at Atlantic City were computed with Pore and Cummings' program (12) by the Coast and Geodetic Survey for this study for a 19-year epoch for the months of September, representing the hurricane season, and January, representing the winter surge season. The resulting probability distributions of astronomical high tides for these months and the adopted class interval subdivisions are depicted in figures 5-3 and 5-4. The probabilities for each class interval are tabulated in table 5-2.

At a few locations on the United States coast the tidal wave is sufficiently different from a cosine wave that equation (23) would be inappropriate. In this case equation (23) would be expanded to represent the tidal oscillation by more than one constituent, relative to A_x.

Table 5-1

SEA LEVEL VARIATION AT ATLANTIC CITY, NEW JERSEY

Year	Mean annual sea level (feet above gage zero)		Difference from 1941-59 epoch* (feet)
	Observed	Smoothed (fig. 5-1, equation (20))	
1910	--	6.09	-.51
1911	--	6.10	-.50
1912	6.01	6.11	-.49
1913	6.08	6.13	-.47
1914	6.20	6.14	-.46
1915	6.26	6.15	-.45
1916	6.17	6.16	-.44
1917	6.18	6.18	-.42
1918	6.23	6.19	-.41
1919	6.37	6.20	-.40
1920	6.31	6.22	-.39
1921		6.23	-.37
1922		6.24	-.36
1923	6.19	6.25	-.35
1924	6.22	6.27	-.33
1925	6.13	6.28	-.32
1926	6.17	6.29	-.31
1927	6.33	6.30	-.30
1928	6.16	6.32	-.28
1929	6.18	6.33	-.27
1930	6.20	6.34	-.26
1931	6.38	6.36	-.24
1932	6.37	6.37	-.23
1933	6.49	6.38	-.22
1934	6.30	6.39	-.21
1935	6.44	6.41	-.19
1936	6.36	6.42	-.18
1937	6.51	6.43	-.17
1938	6.50	6.44	-.16
1939	6.55	6.46	-.14
1940	6.55	6.47	-.13
1941	6.49	6.48	-.12
1942	6.58	6.50	-.10
1943	6.49	6.51	-.09
1944	6.60	6.52	-.08
1945	6.67	6.53	-.07
1946	6.64	6.55	-.05
1947	6.59	6.56	-.04

*"Smoothed" value minus 6.60 ft.

Table 5-1 Continued

SEA LEVEL VARIATION AT ATLANTIC CITY, NEW JERSEY

Year	Mean annual sea level (feet above gage zero)		Difference from 1941-59 epoch* (feet)
	Observed	Smoothed (fig. 5-1, equation (20))	
1948	6.69	6.57	-.03
1949	6.52	6.58	-.02
1950	6.49	6.60	-.00
1951	6.64	6.61	.01
1952	6.63	6.62	.02
1953	6.63	6.64	.04
1954	6.54	6.65	.05
1955	6.64	6.66	.06
1956	6.73	6.67	.07
1957	6.56	6.69	.09
1958	6.75	6.70	.10
1959	6.56	6.71	.11
1960	6.70	6.73	.13
1961	6.84	6.74	.14
1962	6.84	6.75	.15
1963	6.71	6.76	.16
1964	6.69	6.78	.18
1965	6.68	6.79	.19
1966	6.64	6.80	.20
1967	6.80	6.81	.21
1968	6.82	6.83	.23
1969		6.84	.24
1970		6.85	.25

*"Smoothed" value minus 6.60 ft.

Table 5-2

PROBABILITY DISTRIBUTION OF ASTRONOMICAL HIGH TIDE
AT ATLANTIC CITY, NEW JERSEY

January		September	
Height above mean sea level (ft)	Probability	Height above mean sea level (ft)	Probability
1.0	.016	1.6	.038
1.2	.035	1.8	.049
1.4	.065	2.0	.064
1.6	.092	2.2	.065
1.8	.128	2.4	.088
2.0	.115	2.6	.106
2.2	.100	2.8	.125
2.4	.097	3.0	.153
2.6	.087	3.2	.120
2.8	.070	3.4	.085
3.0	.059	3.6	.058
3.2	.044	3.8	.038
3.4	.040	4.0	.017
3.6	.028		
3.8	.021		
4.0	.003		
	1.000		1.000
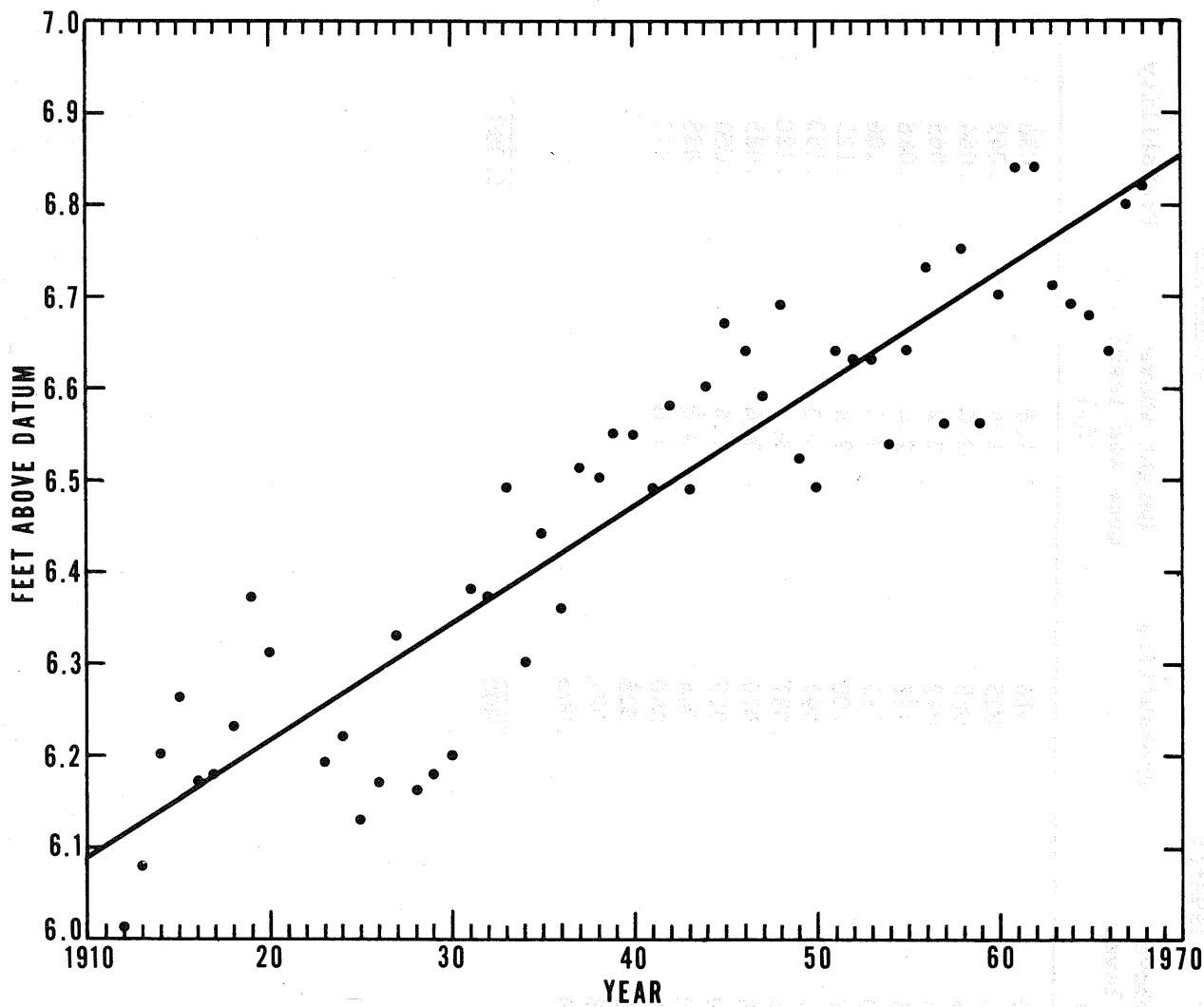
Figure 5-1. Trend in mean sea level at Atlantic City, N.J. Datum is gage zero. This is 4.53' below mean low water and 6.60' below local mean sea level for 1941-59 epoch.

Figure 5-2. Monthly variation in sea level, Atlantic City, N.J. Derived from semi-annual (SSA) and annual (SA) tide prediction harmonics.

Figure 5-3. Frequency distribution of predicted high tide, Atlantic City, N.J. September 1950-68.

Figure 5-4. Frequency distribution of predicted high tide, Atlantic City, N.J. January 1950-68.

Chapter VI

COMBINATION OF HURRICANE SURGE AND ASTRONOMICAL TIDE
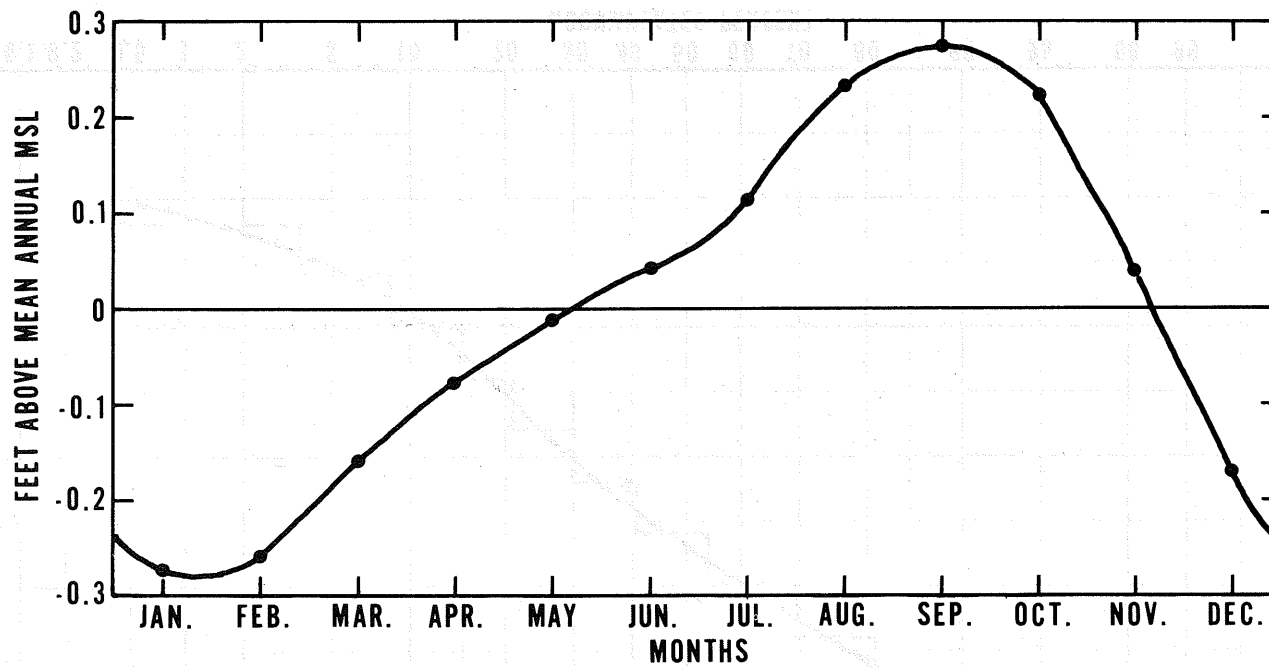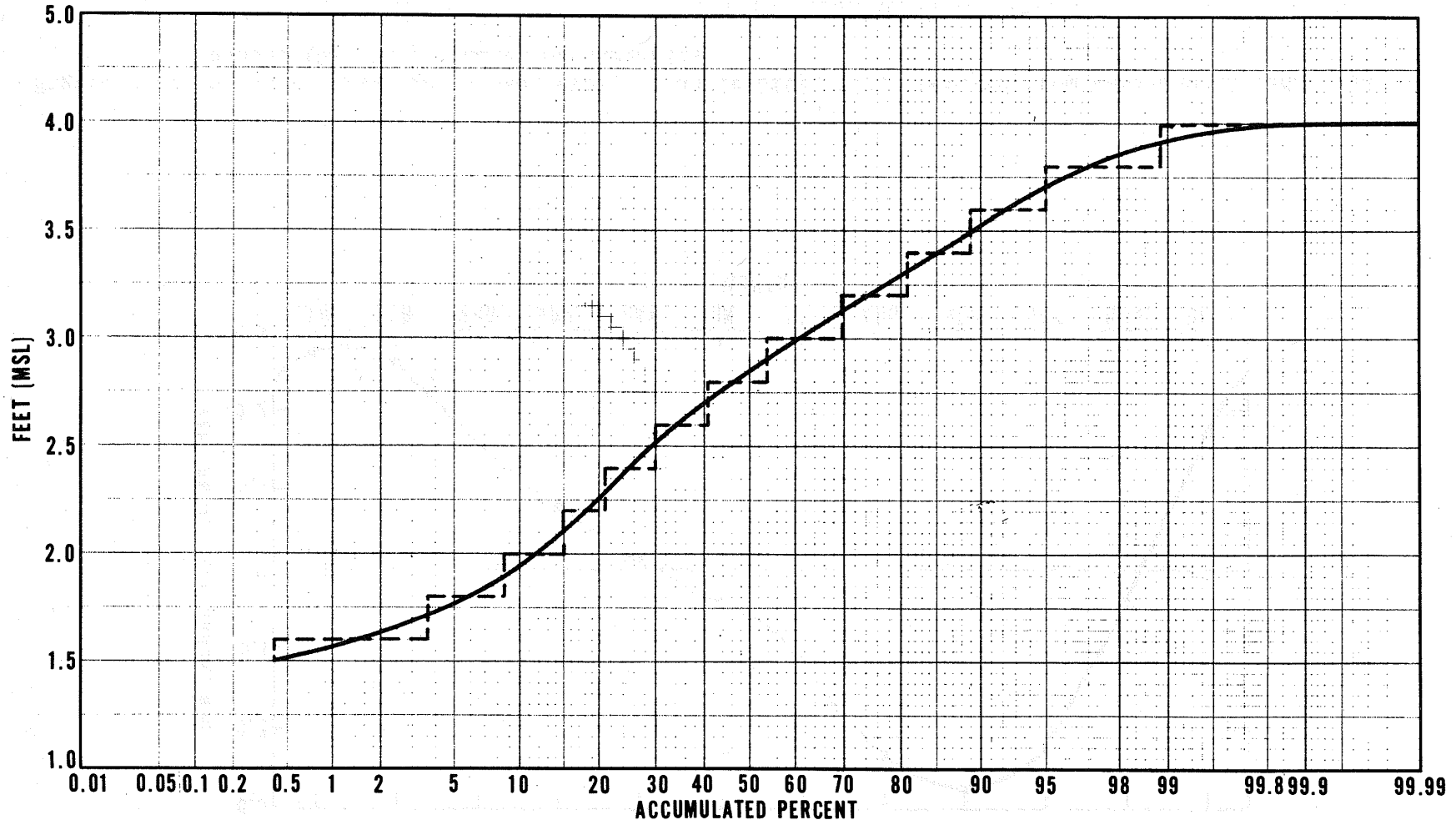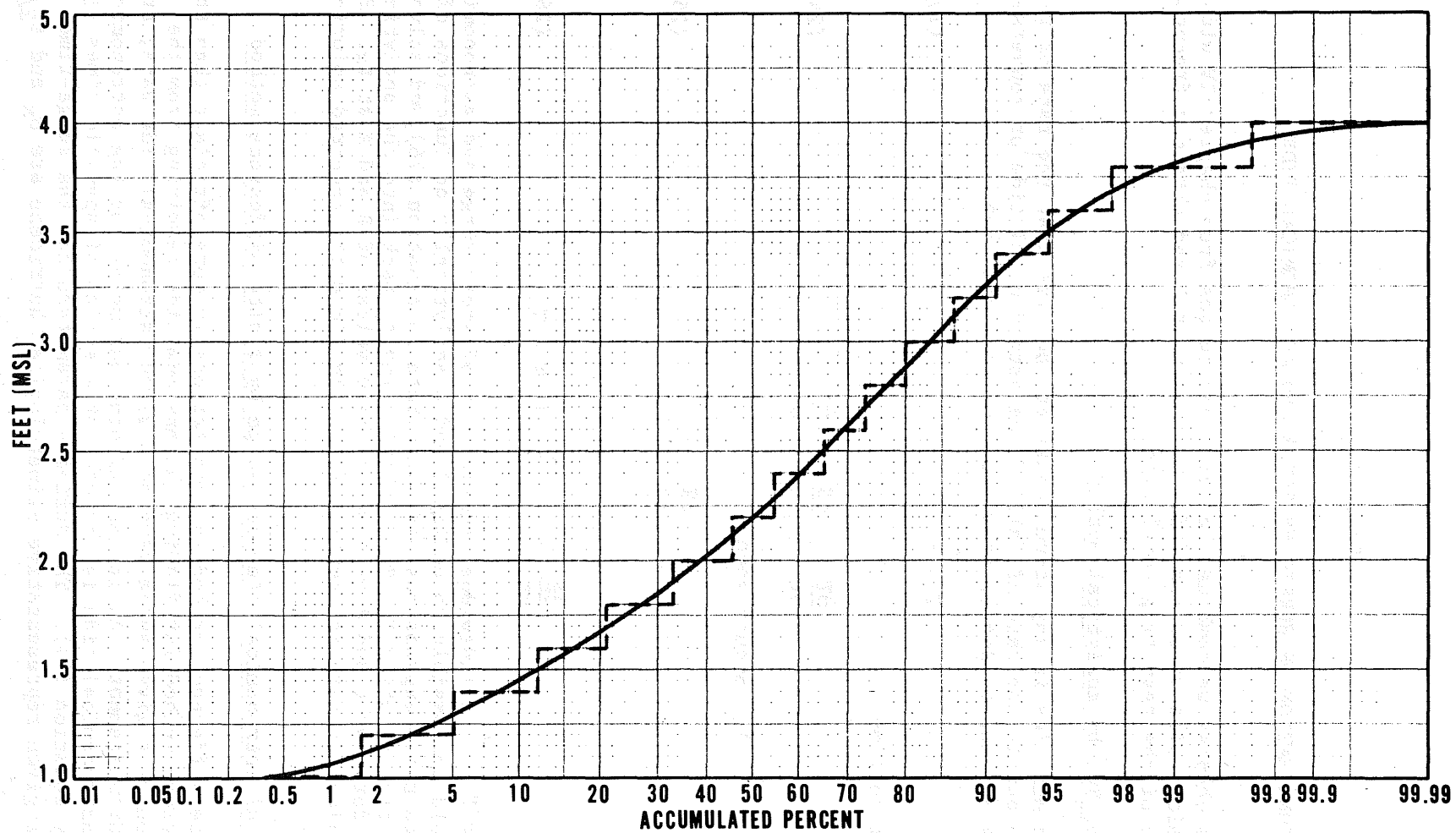
In this chapter we combine the hurricane surges from chapter IV with the astronomical tide variation defined in chapter V and obtain a frequency distribution of the resulting total tide.

Maximum tide, T_x, by analytical method

The maximum tide in any storm occurs at the time that the rate of rise of the surge equals the rate of fall of the astronomical tide or conversely. This is made evident by differentiating the basic equation

$$T = S + A \tag{1}$$

with respect to time

$$\frac{\partial T}{\partial t} = \frac{\partial S}{\partial t} + \frac{\partial A}{\partial t} \tag{24}$$

The maximum tide, T_x, occurs when

$$\frac{\partial T}{\partial t} = 0 \tag{25}$$

thus

$$\frac{\partial S}{\partial t} = - \frac{\partial A}{\partial t} \quad \text{at } T = T_x \tag{26}$$

To solve for T_x in an individual combination of storm surge and astronomical tide, it would be possible to define S and A analytically as functions of t, differentiate these expressions and substitute in equation (26), and solve for t_x, the time at which $T = T_x$. Substituting t_x back into the analytical expressions for S vs t and A vs t would yield values of S and A at t_x. Placing these values in turn in equation (1) would yield the required solution of T_x.

Combination of astronomical tide and surge by finite difference method

A finite difference method is computationally more efficient than the above analytical method for finding the maximum tide resulting from the superposition of a given surge wave on a given astronomical tide wave, at a given time displacement. A_x is the defining parameter for the astronomical tide. The astronomical tide is computed at a series of specific times t_1, t_2, etc., by equation (23). The defining parameters for the surge-time profile of a given representative climatological hurricane are S_x and $t_{2/3}$.

S_1, S_2, etc., are computed at t_1, t_2, etc., from equation (10). Summing the corresponding S's and A's yields T_1, T_2, etc.; the highest value is found by scanning this series and is sufficiently close to T_x if Δt is small enough. The adopted time increment was 1/80th of a mean lunar day or .311 hour. Noting equation (26) and that both S and A are represented by symmetrical waves, all pertinent combinations are taken into account by scanning only on rising S combined with falling A or vice versa but not both.

Phase displacement of surge from astronomical tide

The storm-surge profile of each representative climatological hurricane is combined with each representative astronomical tide cycle at 41 phase displacements ranging from coincidence of maximum surge with maximum astronomical tide to coincidence of maximum surge with low astronomical tide. Computationally, the procedure is to combine S_1, S_2, etc., with A_2, A_3, etc., for a phase displacement of $1\Delta t$; with A_3, A_4, etc., for a phase displacement of $2\Delta t$, etc.

Each of the 41 phase displacements is assigned a probability of .025 except for the first and the last which have a probability of .0125.

Calculated frequency of maximum tide, T_x, alongshore hurricanes

The surge-time profile for each of the 432 alongshore representative climatological hurricanes was combined with 13 different astronomical high tides ranging in 0.2 ft increments from 1.6 ft above sea level to 4.0 ft above sea level at each of 41 phase displacements, as has just been described. The frequency, F_c, of each combination is

$$F_c \left[(T_x)_{d,r,i,f,a,z} \right] = F_d P_r P_i P_f P_a P_z \tag{27}$$

$F_c \left[(T_x) \right]$ means "frequency of this particular T_x." P_z is the phase displacement probability and P_a is the astronomical high tide probability for September, from table 5-2. Arraying the 432x13x41 T_x's in order of magnitude from the largest downward and accumulating their individual frequencies yields the calculated tide frequency relation for alongshore hurricanes. This is shown in figure 6-1. In the diagram the frequency is delineated in terms of "return period," the reciprocal of the annual frequency.

Observed total tides from alongshore hurricanes

The six total tides from alongshore hurricanes at Atlantic City that are of largest magnitude when normalized for trend in sea level are listed in table 6-1. The September 1938 tide record was lost in the storm at Atlantic City and the Sandy Hook tide has been substituted. These six tides

64

are plotted in figure 6-1 assuming they represent a 58-year record, since establishment of the gage in 1912, and tend to confirm the lower end of the calculated frequency curve.

Calculated frequency of maximum tide, T_x, landfalling hurricanes

The surge for each representative climatological landfalling hurricane is defined by three parameters, S_x, $t_{2/3}$, and $d_{2/3}$. In line with our practice of replacing smooth curves with steps, the surge-distance profile is conceptually separated into steps at standard surge heights as illustrated in figure 6-3. The frequency with which one of these steps passes over a given coastal point is the product of the overall frequency of the landfalling hurricane, in storms per mile per year, the length of the step in miles, and the storm probability P_s defined in equation (6). We construct a surge-time profile for each step using the mean surge height for the step as S_x and the $t_{2/3}$ parameter for the storm. Each of the surge time profiles was then combined with the spectrum of astronomical tides and phase displacements in the manner that has been described. The complete expression for the frequency of a maximum tide from a particular combination of storm characteristics, astronomical tide, phasing displacement, and distance step along the surge-distance profile is

$$F_c \left[(T_x)_{b,r,i,f,a,z} \right] = F_h \left\{ (d_A)_b - (d_B)_b \right\} P_r P_i P_f P_a P_z \qquad (28)$$

where the subscript b is the index of standard surge heights.

Maximum total tides are calculated for each combination indicated, and the frequency of that particular total tide from equation (28). The resulting calculated tide-frequency curve for landfalling hurricanes is shown in figure 6-2.

Comparison of figure 6-1 with 6-2 shows that the most extreme dangerous high tides on the southern New Jersey coast would result from a hurricane entering the coast. At intermediate levels alongshore hurricanes, because of their much greater frequency in this region, produce most of the high storm tides.

Observed tides from landfalling hurricanes

The two historical tides of more than 4 ft from landfalling hurricanes at Atlantic City are shown in the lower part of table 6-1. Interpreted as the record for 58 years, these are plotted on the frequency diagram, figure 6-2.

In comparing the plotted points with the computed curve, it should be noted that both of the observed points are from distant hurricanes, (table 6-1). In representing the surge-distance profile by the Gaussian curve, no great accuracy has been sought or obtained at great distances or with surges of less than two or three feet.

Table 6-1

MAXIMUM TIDES FROM HURRICANES, ATLANTIC CITY, N.J.
1912-1969

| Date | Observed | | | Adjustment for sea level trend (ft) | Adjusted max tide (ft msl) | Distance track to coast (naut. mi.) |
	ft above gage zero	ft msl this report*	ft msl Corps of Engineers report**			
Hurricanes passing at sea						
Sept. 14, 1944	13.8	7.2	7.6	+0.1	7.3	30
Sept. 12, 1960	12.2	5.6	6.1	-0.1	5.5	45
Sept. 21, 1938	9.6#	5.0#	4.1	+0.2	5.2#	90
Sept. 18, 1936	10.9	4.3	4.7	+0.2	4.5	45
Sept. 27, 1956	11.1	4.5	4.9	-0.1	4.4	130
Sept. 21, 1961	11.0	4.4	--	-0.1	4.3	115
Landfalling hurricanes						Distance coastal entry point from Atlantic City (naut. mi.)
Aug. 23, 1933	11.2	4.6	5.0	+0.2	4.7	240
Oct. 15, 1954	10.8	4.2	4.6	-0.1	4.1	150

#Sandy Hook, N.J.
*local msl for 1941-59 epoch, 6.60' above gage zero
**mean sea level datum, 1929 adjustment, 6.23' above gage zero

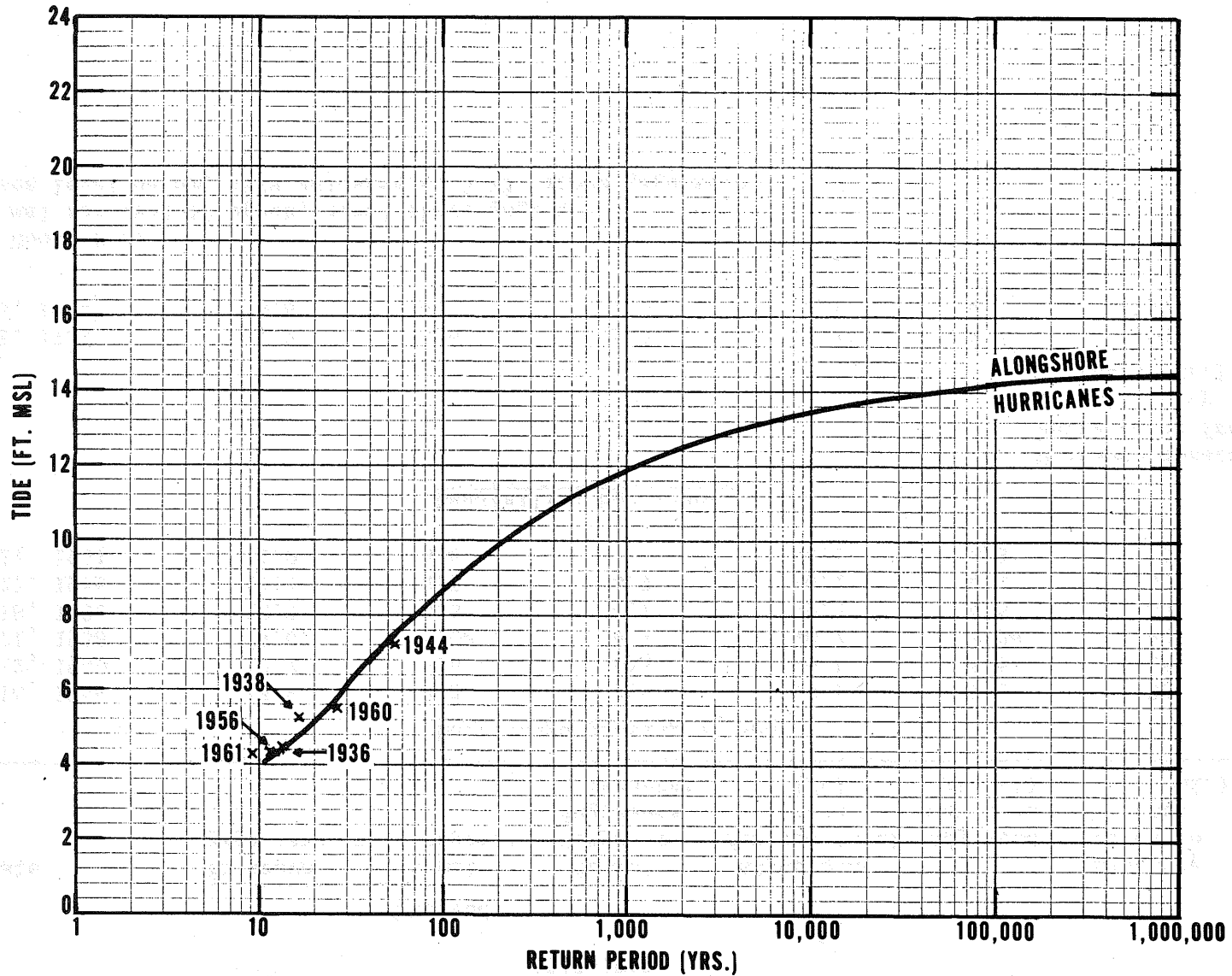Figure 6-1. Tide frequency from alongshore hurricanes, Atlantic City, N.J. by joint probability method. X - observed tides from these storms 1912-1969.
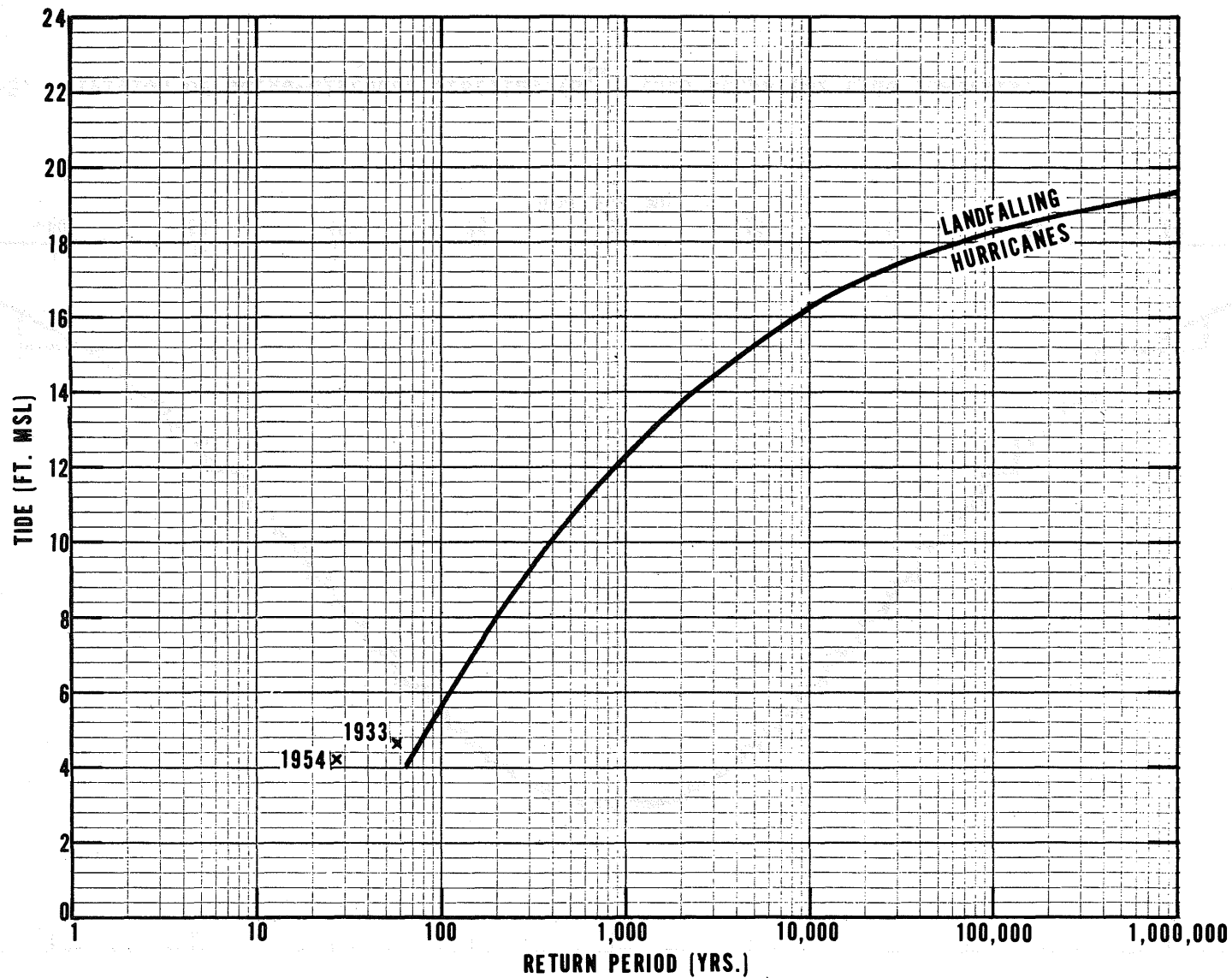
Figure 6-2. Tide frequency from landfalling hurricanes, Atlantic City, N.J., by joint probability method. X - observed tides from these storms 1912-1969.
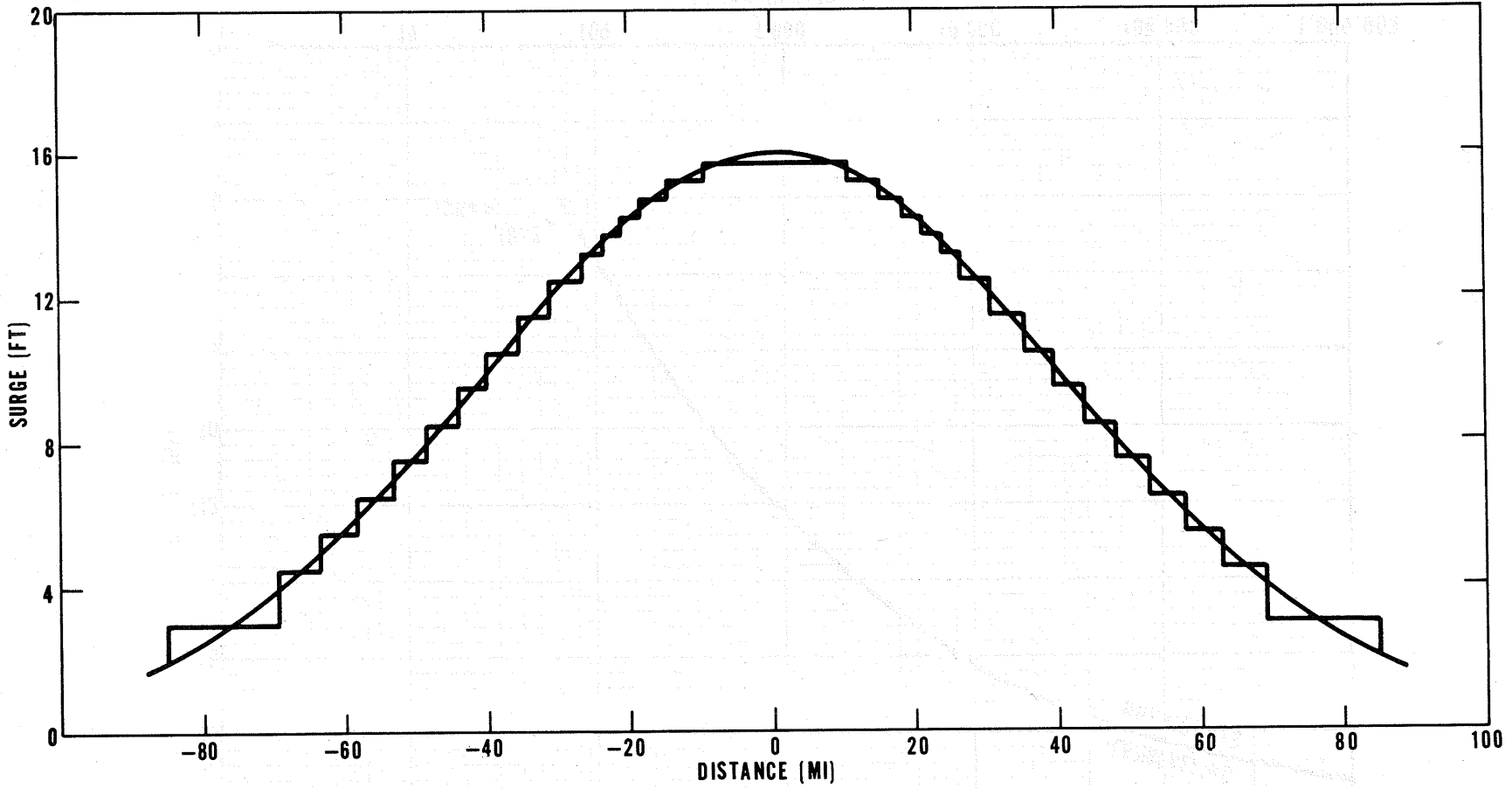
Figure 6-3. Division of surge-distance profiles (S_{1x}) into steps for tide analysis.

Chapter VII

WINTER STORM SURGES

The purpose of this chapter is to assess the magnitude and frequency
of storm surges on the southern New Jersey coast from northeasters. These
storms, like hurricanes, are cyclones (a wind system in the counterclock-
wise direction about a central low pressure). The most extreme northeasters
are of larger lateral extent, lesser intensity, and longer duration than
typical hurricanes. This statistical assessment of surges is based entirely
on analysis of the tide gage record at Atlantic City and, unlike the treat-
ment of hurricane surges in chapter IV, there is no calculation of surges
from hypothetical, climatologically representative storms. Northeaster
total tides are synthesized by combination of surges and astronomical tide
in the same manner as the hurricanes. This is covered in chapter VIII.
The present chapter is restricted to surge statistics.

Surge data, 1955-1969

The hourly surge has been evaluated by the Techniques Development
Laboratory of the Weather Bureau from November 1 through April 30 (here-
after called a "winter") for several coastal stations, including Atlantic
City, continuously since November 1955. These values are plotted as con-
tinuous graphs (unpublished) of surge height vs. time. These graphs were
scanned in the present study and statistics assembled on all surges showing
heights of 2 feet or more at Atlantic City.

Surge data, 1922-1955

For the "winters" 1922 through 1955, surge data were assembled for
the present study by the Oceanography Division of the Coast and Geodetic
Survey. This was done in the following steps. Observed high and low
tides at Atlantic City were compared visually with the predicted astro-
nomical high and low tide, and instances of 2 feet or more of excess of
observed over predicted noted and tabulated. Hourly predicted tides were
then recomputed for these dates by Pore and Cummings' computer program (12)
(equation (19)) and these hourly predictions subtracted from the tabulated
observed total tides (equation (4)), thus yielding hourly values of the
surge.

These surge values depend numerically on the astronomical tides, in
turn referred to a standard H_0. In the present study all surge values
were adjusted for secular trend in sea level by equation (22).

Maximum annual surge

The most popular method of statistical analysis of a time series of
hydrologic data is to fit a curve of prescribed mathematical characteristics

to the "annual series," that is to the array consisting of the largest value in each year listed in order of magnitude. The Weather Bureau has done this in the frequency analysis of extreme rainfall, using the procedure developed by Gumbel (17) for fitting the Fisher-Tippett Type 1 distribution. The Rainfall Frequency Atlas of the United States (18) uses this method, as do several later papers which amplify this Atlas. We adopt the Gumbel procedure as suited to our statistical purpose in treatment of surges.

The maximum surges each winter (Nov-Apr) at Atlantic City, together with sea-level adjustments, are listed in table 7-1.

The adjusted maximum seasonal surge heights are plotted in figure 7-1 on an extreme probability frame of reference. The abscissa is so designed that data distributed according to Gumbel's extreme probability theory will plot in a straight line. The curve shown is a machine-computed least squares regression fit.

Frequency of all surges

The requirement here is not for the frequency of maximum annual surges only but for the frequency of any particular surge height, occurring as a maximum annual value or not. As with other classes of hydrologic data, the highest storm surge values are maximum annual values. At more moderate levels, however, the maximum annual values in some years are less than the second or third highest value in other years.

We estimate the frequency of the moderate-level surges by listing all surges of 2 feet or more during the years for which we have complete record, 1955-69, table 7-2. These frequencies are plotted in figure 7-2. This type of plot is sometimes called a partial duration series (18).

Adopted winter surge frequencies

The maximum annual frequency distribution transposed from figure 7-1, and the partial duration frequencies from figure 7-2, are combined in figure 7-3, curves A and B, respectively. We construct a transition curve, curve C, recalling that curve A is based on 14 years of data while curve B is based on 47 years. Curve C is adopted as the best estimate of the probabilities of indicated surge heights in any one year. Surge heights and probabilities are extracted from this curve for combination with the astronomical tide in chapter VIII.

Critique of outlier

The surge on November 25, 1950, in a famous and damaging northeaster is by far the highest of record and on figure 7-1 appears as what is known in the parlance of statisticians as an "outlier." Such outliers should be

examined as closely as possible in analyses of this kind, both to search
for possible error and establish the validity of the observation, and to
develop a background of understanding of the event as a guide to assessing
its frequency.

The original tide recorder chart was examined and the conclusion
reached that the record is entirely reliable. The Tides and Currents
Branch, Oceanography Division, Coast and Geodetic Survey which has custody
of these records concurred. The peak surge of 6.4 ft occurred on falling
tide in a brief sharp wave which has the appearance of a resurgence. In
a separate peak two and a half hours earlier, at the time of high astro-
nomical tide, the surge was 5.1 ft. The astronomical tide, observed tide,
and computed surge are shown in figure 7-4.

Pore has computed the surge in this storm for 27 tide gages along the
East Coast (not reproduced here). These reveal a consistent pattern as to
magnitude and timing of the surge peak, lending weight to the validity of
the Atlantic City profile. The highest absolute computed surge was 8.7 ft
at Sandy Hook, N.J., with the Battery, New York City showing 8.1 ft.

The extrapolated mean recurrence interval of a surge of 6.4 ft from
the fitted curve of figure 7-1 is 270 years. It is not positive that the
true recurrence interval of this winter surge level is really this great.
Several alternate interpretations are considered in the next chapter.

Apparent semidiurnal oscillation in surges

Some surges computed at hourly intervals by subtracting the computed
astronomical tide from the observed total tide, appear to show a semi-
diurnal oscillation with an amplitude of a foot or more. Figure 7-5 is
an example of this. The principal cause of the surge is wind, which has
no known periodicity of this kind. A timing discrepancy in either the
observed tide or the astronomical tide would, of course, introduce an
apparent periodicity in the apparent surge. A 15-minute timing discrepancy
when astronomical high tide is 3 ft above mean sea level would occasion
a spurious semidiurnal wave in the apparent surge with an 0.5 ft amplitude.
If due to a timing discrepancy, the spurious maxima and minima of the
surge would appear at the time that the astronomical tide is rising or
falling most rapidly. This was indeed the case for the storm of figure
7-5 and for several other storms.

The storm surge and the astronomical tide are to be combined in a
random manner to synthesize total tide, assuming that surge and astronomi-
cal tide are independent. It is necessary, then, to eliminate this spuri-
ous oscillation which is not independent of the phasing of the astronomical
tide. In concept, the surge could be recomputed with various time adjust-
ments and the surge accepted that had the least semidiurnal periodicity in
it. In practice this is unnecessary; the same result is obtained by simply
smoothing the surge profile by eye, reducing the peaks and increasing the
troughs in equal amount.

72

Those surges appearing to have a spurious semidiurnal oscillation with
an amplitude of one foot or more were smoothed in this manner. The peak
of the smoothed profile is listed in table 7-1 ("smooth" column) and used
for subsequent statistical analysis. Apparent semidiurnal periodicities
with amplitudes of less than one foot were not adjusted. There is further
comment on this in chapter X.

To account for the spurious surge oscillation we examined the origi-
nal tide gage record of the case in figure 7-5 and found that an instru-
mental or observational timing discrepancy of more than five minutes is
unlikely. Computational error is also rejected as a possibility.

This leaves the conjecture that under storm conditions the timing
of the astronomical tide may shift thus introducing an apparent oscilla-
tion in surges which are computed as departures from the published pre-
dicted astronomical tides. This is not unreasonable. The normal periodic
tide involves wave dynamics, with depth of water an influencial factor;
transport of water, with greater volumes at greater depths; and currents,
which are modified by wind.

Time and distance shape of winter surges

For combining with the astronomical tide (chapter VIII) it is nec-
essary to specify the temporal variation of the surge and also the
spatial variation, if any. As to spatial variation, the winter surges
are given the same treatment as the alongshore hurricanes. It is assumed
that the surge is the same along long stretches of coast (no spatial vari-
ation). The validity of this is borne out by comparing Atlantic City and
Sandy Hook surges in a number of storms. They average close to the same
height and differ very little in several individual storms.

For temporal variation of the surge we use as representative the
surge time profile for those storms since 1923 having a peak adjusted
surge (table 7-1 and table 7-2) of 3.0 ft or more. There are 21 such
storms. For a degree of smoothing these were grouped by shape and aver-
aged. This grouping resulted in the 1950 storm being kept in a class by
itself, 14 other storms being averaged by pairs into seven curves, while
the remaining six storms were averaged into two curves based on three storms
each. In averaging, since the intent is to maintain shape about the surge
peak, the peak surges were aligned. The maximum consecutive 13 hours of
smoothed average surge profile then becomes a standard surge shape. The
tabulation is shown in table 7-4 and a plot of these shapes in figure 7-6.

Surge height and surge shape as separate variables

In the joint probability approach maximum surge height, S_x, and the
surge shape (time variation of the surge) are separate variables, each
with their own probabilities, though not necessarily statistically independent

variables. Visual comparison of the surge shapes with S_x shows no clear trends or relationship, excepting that the highest surge, in November 1950, is associated with a sharply peaked time profile.

Beyond this, some of the higher surges are of long duration and others are more sharply peaked. The second highest surge, in the damaging March 1962 storm, was of long duration. An experiment in varying the combination of surge shape with surge height and the resulting decision, are covered in the next chapter. In combining a surge height with a particular surge shape the shape profiles of figure 7-6 are interpreted in a relative manner. That is, each of the surge heights of the pattern surge (table 7-4) is multiplied by the ratio $S_x/(S_x)_p$ to give the computed surge-time profile, where S_x is the statistical maximum surge height, and $(S_x)_p$ the maximum surge on the pattern profile in the table.

Table 7-1

MAXIMUM SEASONAL WINTER SURGES (NOV-APR) ATLANTIC CITY, N.J., 1922-69

Season	Maximum Surge from S = T-A (ft)	Smoothed	Reference Sea Level (ft above gage zero)	Sea Level for Year (ft above gage zero)	Sea Level Correction (ft)	Adjusted Surge (ft)	Date
1922-23	2.2		6.60	6.25	+.35	2.6	1-8-23
1923-24	3.3		"	6.27	+.33	3.6	3-11-24
1924-25	2.3		"	6.28	+.32	2.6	1-2-25
1925-26	2.5		"	6.29	+.31	2.8	2-4-26
1926-27	3.0		"	6.30	+.30	3.3	2-20-27
1927-28	3.1		"	6.30	+.30	3.4	12-4-27
1928-29	3.3		"	6.33	+.27	3.6	4-16-29
1929-30	2.4		"	6.33	+.27	2.7	12-23-29
1930-31	2.7		"	6.36	+.24	2.9	3-8-31
1931-32	3.5	3.0	"	6.37	+.23	3.2	3-6-32
1932-33	3.8	2.8	"	6.37	+.23	3.0	11-9-32
1933-34	1.6#		"	6.39	+.21	1.8	2-26-34
1934-35	2.3		"	6.41	+.19	2.5	1-23-35
1935-36	3.3		"	6.41	+.19	3.5	11-17-35
1936-37	2.7		"	6.43	+.17	2.9	2-5-37
1937-38	2.6		"	6.44	+.16	2.8	2-20-38
1938-39	2.1		"	6.46	+.14	2.2	3-12-39
1939-40	2.5		"	6.47	+.13	2.6	2-14-40
1940-41	2.1		"	6.48	+.12	2.2	3-1-41
1941-42	2.7		"	6.50	+.10	2.8	3-3-42
1942-43	2.3		"	6.51	+.09	2.4	1-28-43
1943-44	2.9		"	6.52	+.08	3.0	1-4-44
1944-45	2.4		"	6.52	+.08	2.5	11-17-44
1945-46	3.0		"	6.53	+.07	3.1	12-1-45
1946-47	2.6		"	6.56	+.04	2.6	2-21-47
1947-48	3.1		"	6.56	+.04	3.1	11-1-47
1948-49	2.2		"	6.57	+.03	2.2	11-29-48
1949-50	1.8#		"	6.60	+0	1.8	2-15-50

Table 7-1 - Continued

MAXIMUM SEASONAL WINTER SURGES (NOV-APR) ATLANTIC CITY, N.J., 1922-69 - Continued

Season	Maximum Surge from S = T-A (ft)	Smoothed	Reference Sea Level (ft above gage zero)	Sea Level for Year (ft above gage zero)	Sea Level Correction (ft)	Adjusted Surge (ft)	Date
1950-51	6.4		6.60	6.60	+0	6.4	11-25-50
1951-52	2.4		"	6.62	-.02	2.4	1-7-52
1952-53	2.7		"	6.62	-.02	2.7	12-22-52
1953-54	3.9		"	6.64	-.04	3.8	11-7-53
1954-55	2.0		"	6.66	-.06	1.9	3-22-55
1955-56	4.0	3.4	6.36	6.67	-.31	3.1	1-10-56
1956-57	2.5		6.36	6.69	-.33	2.2	2-28-57
1957-58	3.1		"	6.70	-.34	2.8	1-25-58
1958-59	2.2		"	6.70	-.34	1.9	12-30-58
1959-60	3.1		"	6.73	-.37	2.8	2-18-60
1960-61	4.1		"	6.74	-.38	3.8	2-4-61
1961-62	4.7		"	6.75	-.39	4.3	3-7-62
1962-63	4.1		"	6.75	-.39	3.7	12-6-62
1963-64	4.5		"	6.78	-.42	4.1	1-13-64
1964-65	2.8		"	6.79	-.43	2.4	2-25-65
1965-66	3.6		"	6.80	-.44	3.2	1-23-66
1966-67	3.2		"	6.81	-.45	2.8	2-7-67
1967-68	2.9		"	6.83	-.47	2.5	1-13-68
1968-69	4.6		"	6.83	-.47	4.2	11-12-68

#estimated without computing all hours during storm.

Table 7-2

FREQUENCY OF WINTER (NOV-APR) SURGE HEIGHTS. ATLANTIC CITY, N.J.
1955-68

Surge Height (ft)	Occurrences in 14 years	Accumulated Occurrences	Frequency per Year
4.3	1	1	.07
4.2	1	2	.14
4.1	1	3	.21
3.8	1	4	.29
3.7	2	6	.43
3.2	1	7	.50
3.0	2	9	.64
2.9	1	10	.72
2.8	4	14	1.00
2.7	3	17	1.2
2.6	3	20	1.4
2.5	1	21	1.5
2.4	5	26	1.9
2.3	4	30	2.1
2.2	11	41	2.9
2.1	6	47	3.4
2.0	4	51	3.6
1.9	8	59	4.2
1.8	10	69	4.9
1.7	8	77	5.5
1.6	5	82	5.9

Surge heights above have been adjusted for sea level trend in the same manner as Table 7-1.

Table 7-3

FREQUENCIES OF MAXIMUM WINTER (NOV-APR) SURGE HEIGHTS, ATLANTIC CITY, N.J.

Surge (ft)	Frequency* (per season)
2.0	1.2
2.2	.80
2.4	.60
2.6	.45
2.8	.30
3.0	.20
3.2	.16
3.4	.11
3.6	.08
3.8	.05
4.0	.04
4.2	.03
4.4	.019
4.6	.016
4.8	.011
5.0	.009
5.2	.006
5.4	.005
5.6	.0035
5.8	.0027
6.0	.0021
6.2	.0013
6.4	.0011

*from curve C, figure 7-3.

Table 7-4

HOURLY VARIATION OF WINTER (NOV-APR) SURGES (FT) ATLANTIC CITY, N. J.

| No.	Date	10	9	8	7	6	5	4	3	2	1	0	1	2	3	4	5	6	7	8	9	10	Group A	Group B
1	1/27/33	2.7	2.9	3.0	2.9	3.1	2.7	2.8	2.9	2.9	3.0	3.1	2.9	2.7											
	11/17/35	3.4	3.3	3.2	3.1	3.1	3.1	3.4	3.2	3.3	3.4	3.5	3.4	3.2											
	2/20/27	3.2	3.0	3.2	3.0	3.0	3.0	2.8	3.1	3.1	3.0	3.3	3.3	3.1											
	AV	3.1	3.1	3.1	3.0	3.1	2.9	3.0	3.1	3.1	3.1	3.3	3.2	3.0										0.15	
2	10/31-11/47									2.9	2.9	3.1	2.9	2.8	2.6	2.4	2.3	2.4	2.5	2.6	2.6	2.6		
	4/16/29									2.5	3.3	3.6	3.4	3.2	2.9	2.4	3.1	3.1	3.3	2.7	2.8	3.0		
	3/11/24									3.2	3.5	3.6	3.2	2.7	2.8	2.7	2.8	2.6	2.9	2.8	3.1	3.2		
	AV									2.9	3.2	3.4	3.2	2.9	2.8	2.5	2.7	2.7	2.9	2.7	2.8	2.9	0.15	
3	3/6/32				1.1	1.5	1.8	2.1	2.6	3.0	3.2	3.2	3.1	2.9	2.7	2.2	1.4							
	2/19/64				1.2	1.9	2.5	2.6	2.8	3.0	3.2	3.0	2.6	2.3	2.4	2.1	1.5							
	AV				1.2	1.7	2.2	2.4	2.7	3.0	3.2	3.1	2.8	2.6	2.6	2.2	1.4						.10	
4	11/25/50				2.5	2.5	3.2	3.9	4.7	4.1	3.4	6.4	5.0	4.2	3.6	3.4	3.0							
	1/13/64				2.3	2.6	3.0	3.4	3.1	3.2	3.4	4.3	3.5	3.2	2.7	2.4	1.9							
	AV				2.4	2.6	3.1	3.6	3.9	3.6	3.4	5.4	4.2	3.7	3.2	3.4	2.4						.10	
5	1/1/32					2.2	2.4	2.5	2.2	2.8	2.3	3.1	3.3	3.0	2.9	2.8	2.6	2.6						
	11/9-10/32					3.3	3.4	3.4	3.6	3.5	3.7	3.9	4.0	3.9	3.7	3.3	3.0	2.6						
	AV					2.8	2.9	3.0	2.9	3.2	3.0	3.5	3.6	3.4	3.3	3.0	2.8	2.6					.10	
6	11/3/62		1.5	1.8	2.1	1.9	2.3	2.1	2.5	2.3	2.7	3.1	3.1	2.0	1.3									
	12/6/62		2.1	2.1	2.2	2.2	2.3	2.5	2.7	2.9	2.9	3.9	1.1	2.3	2.1									
	AV		1.8	2.0	2.2	2.0	2.3	2.3	2.6	2.6	2.8	3.5	2.1	2.2	1.7								.10	
7	3/8/61									2.8	3.2	3.1	2.9	2.5	2.9	3.0	2.2	2.0	2.1	2.2	2.1	1.8		
	3/6/62									3.9	4.5	4.1	3.7	3.8	4.3	3.6	3.6	4.0	3.9	4.2	4.3	4.2		
	AV									3.4	3.8	3.6	3.3	3.2	3.6	3.3	3.4	3.0	3.0	3.2	3.2	3.0	.10	
8	2/4/61						2.5	3.0	3.5	3.9	4.0	3.7	3.2	2.9	2.7	2.7	2.8	2.4	2.1					
	11/12/68						2.7	3.4	3.2	4.0	4.4	3.2	3.1	2.8	3.3	3.5	3.0	2.8	2.7					
	AV						2.6	3.2	3.4	4.0	4.2	3.4	3.2	2.8	3.0	3.1	2.9	2.6	2.4				.10	
9	12/4-5/27					2.0	2.5	2.8	2.8	2.5	2.5	3.4	2.3	2.0	2.1	2.0	2.1	2.1						
	1/23/66					2.3	2.8	2.7	2.9	2.7	3.0	3.4	3.3	3.1	2.5	2.1	2.6	1.9						
	AV					2.2	2.6	2.8	2.8	2.6	2.8	3.4	2.8	2.6	2.3	2.0	2.4	2.0					.10	1.00
10	11/25/50					2.5	3.2	3.9	4.7	4.1	3.4	6.4	5.0	5.3	3.6	3.4	3.0	2.8					1.00	1.00
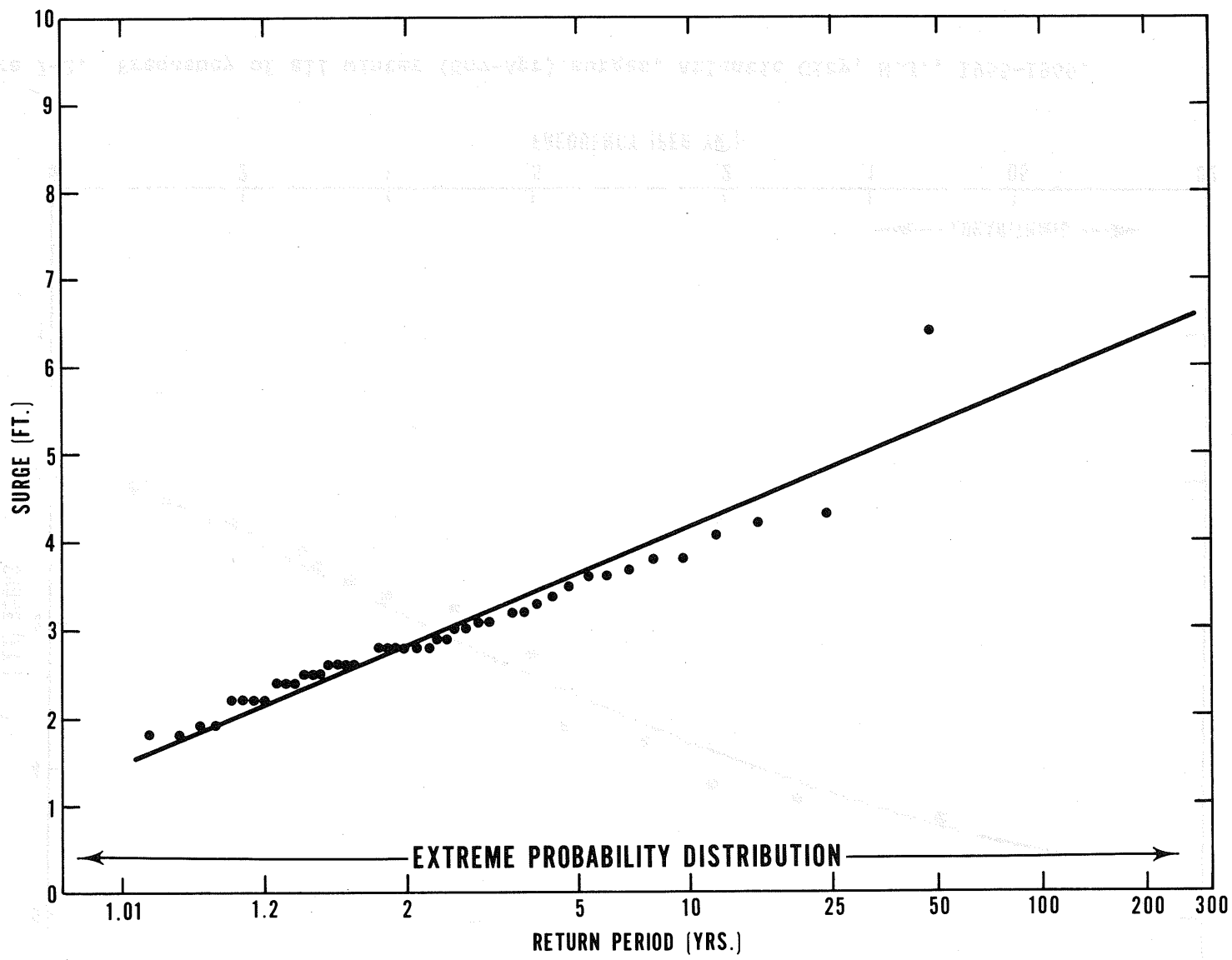
Figure 7-1. Frequency of maximum annual winter (Nov-Apr) surge heights (ft.)
Atlantic City, N.J., 1922-1969.

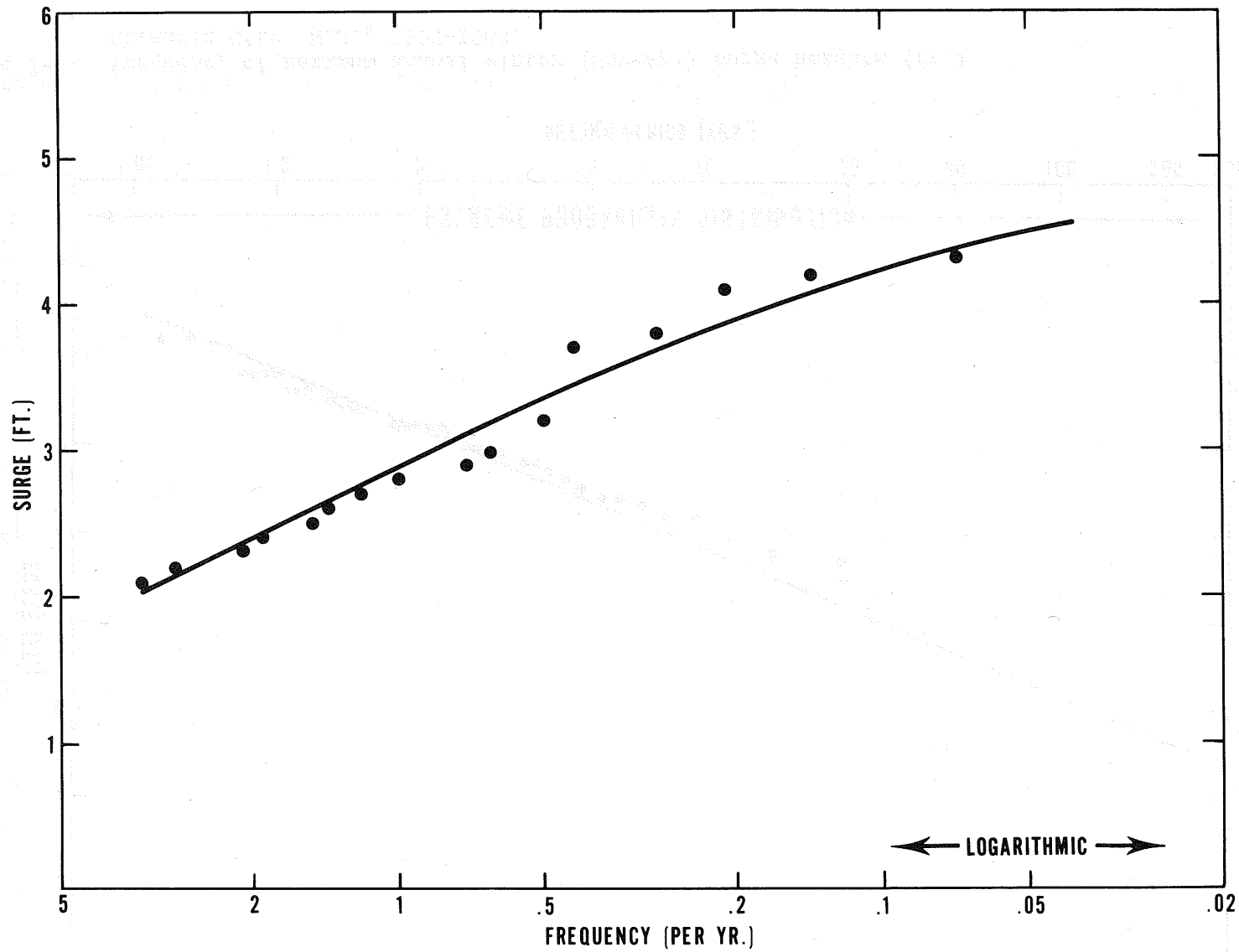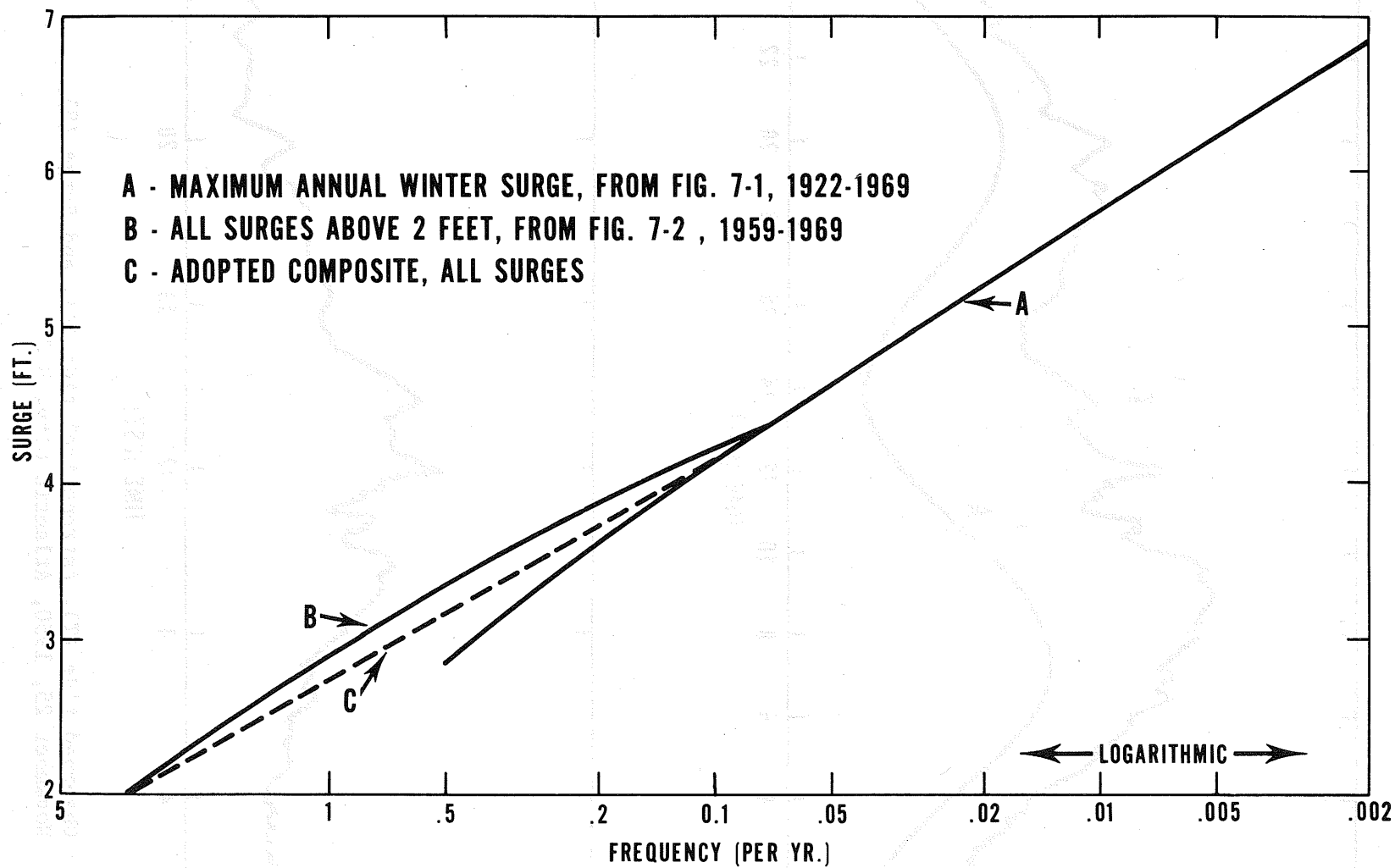Figure 7-2. Frequency of all winter (Nov-Apr) surges, Atlantic City, N.J., 1955-1969.

A - MAXIMUM ANNUAL WINTER SURGE, FROM FIG. 7-1, 1922-1969
B - ALL SURGES ABOVE 2 FEET, FROM FIG. 7-2 , 1959-1969
C - ADOPTED COMPOSITE, ALL SURGES

Figure 7-3.   Composite winter surge frequency, Atlantic City, N.J.
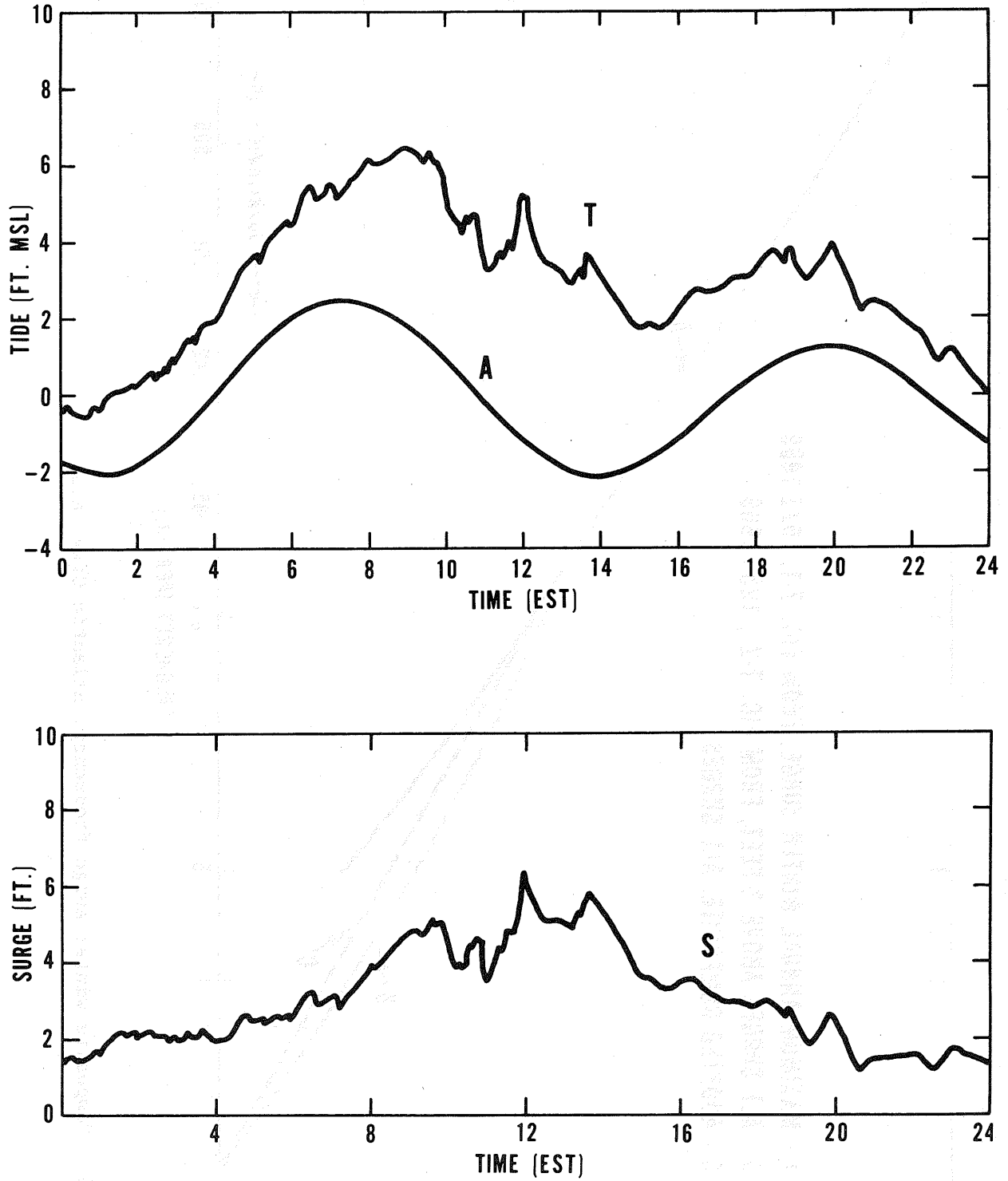
Figure 7-4. Observed tide (T), Astronomical tide (A), and Surge (S), November 25, 1950, Atlantic City, N.J.
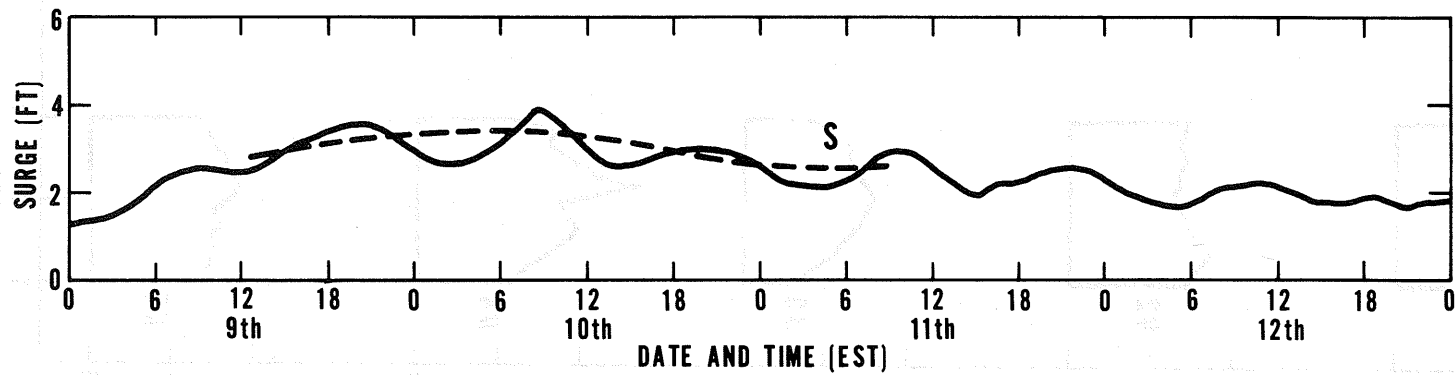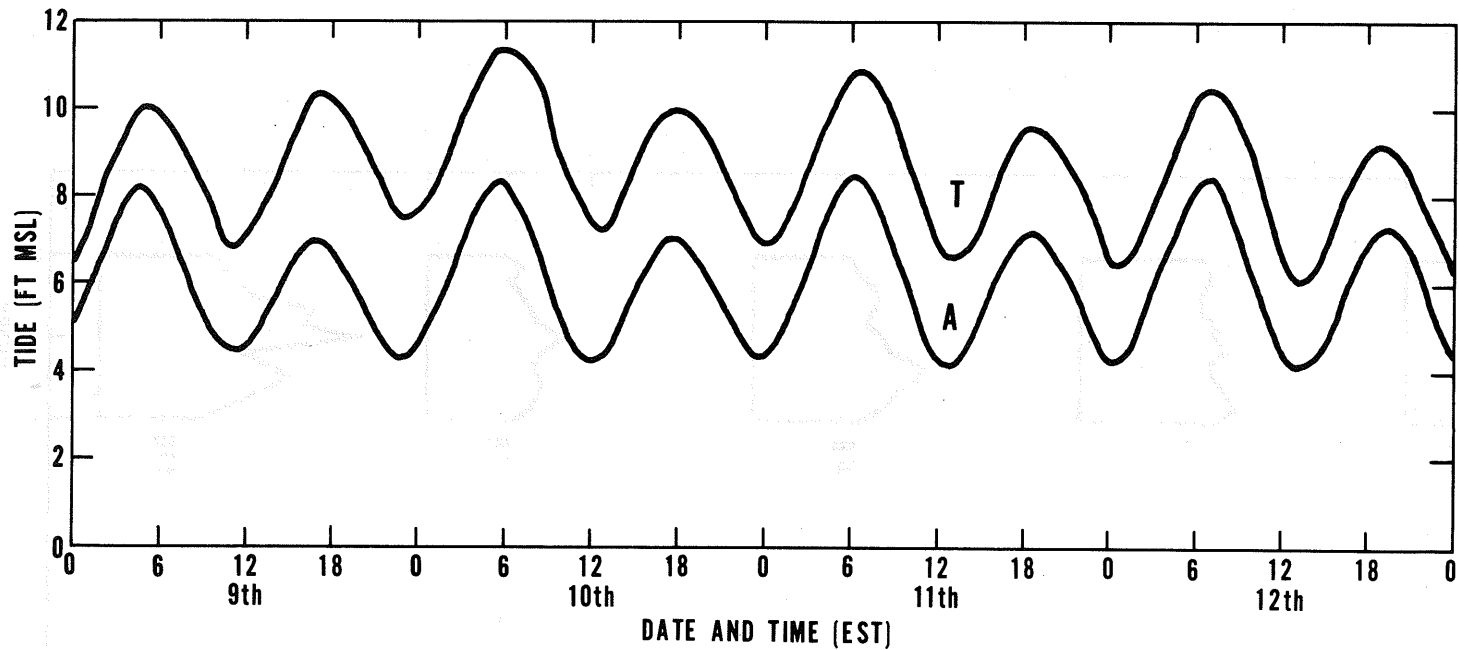
Figure 7-5.   Observed tide (T), Astronomical tide (A), and Surge (S), January 9-11, 1956, Atlantic City, N.J., illustrating apparent 12.4-hr. oscillation in surge. Dashed curve, surge smoothed by eye. (Astronomical tide based on H_o of 6.36' above gage zero.)
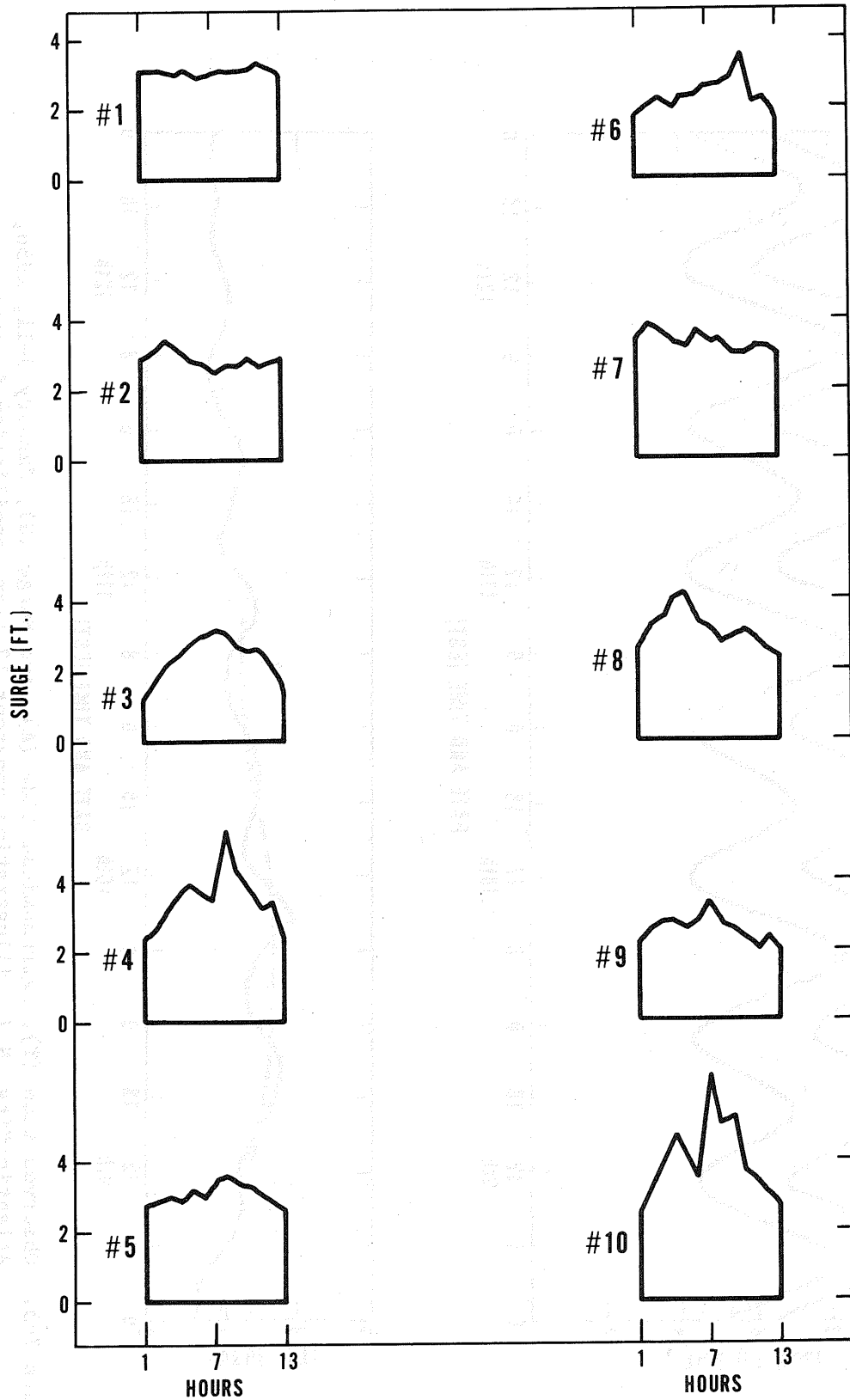
Figure 7-6. Surge time profile patterns. Winter surges (Nov-Apr), Atlantic City, N.J. From table 7-4.

Chapter VIII

COMBINATION OF WINTER STORM SURGE AND ASTRONOMICAL TIDE

The concept in combining winter (Nov-Apr) surges with the astronomical tide to estimate frequencies of total tide is the same as for hurricanes, namely, that the storm surge and the astronomical tide are essentially independent phenomena. Climatologically estimated surges can be expected to be superimposed on the full spectrum of astronomical tides at the full spectrum of phasing displacements. In making the combination there are certain procedural differences from hurricanes due both to differences in the storms and differences in the form of the data. These differences are covered in this chapter.

The climatology of surges at Atlantic City is covered in chapter VII, where a frequency distribution of maximum winter surge heights is found in table 7-3, and a portrayal of the time shape of these surges in figure 7-6. The frequency of the maximum total tide for a particular combination of maximum surge, surge time shape, astronomical tide, and phasing displacement is

$$F_c \left[(T_x)_{w,t,a,z} \right] = F_w P_t P_a P_z \qquad (29)$$

where F_w is the maximum surge frequency from table 7-3, P_t is the time shape probability, and P_a and P_z are the astronomical tide and phasing displacement probabilities, as previously defined.

Time increment for tide-surge combination

Observed tides (total tide) are summarized and tabulated by the Coast and Geodetic Survey at one-hour intervals. To match these data series, in computing a surge by subtracting A from T (equation (4)), the astronomical tide is also computed at one-hour intervals. A is computed beginning 6 hours before high tide, and ending 6 hours after high tide by equation (23). The 13 S's are combined with these 13 A's and scanned for T_x at each of the 13 possible phasing displacements. P_z is 1/13.

To obtain 13 consecutive A's to combine with the 13 S's as the phase shifts, the astronomical tide wave is repeated.

Surge time pattern

As a matter of convenience, symmetry was not enforced on the surge time profiles of figure 7-6, and they were combined "as is" from table 7-4 with the astronomical tide.

Variation of interrelationship between surge height and surge shape

To measure the sensitivity of the computed total tide to the treatment of surge shape, the total tide frequency distribution was computed with three different combinations of S_x with different surge shapes:

    a. All surges shaped like number 10 of figure 7-6. (extreme peaking).

    b. All surges shaped like number 1 of figure 7-6 (extreme flatness).

    c. Distributing the lower 99 percent of maximum surges over surge patterns 1 thru 9, in accordance with the "group A" probabilities of table 7-4; assigning pattern 10 to the upper 1% of maximum surges, thus allowing for maximum peaking of the highest surges.

The results of these tests are shown in figure 8-1. The most extreme difference in the tide height at moderate return periods is about 0.6 ft, decreasing to about 0.3 at the .005-per-yr frequency level.

Combining all surges with all shapes was also tried and gave a curve (not shown) slightly above B at the right end and below B at the left end. The curve B combination, providing selective peaking of the highest surges, was adopted as the final procedure.

Variation of total tide frequency with maximum surge frequency

Fitting a curve to the series of maximum annual surge heights (figure 7-1) yields an extrapolated estimated return period of 270 years for a surge height of 6.4 ft, the maximum observed in the November 1950 storm. The question can legitimately be raised as to whether the return period of this height is in reality that long. For testing purposes we set this surge height at the 100-yr return period, with an adjusted frequency curve as shown in figure 8-2, curve B. The resulting total tides with the two frequency distributions of S_x are shown in figure 8-3. The modification increases tides at a given frequency a maximum of 0.2 ft. We adopt the straight line fit after comparison with observed maximum tides (next paragraph).

Amalgamation of computed and observed winter tides

Plotted together in figure 8-4 are the four highest maximum annual winter tides at Atlantic City for 47 years from table 8-1, the least squares regression line fitted by the Gumbel theory to this series, and the computed tide frequency, the B curve of figures 8-1 and 8-3. Also shown is the maximum annual winter surge curve from figure 7-1. The compromise curve A has been constructed as best depicting the probable frequency of winter maximum

tides. This goes through the observed data at return periods of less than
about 20 years and transitions to computed tides for longer return periods.
Curve A maintains a better spacing with the surge frequency curve than does
the fitted straight-line total tide curve, curve B. The latter converges
with the surge curve at long return periods, which is unrealistic.

The computed total tide curve fails to replicate observations in the
2- to 20-year return-period range, and exceeds the observed tide curve by
about 0.9 ft. We surmise that failure to remove all of the spurious
periodicity in the apparent surge contributes to at least part of this
difference.

Table 8-1

MAXIMUM ANNUAL WINTER (NOV-APR) TIDES (FT MSL)
ATLANTIC CITY, N.J., 1911-1968

Year	Highest tide (ft msl)*	Adjustment to 1941-59 msl (ft)	Adjusted tide (ft msl)*	Date
1911-12	3.6	+.5	4.1	1-4-12
1912-13	3.6	+.5	4.1	11-24-12
1913-14	4.1	+.5	4.6	1-4-14
1914-15	4.8	+.5	5.3	12-7-14
1915-16	4.0	+.5	4.5	12-7-15
1916-17	3.4	+.4	3.8	12-22-16
1917-18	4.8	+.4	5.2	4-11-18
1918-19	4.4	+.4	4.8	12/17,18/18
1919-20	5.0	+.4	5.4	2-5-20
1920-21	-	-	-	-
1921-22	-	-	-	-
1922-23	4.0	+.4	4.4	3-6-23
1923-24	4.5	+.3	4.8	3/21,22/24
1924-25	3.9	+.3	4.2	1-2-25
1925-26	4.0	+.3	4.3	12-3-25
1926-27	4.6	+.3	4.9	2-20-27
1927-28	4.1	+.3	4.4	12-5-27
1928-29	4.0	+.3	4.3	4-16-29
1929-30	4.0	+.3	4.3	1-15-30
1930-31	4.9	+.2	5.1	3-4-31
1931-32	4.3	+.2	4.5	3-6-32
1932-33	5.2	+.2	5.4	11-10-32 1-26-33
1933-34	3.6	+.2	3.8	12-5-33
1934-35	3.8	+.2	4.0	12-8-34
1935-36	4.9	+.2	5.1	11-17-35
1936-37	4.5	+.2	4.7	4-26-37
1937-38	4.1	+.2	4.3	12-4-37
1938-39	3.7	+.2	3.9	12-9-38
1939-40	4.7	+.1	4.8	1-24-40
1940-41	4.4	+.1	4.5	12-29-40
1941-42	4.8	+.1	4.9	3-3-42
1942-43	4.2	+.1	4.3	12-9-42 2-6-43
1943-44	4.5	+.1	4.6	1-4-44
1944-45	5.4	+.1	5.5	11-30-44

*msl 6.60' above gage zero

Table 8-1 Continued

MAXIMUM ANNUAL WINTER (NOV-APR) TIDES (FT MSL) ATLANTIC CITY, N.J. 1911-1968

Year	Highest tide (ft msl)*	Adjustment to 1941-59 msl (ft)	Adjusted tide (ft msl)*	Date
1945-46	4.8	+.1	4.9	12-2-45
1946-47	4.2	+.1	4.3	11-11-46
				4-21-47
1947-48	5.5	0	5.5	11-1-47
1948-49	4.4	0	4.4	11/29,30/48
1949-50	3.9	0	3.9	2-15-50
1950-51	6.6	0	6.6	11-25-50
1951-52	4.8	0	4.8	11-1-51
1952-53	4.4	0	4.4	12-22-52
1953-54	4.6	0	4.6	11-6-53
1954-55	4.5	-.1	4.4	4-24-55
1955-56	4.8	-.1	4.7	1-10-56
1956-57	4.3	-.1	4.2	2-15-57
1957-58	4.7	-.1	4.6	4-3-58
1958-59	4.2	-.1	4.1	12-12-58
1959-60	4.9	-.1	4.8	12-29-59
1960-61	5.0	-.1	4.9	1-16-61
1961-62	6.8	-.2	6.6	3-7-62
1962-63	4.6	-.2	4.4	11/3,10,16/62
1963-64	4.5	-.2	4.3	11-7-63
1964-65	4.5	-.2	4.3	1-17-65
1965-66	5.5	-.2	5.3	1-23-66
1966-67	4.7	-.2	4.5	2-7-67
				4-27-67
1967-68	4.5	-.2	4.3	12-29-68

*msl 6.60' above gage zero

A - ALL SURGES FLAT SHAPE (SHAPE NO. 1 FIG. 7-6)

B - MIXED RELATION. HIGHEST 1% SURGES. SHAPE NO. 10.
99% SURGES SHAPE NOS. 1-9

C - ALL SURGES PEAKED SHAPE (SHAPE NO. 10, FIG. 7-6)

EXTREME PROBABILITY DISTRIBUTION
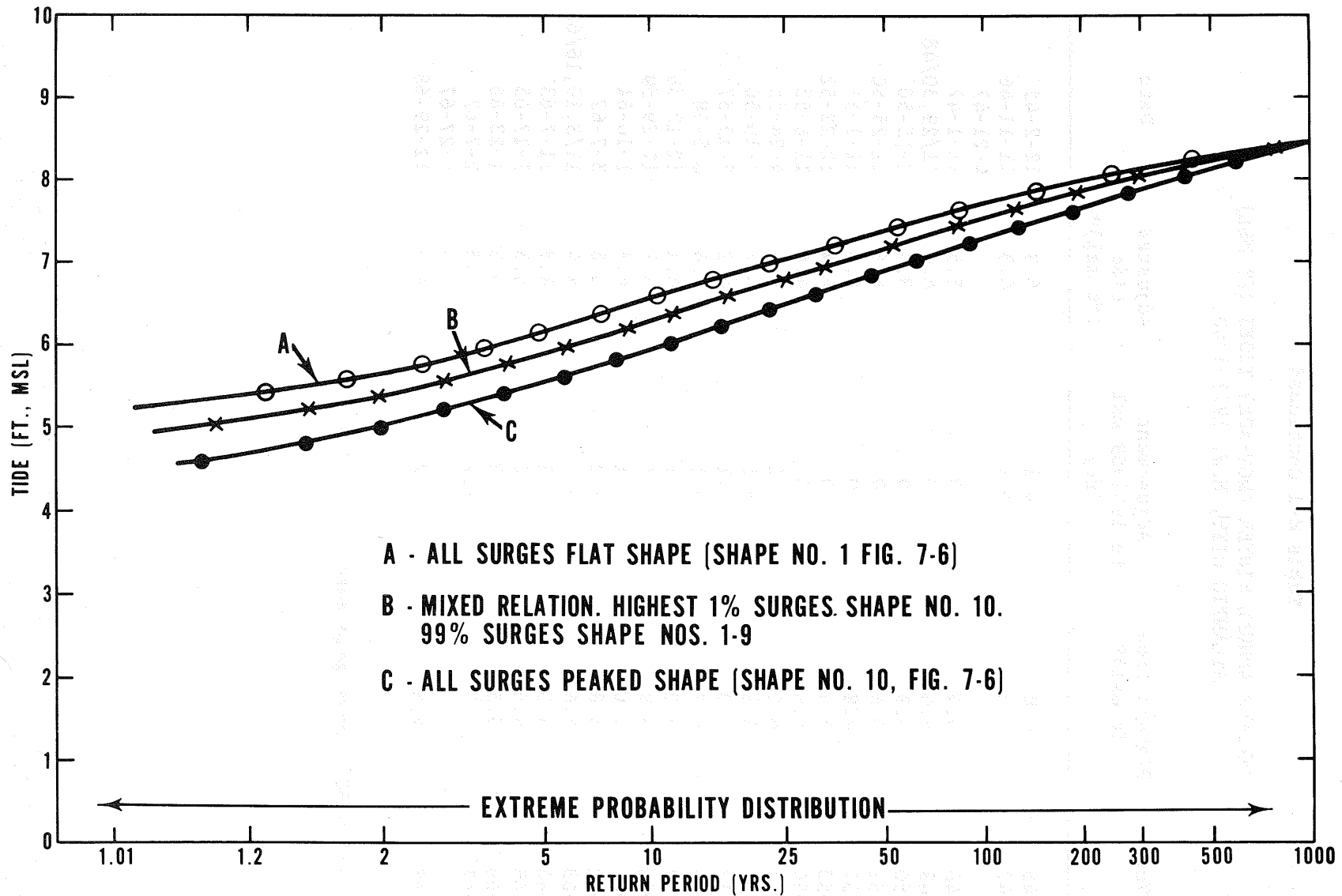
Figure 8-1. Test of effect of surge height – surge shape relationship on computed winter maximum tides.
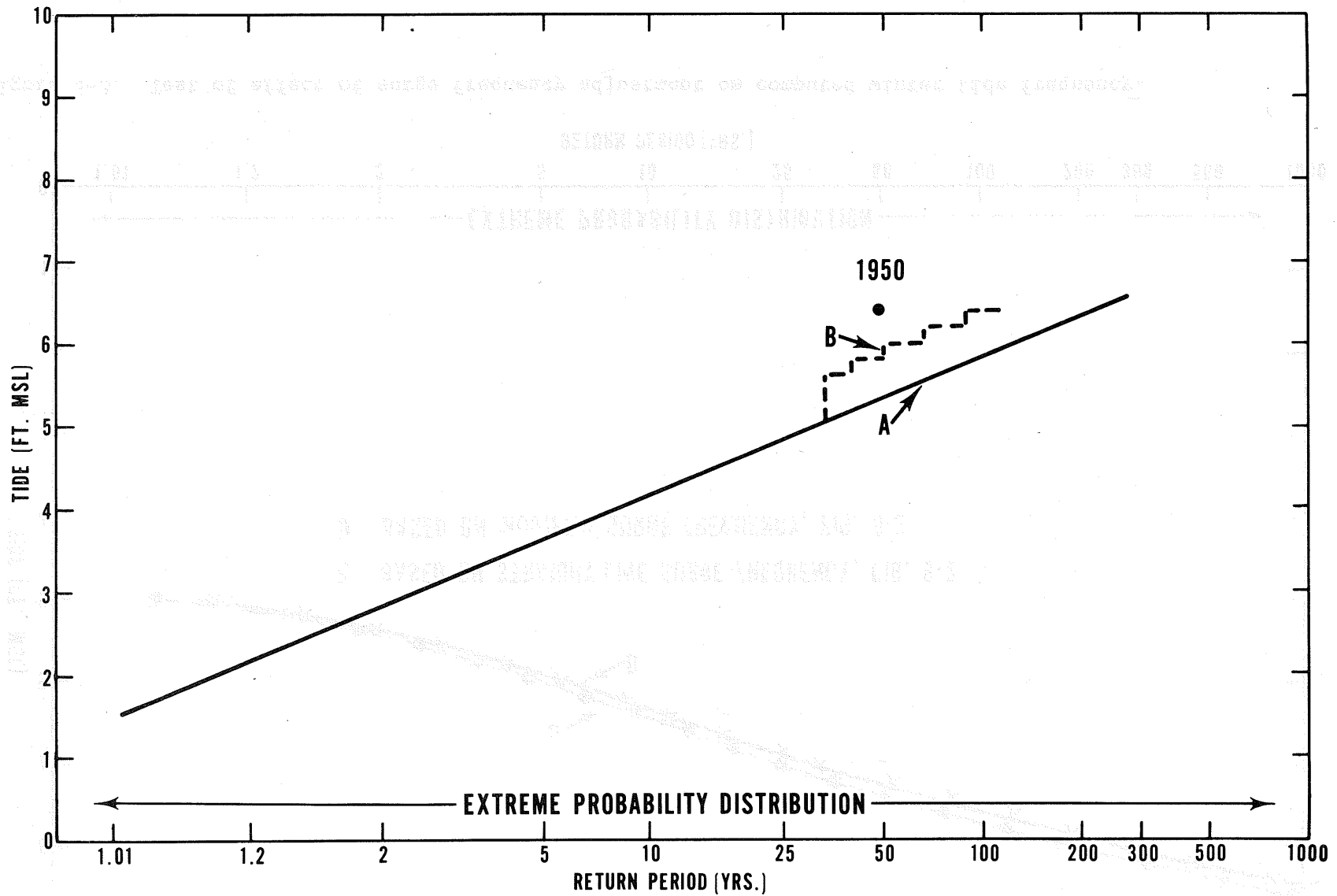
Figure 8-2. Modification of winter surge frequency for testing effect on total tide frequency
A. Frequency of maximum annual winter (Nov-Apr) surge, Atlantic City, N.J. From
figure 7-1. B. Modification.
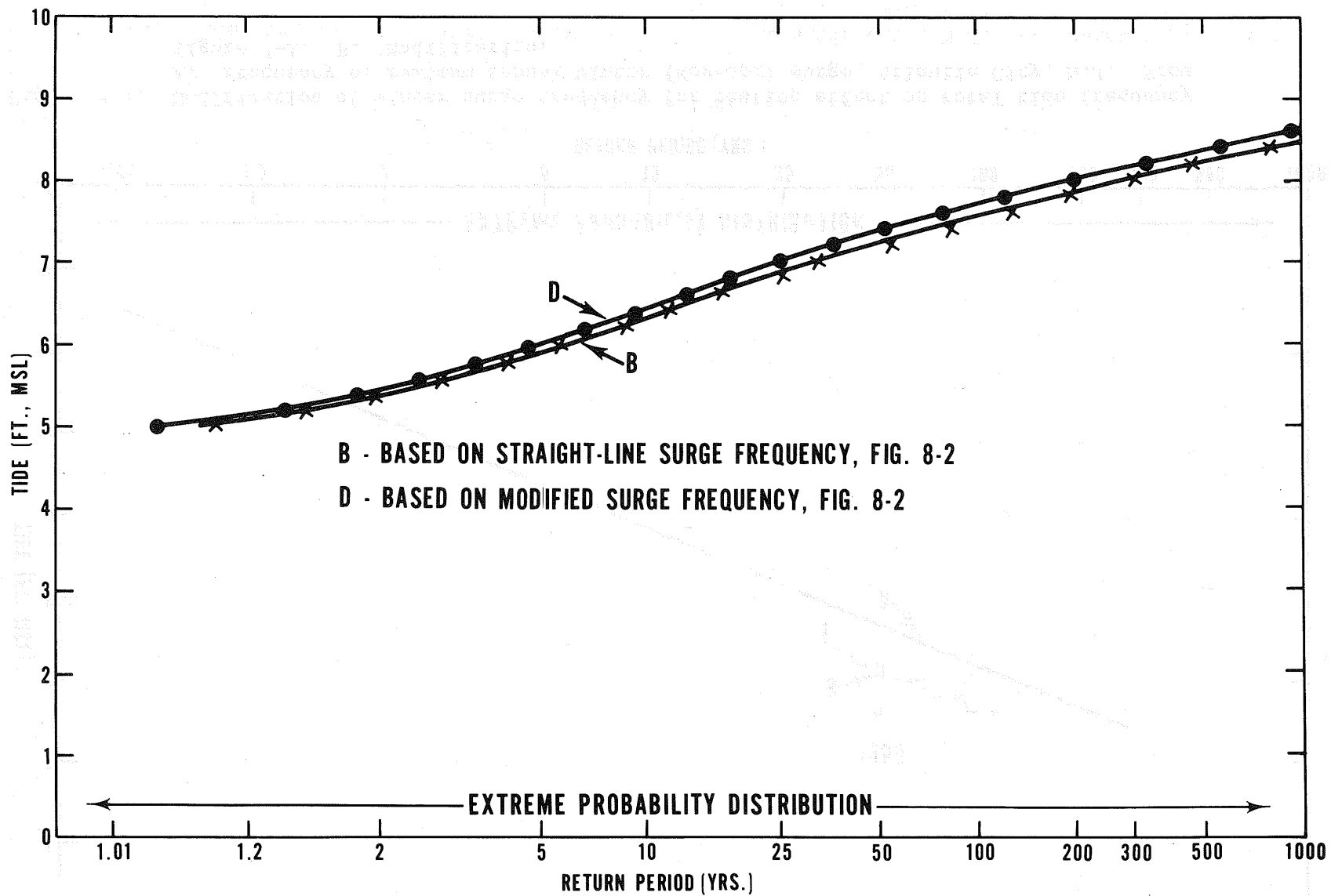
Figure 8-3. Test of effect of surge frequency adjustment on computed winter tide frequency.
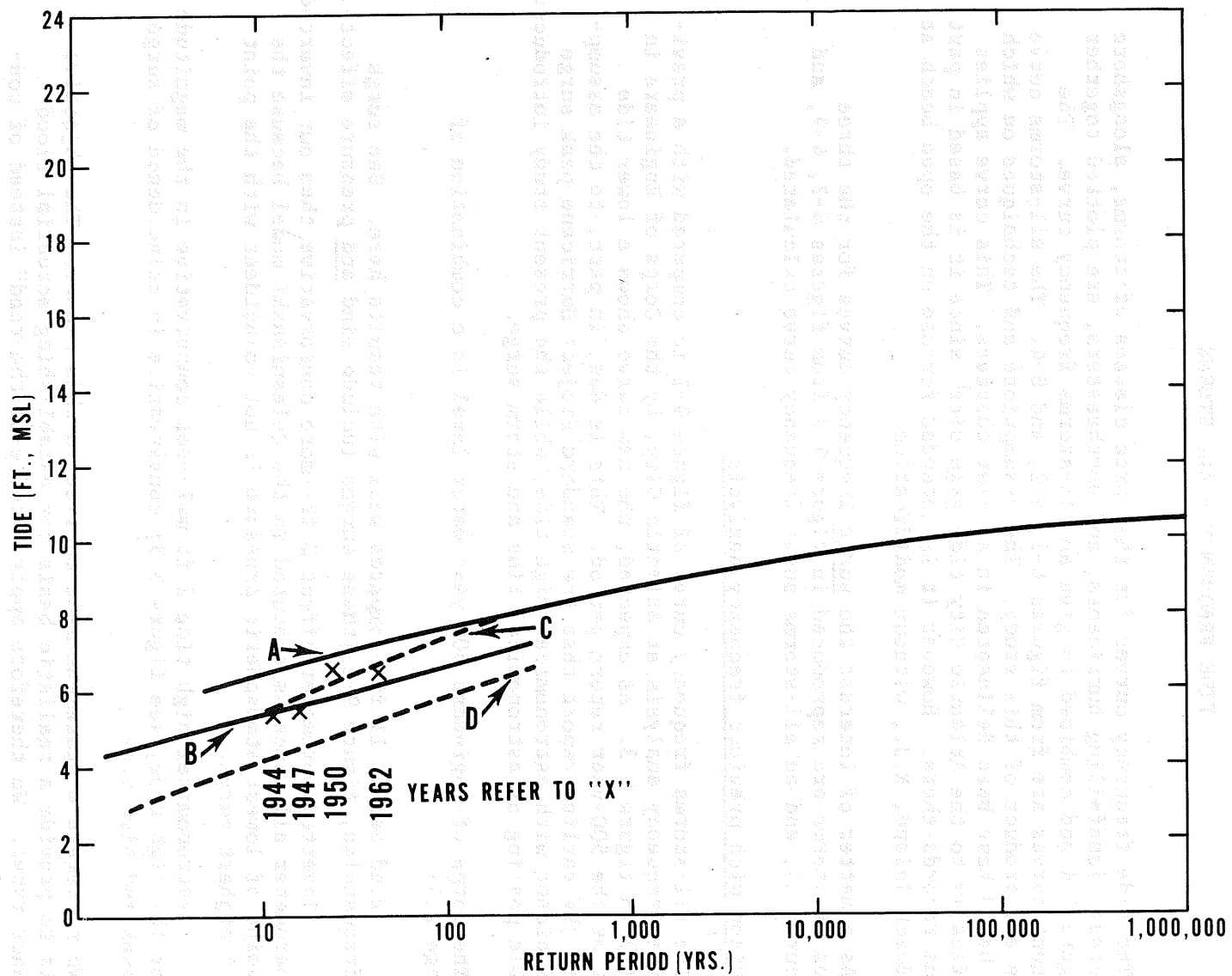
Figure 8-4. Tide frequency from winter (Nov-Apr) storms, Atlantic City, N.J. A. Joint probability method. B. Gumbel analysis of maximum annual observed winter tides. C. Adopted frequency. D. Surge (ft). From figure 7-1.

Chapter IX

TIDE FREQUENCY - ALL STORMS

The tide frequency curves for the three classes of storms, alongshore hurricanes, landfalling hurricanes, and northeasters, are plotted together on figure 9-1 and combined to give an all-storms frequency curve. The component curves are from figures 6-1, 6-2, and 8-4. The all-storms curve is the end product of this study. The assumptions and techniques on which it is based have been delineated in earlier chapters. This curve applies specifically to the Atlantic City tide gage site, since it is based in part on tide records there. However it is intended for use on the open beach at Long Beach Island, N.J., without modification.

As a matter of interest the surge frequency curves for the three classes of storms are reproduced in figure 9-2 from figures 4-7, 4-9, and 7-3 (curve C), and an all-storms surge frequency curve calculated.

Comparison with previous frequency analysis

The all-storms frequency curve of figure 9-1 is compared with a previous tide frequency analysis at Atlantic City, by the Corps of Engineers in 1963 (1) in figure 9-3. As expected, the new curve shows a lower tide height at the 500-year return period. This is due, in part, to the assumption in the earlier report that the Standard Project Hurricane peak surge is coincident with astronomical high tide, while the present study introduces variable phasing of astronomical tide and storm surge.

The Corps of Engineers 500-year water level is a combination of (1, page 21):

Wind set-up 11 ft--compares well with results here. See surge frequencies, figure 9-2 (these surges include wind and pressure effect).

Inverted barometer effect 3 ft--more conservative than our inverted barometer allowance as executed in the Jelesnianski model because the point of lowest atmospheric pressure is not coincident with the point of highest surge.

Astronomical high tide 2 ft msl--not conservative in the magnitude of the high tide, see figure 5-3; conservative in coincidence of surge peak and high tide.

We reiterate a statement made earlier in this report. The objective here is to provide a realistic basis for establishing actuarial flood insurance rates. We therefore apply "middle-of-the-road" instead of conservative judgments at various points. In view of the numerous uncertainties, A HIGHER DEGREE OF CONSERVATISM MAY BE APPROPRIATE FOR CONSTRUCTION DECISIONS INVOLVING THE SAFETY OF PERSONS.
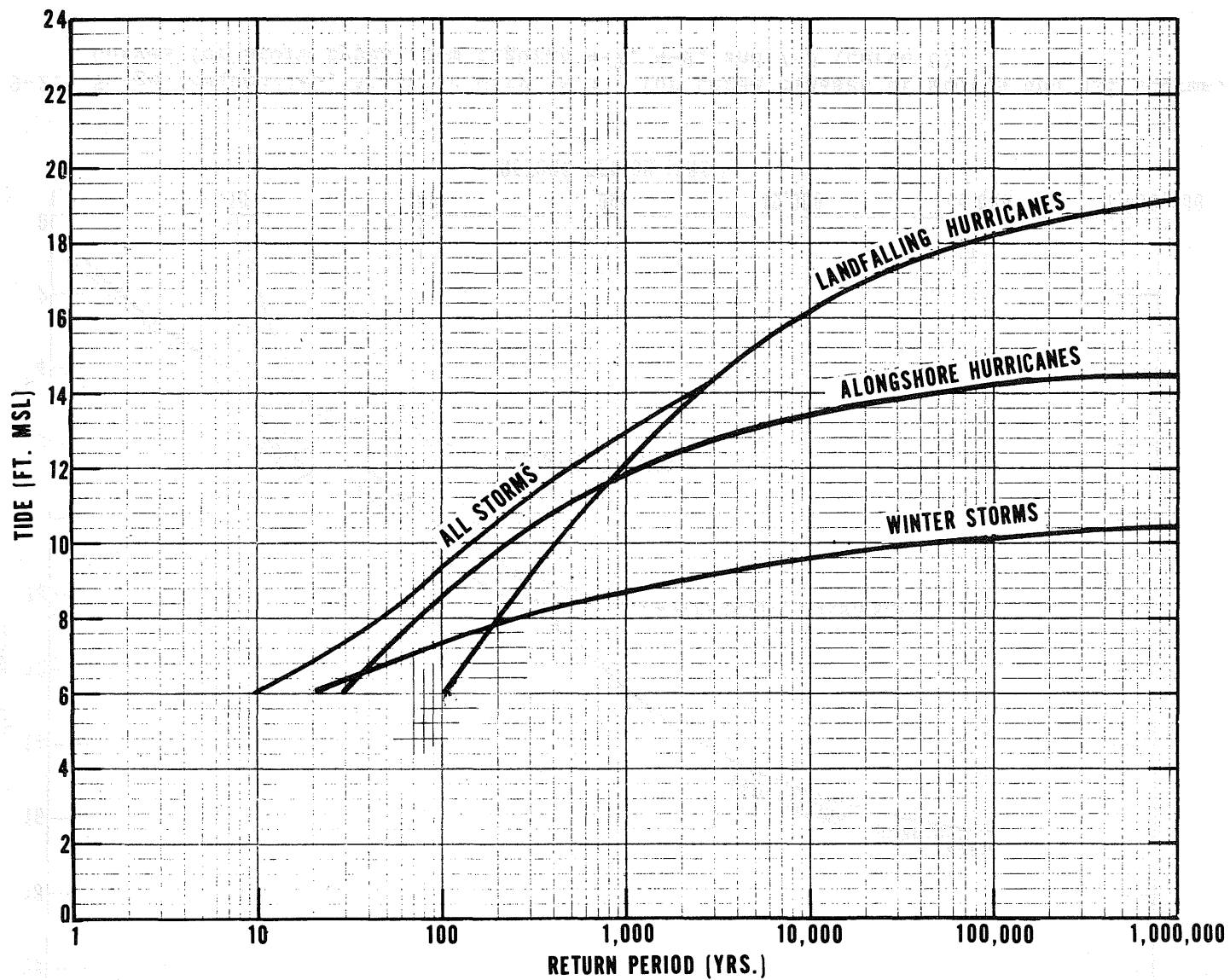
Figure 9-1. Tide frequencies, Atlantic City, N.J., by joint probability method. Curves for storm types from figures 6-1, 6-2, and 8-4.
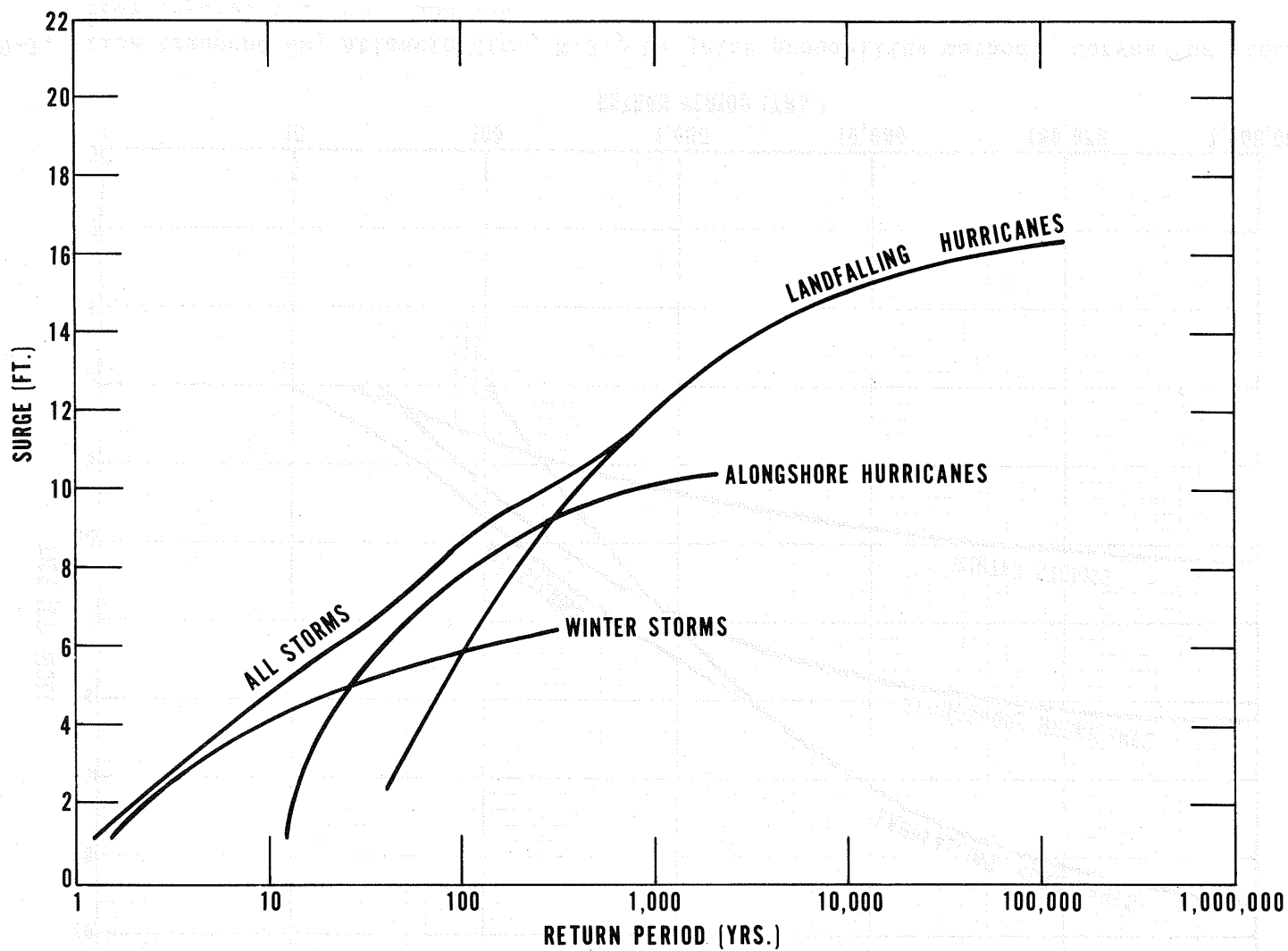
Figure 9-2. Surge frequencies, Atlantic City, N.J., for three classes of storms and all storms.
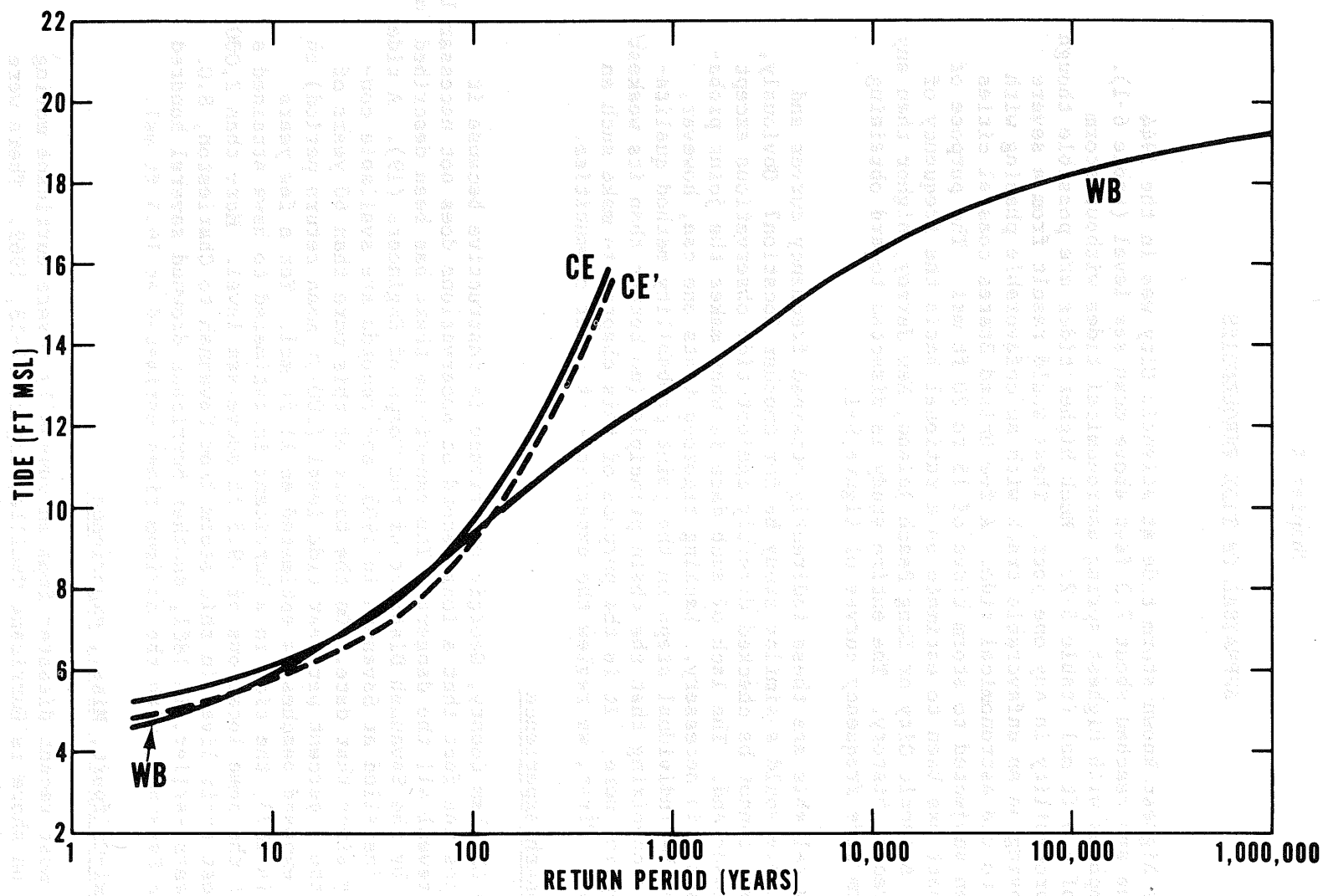Curves for storm types from figures 4-7, 4-9, and 7-3 (curve C).

Figure 9-3. Tide frequency all storms, Atlantic City, N.J. WB - Weather Bureau, from figure 9-1. CE - Corps of Engineers, 1963. CE' - CE adjusted for difference in msl datum in the two analyses.

Chapter X

APPRAISAL OF TIDE FREQUENCIES

The highest known storm tide at Atlantic City was in the 1944
hurricane and reached about 7.3 feet above mean sea level (table 6-1).
This compares with highest spring astronomical tides without storm
effect of 4.0 ft msl (table 5-2). Much higher tides are possible though
of low probability in any one year. These would result from a severe
storm moving on an unfavorable track with an unfavorable phasing with
respect to the astronomical tide. A few United States coastal cities
have been subjected to storm tides of 15 to 20 ft msl. The purpose of
this report has been to estimate on a rational basis the frequency of
tides at Atlantic City or Long Beach Island, New Jersey, higher than any
during recent history. The entire study is directed toward obtaining
the storm tide frequency curves of figure 9-1.

How reliable are these indirectly obtained frequency curves and
how reliable would a similar study be for another location? Obviously,
the curves cannot be checked directly against tide observations except
at the lower end. The lack of such data is what makes the joint proba-
bility analysis necessary. Lacking rigorous tests one can, however,
appraise the individual steps in the joint probability method qualita-
tively, recognizing that the chain principle (no better than its weakest
link) applies here. It is the purpose of this chapter to make such an
appraisal. First, we review the experience of other communities.

The Savannah experience

The Chatham County, Georgia experience is instructive because it
illustrates the fact that a long record of observations does not necessarily
clearly reveal all the dangers. The experience there has been described in
a report by the Savannah District of the Corps of Engineers (19). A tide
gage was installed at Savannah in 1903, and records are available con-
tinuously since that date. On the basis of this more than 60 years of
record, the 1 percent per year tide level (100-yr mean return period) on
the more exposed beaches is estimated as 11 ft msl. Yet a few years
before, in 1893, the tide in a hurricane is estimated to have attained a
height at the same locations of 19.5 ft above sea level. More than 2,000
people lost their lives in this storm from Savannah to Charleston, S.C.
Twelve years earlier, in 1881, another hurricane drowned several hundred
people in Savannah, with the maximum tides estimated at 16.5 ft msl.

The Biloxi-Gulfport, Miss., experience

The most recent disaster from an unusually severe hurricane moving
directly on shore is Hurricane Camille, August 17-18, 1969. There were
a number of deaths to persons who failed to evacuate after dissemination

of warnings. Coastal high water elevations in Hurricane Camille, based on a survey by the Corps of Engineers, are graphed in figure 10-1.

Appraisal of hurricane climatology

The climatological hurricane parameters that generate surge (and therefore tide) frequencies in this study are basic storm frequency, and intensity, radius of maximum winds, forward speed, and direction of motion probabilities. The direction of motion of landfalling hurricanes is covered on page 15 and will not be reviewed again here.

Storm frequency--alongshore hurricanes. There are sufficient tropical storm tracks for this to be fairly definite.

Storm frequency--landfalling hurricanes. Landfalling hurricanes in New Jersey are rare and the real climatological frequency is somewhat indefinite. The basis for estimating a frequency of .0002 storms per nautical mile per year is found on page 11 . The comparison of calculated tide frequency with observed hurricane tides (only two) in figure 6-2 tends to support this adopted frequency. A lower basic frequency would shift the curve to the right away from the observed tides.

Forward speed. The forward speed is obvious from published tracks and this factor is fairly definite. The influence of forward speed on surges may be judged from figures 3-8 and 4-8.

Radius of maximum winds. This is the most difficult hurricane parameter to determine. The computed surge varies about 2.5 feet for storms of standard intensity from the smallest climatological R (30 miles) to the largest (45 miles). This is indicated by comparing curves of figure 4-1 for landfalling storms and the respective curves of figure 4-8 for alongshore storms. Accepting the published values of R without modification (figure 3-7) and applying the Jelesnianski model to them would increase surge and tide heights. The judgment factors for not doing this are found on page 14 .

Intensity. In combination with basic storm frequency, the intensity parameter has the greatest influence on surge frequencies. Extreme surges result only from intense hurricanes, regardless of R, forward speed, or direction. The intensity index--depression of pressure at the center-- in some hurricanes has been observed directly; in others indirect estimates were required. In most recent severe hurricanes the central pressure is determined by dropsonde from reconnaissance aircraft. Elaborate efforts were made in (8), (9), and (10) to estimate the central pressure at landfall in hurricanes when not directly observed. In the present study care was exercised to relate the intensity probability and the basic storm frequency, pages 12 and 13 . The probability distribution of central pressures in table 3-3 seems reasonable against the geographical variation pattern of this parameter in (8), though obviously all uncertainties have not and cannot be removed.

Appraisal of Jelesnianski model

Replication of observed storm surges. The ultimate test of a model of this kind is whether it will reproduce historical observed surges. This verification can be made only when tide values at the coast and winds and pressures at sea are available. Jelesnianski has published reconstructed surges at Atlantic City for two alongshore hurricanes, September 1944 and Donna of 1960, in (3), and has also made a comparison in Hurricane Carol of 1955, being prepared for publication. Coastal surge profile for two landfalling hurricanes, Carla of 1961 on the Texas coast and Audrey of 1957 in Louisiana, are worked out in (20). The bottom stress treatment is different in (20) than in the later version, (3). The two Atlantic City replications are reproduced in figure 10-2. The "no bottom stress" curve does not apply to the present study.

The computed surge profile in Camille, by the methods of (3) and furnished by Dr. Jelesnianski, is shown in figure 10-3. It should be noted that this is the instantaneous surge profile at time of maximum surge and not (thus differs from fig. 10-1) a profile of local maximum surge regardless of time.

Group verification. The correspondence of the calculated alongshore storm tide frequency curve of figure 6-1 to the observed tides at the lower end of the curve is a verification of the surge model as well as the hurricane climatology. A bias in the model would tend to shift the curve away from the observed tides.

This is not a strictly independent test, as the two highest observed storms (1944 and 1960) are part of the development data in establishing the bottom friction coefficient and other factors. However, the surge height is not highly sensitive to the particular value of the bottom friction coefficient assumed.

Deductive verification. The Jelesnianski surge model is based on the equations of motion and continuity and takes into account the principal forces or states, which are the stress of wind on water, bottom stress, reduction of atmospheric pressure, inertia, Coriolis forces, and gravity. Do the linearized forms of the equations do violence to the complete equations and do the numerical methods of solution do violence to the linearized equations? The author of the present study is not a specialist in these fields and can only accept the judgment of hydro-dynamicists that they do not.

Dispersion test. A test revealed that the hurricane tide frequencies of figures 6-1 and 6-2 (also fig. 9-1) in the range of greatest interest are not highly sensitive to precision of the surge model in individual storms, provided the model gives values at the proper level on the average. The test was executed as follows. Three surge profiles were derived from each climatological hurricane: the original profile as calculated, a

profile 10 percent lower, and a profile 10 percent higher. This expanded set of representative surges was then combined with the astronomical tide as before, and the frequency established of the resulting total tides. Shifts in the computed tide frequency curve by this operation were found to be negligible at return periods of less than 1000 years.
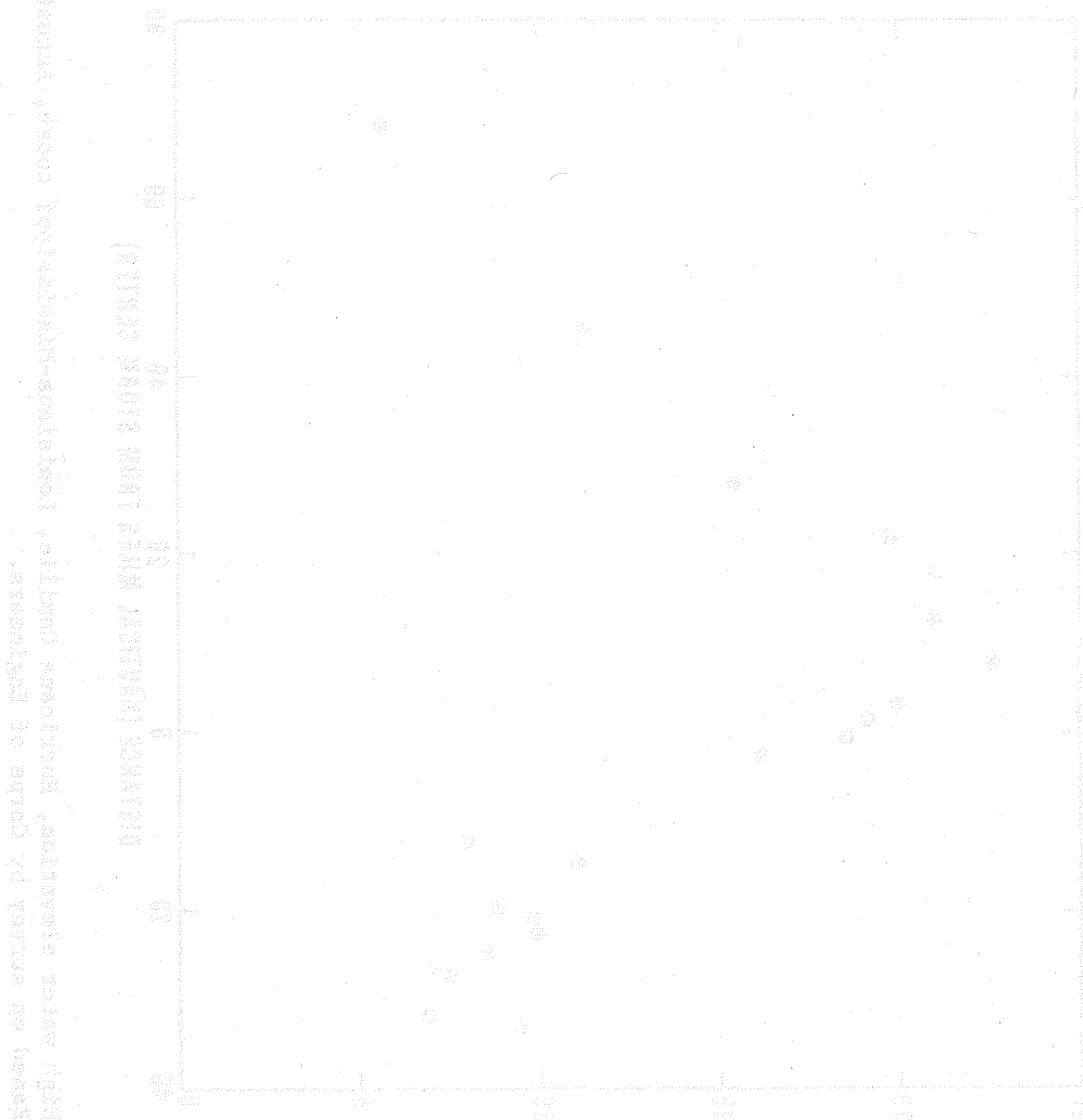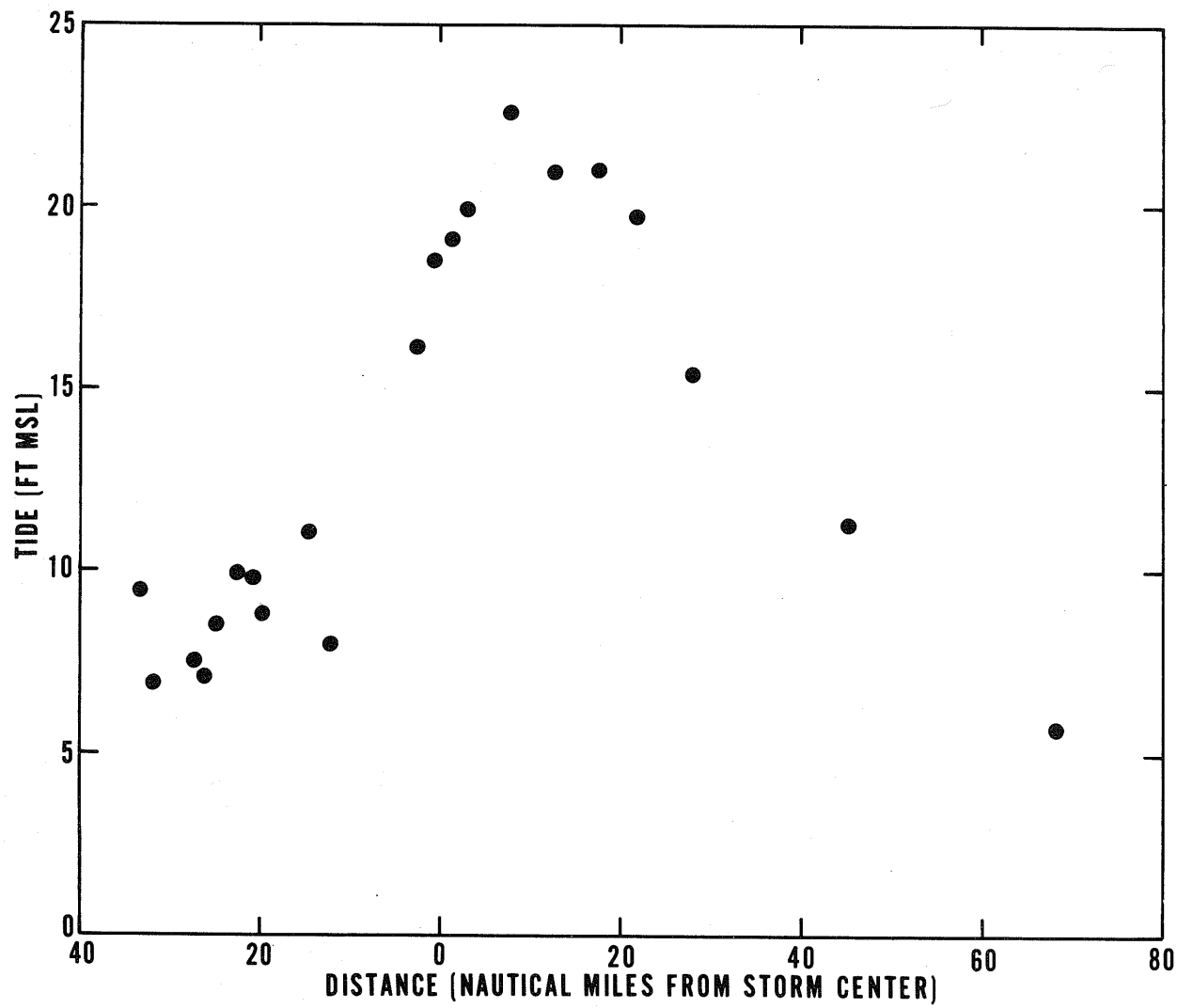
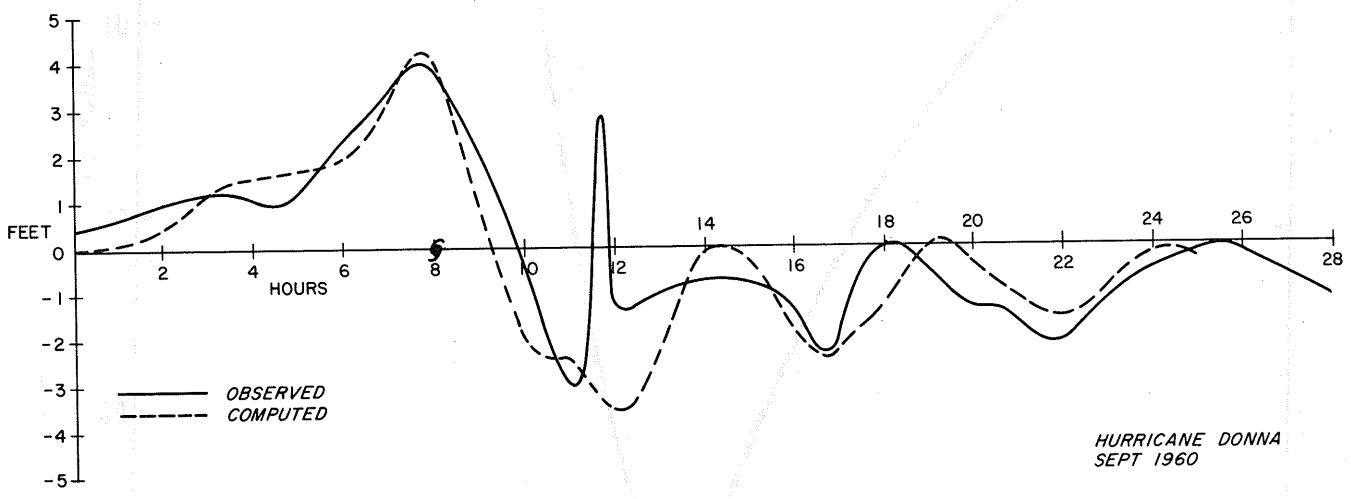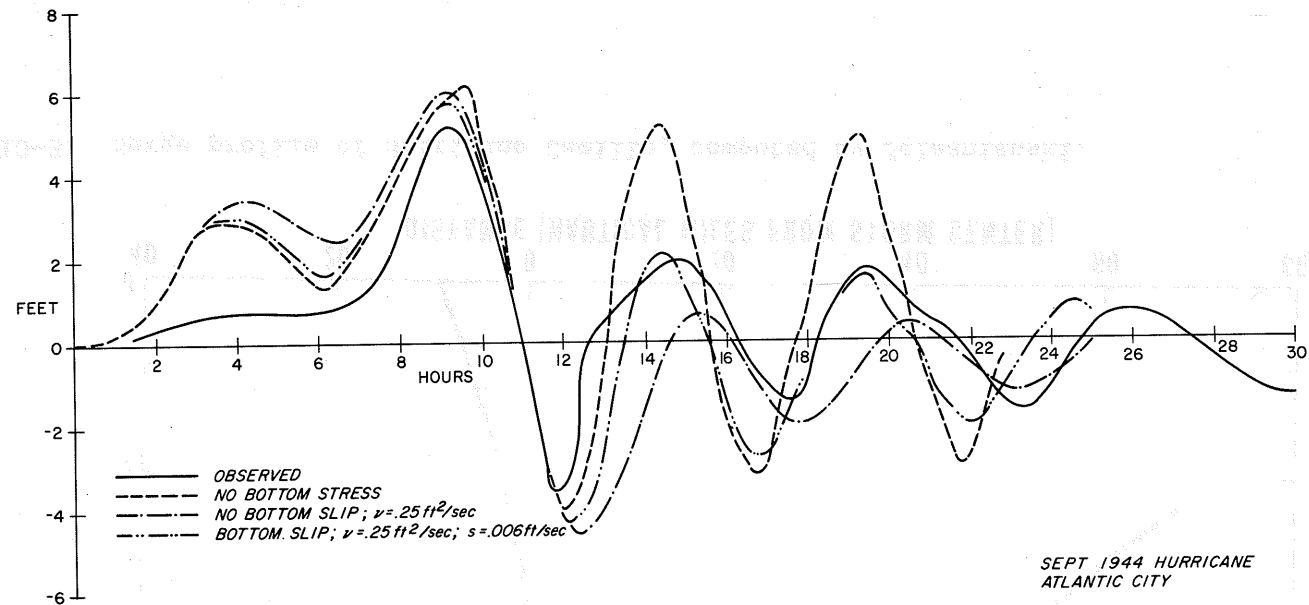Figure 10-1. High water elevation, Hurricane Camille, Louisiana-Mississippi coast, August 17-18, 1969. Based on survey by Corps of Engineers.

Figure 10-2. Computed and observed surges in two hurricanes at Atlantic City, N.J. From (3).
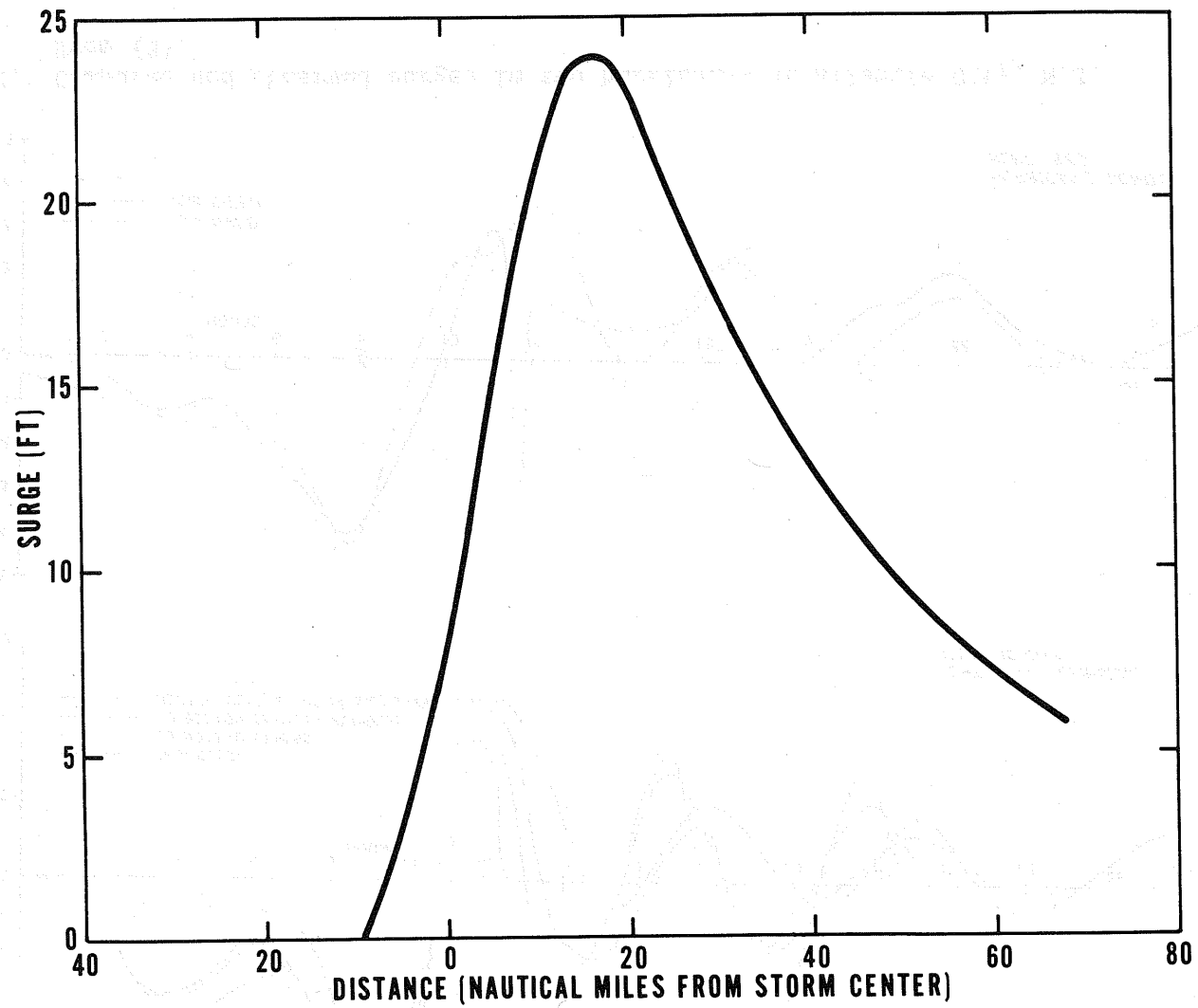
Figure 10-3. Surge profile of Hurricane Camille, computed by Jelesnianski.

Chapter XI

RECOMMENDATIONS

These are the recommendations of the author of this study based on experience in making the study. At the time of preparation of the study they were not ESSA recommendations, but were part of the basis being developed for formulating ESSA recommendations.

Recommendation 1. That tide frequency analyses by the joint probability method be carried out for selected points along all of the eastern and southern coasts of the United States, for flood insurance and other planning purposes.

Recommendation 2. That locations with tide gage records and relatively simple coast and ocean bottom configuration be selected for the next such studies. The tide gage records serve to verify hurricane surge frequencies computed from a dynamic model and supply the basic data for non-hurricane surges.

Recommendation 3. That after gaining the above experience that studies be extended to locations with no or few tide gage records.

Recommendation 4. That a complete verification of the Jelesnianski surge model be run in Hurricane Camille, using existing ocean floor and coastal configurations in two dimensions.

Recommendation 5. That intercomparisons be made between surges computed by the Jelesnianski model and other models that have been used or proposed, including the Marinos and Woodward model.

Recommendation 6. That Jelesnianski's basin adjustment coefficients (fig. 17 of (3)) be re-examined for each major study location, carrying out as many complete dynamic calculations of the surge with as many different hurricanes as may be necessary, using a two-dimensional specification of the ocean depth. The limiting factor is cost of computer time for the dynamic calculations. Jelesnianski's published coefficients are based on a relatively few number of complete runs, all with a one-dimensional specification of the bottom configuration.

Recommendation 7. That the dynamics of surges with curved coasts be further examined, by extension of the Jelesnianski model or by some other method.

Recommendation 8. That methods be organized for adjusting tide frequencies from the outer beach on barrier islands (to which the present study applies) to the adjacent mainland. Many communities requiring flood insurance are in the latter type of location.

106

As in the present study, major dependence will necessarily be on physical analysis, with observed tides as a check, as the major interest is in tides higher than any observed at most locations. The principal physical factors are wind set-up, which tends to raise mainland tide levels adjacent to wide shallow sounds; limitation of inflow through inlets and over islands, which tends to restrict mainland tide levels, and dynamics of traveling tidal waves (e.g., Long Island Sound). Degree of erosion of the barrier island and consequent cross section for admitting the sea can be introduced as an additional probability factor, at least is concept.

Recommendation 9. That the numerical and approximation procedures of the present initial study be re-examined and refined in subsequent studies. For example, in fitting a curve to the surge time (figure 4-3) and surge-distance (figure 4-5) profiles are more terms in the equation for a closer fit warranted? In the several steps of representing a continuous probability distribution (figures 3-5, 5-3, 6-3, etc.) by discrete values, is the choice of class interval the optimum for accuracy without unnecessary calculation?

Acknowledgments

REFERENCES

(1)   Corps of Engineers, Philadelphia District, "Report on Hurricane Study, Atlantic City, N.J." May 1963.

(2)   G. Marinos and J.W. Woodward, "Estimation of Hurricane Surge Hydrographs," _Journal of the Waterways and Harbors Division_, Proceedings of ASCE, No. 5945, May 1968.

(3)   C.P. Jelesnianski, "Numerical Computations of Storm Surges With Bottom Stress," _Monthly Weather Review_, vol. 95, November 1967, pp. 740-756.

(4)   U.S. Coast and Geodetic Survey, "Tide Tables, East Coast, North and South America," 1949-1969.

(5)   G. W. Cry, "Tropical Cyclones of the North Atlantic Ocean," _Technical Paper No. 55_, U.S. Weather Bureau, Washington, 1965.

(6)   G.E. Dunn and Staff, "The Hurricane Season of 1964," _Monthly Weather Review_, vol. 93, No. 3, March 1965, pp. 175-187.

(7)   A.L. Sugg and P.J. Hebert, "The Atlantic Hurricane Season of 1968," _Monthly Weather Review_, vol. 97, No. 3, March 1969, pp. 225-239.

(8)   H.E. Graham and D.E. Nunn, "Meteorological Considerations Pertinent to Standard Project Hurricane, Atlantic and Gulf Coasts of the United States," _National Hurricane Research Project Report No. 33_, U.S. Weather Bureau and Corps of Engineers, Washington, November 1959.

(9)   "Survey of Meteorological Factors Pertinent to Reduction of Loss of Life and Property in Hurricane Situations," _National Hurricane Research Project Report No. 5_, U.S. Weather Bureau, Washington, March 1957.

(10)   H.R. Graham and G.N. Hudson, "Surface Winds Near the Center of Hurricanes (and Other Cyclones)," _National Hurricane Research Project Report No. 39_, U.S. Weather Bureau and Corps of Engineers, Washington, September 1960.

(11)   Paul Schureman, "Manual of Harmonic Analysis and Prediction of Tides," Coast and Geodetic Survey, _Special Publication No. 98_, (Reprinted 1958 with corrections), Washington, 1958.

REFERENCES (Cont'd.)

(12) N.A. Pore and R.A. Cummings, "Fortran Program for the Calculation of Hourly Values of Astronomical Tide and Time and Height of High and Low Water." Weather Bureau Technical Memorandum-TDL-6. 1967.

(13) H.A. Marmer, "Tidal Datum Planes," Coast and Geodetic Survey, Special Publication No. 135, Revised (1951) Edition, Washington, 1951.

(14) L.P. Disney, "Tide Heights Along the Coasts of the United States," Proceedings, ASCE, vol. 81, April 1955, separate No. 666.

(15) S.D. Hicks, "Long Period Variations in Secular Sea-Level Trends," Journal of American Shore and Beach Preservation Association, 1968.

(16) D. Lee Harris, "Characteristics of the Hurricane Storm Surge," Technical Paper No. 48, U.S. Weather Bureau, Washington, 1963.

(17) E.J. Gumbel, "Statistics of Extremes," Columbia University Press, 1958, 375 pp.

(18) D.M. Hershfield, "Rainfall Frequency Atlas of the United States for Durations from 30 Minutes to 24 Hours and Return Periods from 1 to 100 Years," Technical Paper No. 40, U.S. Weather Bureau, Washington, 1961.

(19) Corps of Engineers, Savannah District, "Preliminary Tidal Flood Information for the Coastal Area of Chatham County, Georgia," 1968.

(20) C.P. Jelesnianski, "Numerical Computations of Storm Surges Without Bottom Stress," Monthly Weather Review, vol. 94, No. 6, June 1966, pp. 379-394.